
**Late Neogene to Quaternary paleoproductivity of the
western Indian Ocean and the eastern South Atlantic from
coccolithophore assemblage and coccolith geochemistry**

Dissertation
Zur Erlangung des Doktorgrades der Naturwissenschaften
am Fachbereich Geowissenschaften
der Universität Bremen

vorgelegt von
Deborah Tangunan

Bremen, Oktober 2017

Gutachter:

Prof. Dr. Rüdiger Henrich

Professor of Geology (Sedimentology-Paleoceanography)

Department of Geosciences

University of Bremen

GEO Building, Room 2560

Klagenfurter Strasse

28359 Bremen

Germany

henrich@uni-bremen.de

Prof. José Abel Flores Villarejo

Professor of Micropaleontology and Oceanography

Department of Geology

University of Salamanca

37008 Salamanca

Spain

flores@usal.es

Contents

List of figures.....	i
List of tables.....	ii
List of appendices.....	ii
Preface	iii
Abstract	1
Zusammenfassung	5
CHAPTER 1 General introduction	9
1.1 Coccolithophore biology, morphology and fossil record	11
1.2 Coccolithophores and their role in the global biogeochemical cycles	13
1.3 Coccolithophores as paleoenvironmental proxies.....	14
1.4 The study area	18
1.5 Objectives of the thesis.....	21
1.6 Materials and analytical techniques	22
1.7 Outline of the thesis.....	24
1.8 Declaration of co-author contribution.....	26
CHAPTER 2 Insolation forcing of coccolithophore productivity in the western tropical Indian Ocean over the last two glacial/interglacial cycles <i>Paleoceanography (Tangunan et al., 2017)</i>	27
CHAPTER 3 Variations in coccolithophore productivity off South Africa over the last 500 kyr <i>Quaternary Science Reviews (Tangunan et al., submitted)</i>	57
CHAPTER 4 The last 1 million years of the extinct genus <i>Discoaster</i> : environment and productivity at Site U1476 (Mozambique Channel) <i>Palaeogeography, Palaeoclimatology, Palaeoecology</i> <i>(Tangunan et al., in preparation)</i>	85
CHAPTER 5 Conclusions.....	107
CHAPTER 6 Future direction/outlook.....	113
Appendices	117
References	123
Acknowledgments.....	135

List of figures

1.1	Possible functions of coccoliths.....	11
1.2	Ecological distribution of coccolithophore types.....	12
1.3	Simplified schematic representation of the complex role of coccolithophores in the global carbon cycle.....	14
1.4	Hypothetical scenarios of coccolithophore response to nutrient availability driven by physical processes in a non-upwelling region of the western Indian Ocean.....	15
1.5	Map of the study area	20
1.6	Flowchart of all the analyses performed	23
2.1	Schematic illustrations of surface water hydrography of the equatorial Indian Ocean.....	36
2.2	Age model and sedimentation rates of GeoB12613-1	39
2.3	Coccolithophore assemblage and abundance records of GeoB12613-1	42
2.4	Core GeoB12613-1 productivity records over the last 300 kyr	43
2.5	Spectral power versus frequency plots of coccolithophore-derived parameters.....	45
2.6	GeoB12613-1 stratification and productivity records	49
2.7	GeoB12613-1 stratification and productivity records in comparison to the eastern tropical Indian Ocean records	53
3.1	Mean chlorophyll map of the study area for 2010	64
3.2	Age model and sedimentation rates of the investigated cores	68
3.3	Total coccolith concentrations, diversity and preservation in sediment cores MD96-2077 and Site 1266	70
3.4	Coccolithophore relative abundance and absolute concentrations of MD96-2077 and Site 1266	74
3.5	Productivity records of sediment cores off South Africa	76
3.6	Differences in estimated primary productivity	79
3.7	Paleoceanographic records of the southwest Indian Ocean and the eastern South Atlantic Ocean	81
4.1	Location of IODP Site U1476 plotted on the 2010 average chlorophyll map	90
4.2	Age-depth relationships at Site U1476.....	92
4.3	Calcareous nannofossils of Site U1476	97
4.4	Absolute concentrations of the Plio-Pleistocene <i>Discoaster</i> species.....	98
4.5	Site U1476 coccolithophore productivity and stratification records	100
4.6	Absolute concentrations of indicative calcareous nannoplankton taxa.....	102
4.7	Spectral power versus frequency plots.....	104
5.1	Differences in estimated primary productivity between the eastern and the western tropical Indian Ocean.....	110

List of tables

1.1.	Ecological preferences of indicative species recorded from the study area in Comparison to other studies conducted in other locations.	17
1.2	Geographic locations and water depths of the sediments used for this study.	22
2.1	Radiocarbon dates and calibrated ages for GeoB12613-1	35
4.1	Calcareous nannofossil biostratigraphic events recorded at Site U1476.....	106
4.2	Approximate paleomagnetic boundaries at Site U1476.....	106

List of appendices

1	Scanning electron microscope images of coccolithophores from the western Indian Ocean and South Atlantic	119
2	Light microscope images of Plio-Pleistocene nannofossils from the Mozambique Channel	121

Preface

This thesis was submitted for the degree of Doctor of Natural Sciences (Dr. rer. nat.) at the Department of Geosciences, University of Bremen. This Ph.D. research was conducted at the University of Bremen within the research group *Paleoceanography – Sedimentology* under the supervision of Prof. Dr. Rüdiger Henrich and Dr. Karl-Heinz Baumann. The first thesis reviewer is Prof. Dr. Rüdiger Henrich of the University of Bremen, Germany. The second thesis reviewer is Prof. José Abel Flores Villarejo of the University of Salamanca, Spain.

This project was funded through the German Science Foundation (DFG) Research Center/Cluster of Excellence “The Ocean in the Earth System” *MARUM – Center for Marine Environmental Sciences* in the framework of the project, “Land-ocean interaction and climate variability in low latitudes”. Additional financial support was provided by the *Bremen International Graduate School for Marine Sciences* (GLOMAR) for participation in international conferences and summer schools.

This thesis was written in a cumulative format and thus consists of a collection of three stand-alone research manuscripts, which have been published (1), submitted (1) or will be submitted (1) as joint-author articles to international peer-reviewed journals. A general introduction outlining the research background, objectives and methodology precedes the three research manuscripts. The last two chapters synthesize the main findings and conclusions of this thesis, and present prospects for future research opportunities.

Deborah Tanguan

Bremen, October 2017

Abstract

Recent productivity reconstructions off South Africa have demonstrated the link between climate perturbations and coccolithophore productivity, especially over the glacial/interglacial cycles. These studies suggested enhanced productivity during glacial periods reaching maxima during terminations, and fluctuating in concert with orbital periodicities, suggesting that long-termed climatic variability have controlled the productivity patterns in this region. However most of these studies have focused on the highly productive regions of the northern and eastern Indian Ocean, and the Benguela upwelling area of the South Atlantic, whereas productivity reconstructions outside of these high-nutrient environments remain relatively scarce. Thus this Ph.D. research fills this gap by investigating sediment cores collected off Tanzania (GeoB12613-1), the Natal Valley (MD96-2077), the Mozambique Channel (International Ocean Discovery Program; IODP Site U1476), and the Walvis Ridge (Ocean Drilling Program; ODP Site 1264/1266). The strategic positions of the selected study sites allowed inter-basin and latitudinal comparisons, and accordingly a comprehensive productivity reconstruction of the western Indian Ocean and the eastern South Atlantic over the past 500 kyr, and across the Plio-Pleistocene transition. The coccolithophore assemblage composition and species distributions, preservation, and coccolith fraction geochemistry provided the groundwork for this reconstruction.

Coccolithophore assemblages off Tanzania (GeoB12613-1) are entirely composed of warm water taxa dominated by the deep-dwelling species *Florisphaera profunda*, indicating prevalence of warm tropical conditions with a deep nutricline/thermocline over the past 300 kyr. In contrast, assemblage composition in the Natal Valley (MD96-2077) includes a mixture of coccolithophore species adapted to warm and cold environments, with the abundance of *Gephyrocapsa muelleriae*, suggesting the influence of cold, nutrient-rich surface waters at the location. The abundance of *G. muelleriae* was attributed to the enhanced surface water productivity driven by the subtropical front (STF) migration during the glacial intervals, which allowed the entrance of cold, southern-sourced sub-Antarctic surface water (SASW). A possible influence of the SASW into the area is also shown by the occurrences of *Coccolithus pelagicus* and *C. braarudii*. Both of these species were not encountered off Tanzania (GeoB12613-1) but were found in the Natal Valley (MD96-2077)

as well as in the Plio-Pleistocene sediments of the Mozambique Channel (Site U1476), which suggests that the influence of the SASW could have reached as far as these locations.

The consistently higher abundances of the coccolithophore taxa with affinity for nutrient-enriched environments, such as *G. caribbeanica*, *G. muelleriae*, and small *Gephyrocapsa*, as well as lower abundances of *F. profunda* at the Walvis Ridge (ODP Sites 1264/1266) than in the two Indian Ocean sites indicate that the eastern South Atlantic is more productive than the western Indian Ocean over the last 500 kyr. Here the shifts of the STF have potentially modulated the strengths of the Agulhas Current in the Indian Ocean and the Benguela Current upwelling in the South Atlantic, and played a critical role in the nutricline/thermocline depths, and thus the nutrient availability in these regions. Productivity fluctuations in the Natal Valley (MD96-2077) based on the estimated primary productivity calculated from the relative abundance of *F. profunda* resembled the Benguela upwelling region, with enhanced surface water productivity during the glacial stages. This indicates that the northward shift of the STF during the glacial periods resulted in a weaker Agulhas Current, in the entrance of the nutrient-rich SASW, as well as in a more intense Benguela Current upwelling. By contrast, higher productivity at the Walvis Ridge (ODP Site 1266) occurred during the interglacial periods, which could be the result of the seaward lateral advection of nutrient-rich waters of the Benguela Current during the weakening of the coastal upwelling process or by a localized upwelling event in the area.

In the Mozambique Channel (Site U1476), results show that the transition from warm Pliocene to a cold Pleistocene resulted in a cooler surface water temperature, which further led to intensified mixing and consequent increase in surface water productivity. Here two phases of productivity change were observed, with a major change at 2.4 Myr, coincident with the onset of the Northern Hemisphere glaciation. Based on a low *F. profunda* index and high abundances of upper photic zone dwelling species with an affinity for high nutrient environments (*Gephyrocapsa* spp., *Reticulofenestra* spp., *Calcidiscus leptoporus*), this indicates that a more mixed water column occurred during this time. Consequently, *Discoaster* abundances decreased, accompanied by the successive disappearance of its member taxa during the Plio-Pleistocene transition.

Overall, the coccolithophore productivity record in the western Indian Ocean and the eastern South Atlantic demonstrated good correspondence with previous studies conducted in the eastern Indian Ocean, the area where the warm and oligotrophic surface

waters are mainly derived. This indicates a strong tropical Pacific influence in the western Indian Ocean that is interpreted to be linked to the variations in the intensity of the Walker Circulation. At least for the late Quaternary, a La Niña-like state of the Walker Circulation was observed from 300 to 160 kyr in the western Indian Ocean, and a more El Niño-like phase from 160 kyr and probably continuing to the present day. This is in accordance with the recent modeling studies suggesting that the Walker Circulation has been slowing for the past century, resulting to a more El Niño-like state, leading to a more stratified water column, and thus low productivity in the western Indian Ocean.

Zusammenfassung

Jüngst durchgeführte Produktivitätsrekonstruktionen vor Südafrika haben einen Zusammenhang von Klimavariationen und Coccolithophorenproduktivität im Indischen Ozean während des späten Pleistozäns aufgezeigt. Die Studien belegen Produktivitätszunahmen für Glazialzeiten mit Maxima in den Terminationen und Schwankungen in Orbitalperiodizitäten, was andeutet dass langzeitliche Klimaschwankungen die Produktivitätsmuster in dieser Region kontrolliert haben. Die meisten dieser Untersuchungen konzentrierten sich bisher jedoch auf die hochproduktiven Regionen des nördlichen und östlichen Indischen Ozeans sowie des Benguela-Auftriebs im südöstlichen Südatlantiks, während Produktivitätsrekonstruktionen außerhalb von nährstoffreichen Regionen relativ selten blieben. Die vorliegende Arbeit deckt diese Lücke mit der Bearbeitung von Sedimentkernen vom tanzanischen Kontinentalhang (GeoB 12613-1), aus dem Natal Valley vor Südafrika (Kern MD96-2077), dem Mosambikkanal (IODP-Bohrung U1476) sowie vom Walvis-Rücken (ODP-Bohrungen 1264/1266). Die Lokationen der ausgewählten Kerne erlauben raumzeitliche Vergleiche entlang des Warmwasserweges und ermöglichen dementsprechend umfassende Produktivitätsrekonstruktion im westlichen Indischen Ozean und im östlichen Südatlantik über die letzten 500 ka sowie über den Wechsel von Plio- zu Pleistozän. Das Vorkommen von einzelnen Arten, die Zusammensetzung der Coccolithen-Gemeinschaften, deren Erhaltung sowie geochemische Daten der Coccolithenfraktion liefern dabei die Basis für die hier vorliegenden Untersuchungen.

Die Coccolithophoren-Gemeinschaften aus dem tropischen westlichen Indik (GeoB 12613-1) werden von Warmwasserarten und insbesondere von der tiefliebenden *Florisphaera profunda* dominiert, die auf vorherrschend warm-oligotrophe Bedingungen mit einer tief ausgebildeten Nutri-/Thermokline in den letzten 300 kyr schließen lässt. Im Gegensatz dazu besteht die Gemeinschaft im Natal Valley (MD96-2077) aus Arten, die sowohl an warme als auch an kühlere Bedingungen angepasst sind. Größere Häufigkeiten von *Gephyrocapsa muellerae* deuten hier auf den Einfluss von relativ kaltem, nährstoffreichen subantarktischem Oberflächenwasser (SASW) und einer damit verbundenen Zunahme der Produktivität hin, die durch die nordwärtige Verlagerung der Subtropischen Front (STF) während der Glazialzeiten bewirkt wurde. Der wahrscheinliche

Einfluss vom SASW in der Region zeigt sich auch am Vorkommen von *Coccolithus pelagicus* und *C. braarudii*, die beide nicht vor Tansania, aber in den plio-pleistozänen Sedimenten des Mosambik-Kanals (ODP Bohrung U1476) gefunden wurden, was andeutet, dass der Einfluss des SASW bis hierher gereicht haben kann.

Die durchweg höheren Anteile von Coccolithophoridenarten mit Affinität zu Nährstoff-angereicherten Bedingungen wie *G. caribbeanica*, *G. muelleriae* und kleine *Gephyrocapsa*, sowie geringere Häufigkeiten von *F. profunda* am Walvis-Rücken zeigen, dass der östliche Südatlantik über die letzten 500 ka produktiver als der westliche Indische Ozean gewesen ist. Die Verschiebungen der STF hat sowohl den Agulhas-Strom als auch den Benguela-Auftrieb beeinträchtigt und damit eine wichtige Rolle in der Ausbildung von Nährstoff- sowie Thermokline und damit der Nährstoffverfügbarkeit in diesen Regionen gespielt. Auf relative Häufigkeiten von *F. profunda* basierende Schwankungen der Primärproduktion im Natal Valley (MD96-2077), die eine erhöhte Oberflächenwasserproduktivität während der Glaziale belegen, ähneln denen im Benguela Auftriebsregion. Dies deutet darauf hin, dass die Nordwärtsverschiebung der STF während der Glazialzeiten zu einem schwächeren Agulhas-Strom und erhöhten Einfluss von nährstoffreichem SASW sowie zu einem intensivierten Auftrieb vor SW-Afrika geführt hat. Im Gegensatz dazu kam es während der Interglaziale zu einer höheren Produktivität am Walvis-Rücken, die als Resultat der seewärts gerichteten Advektion des Benguela-Stroms während Zeiten eines abgeschwächten Küstenauftriebs gesehen wird.

Die Ergebnisse aus dem Mosambik-Kanal (Bohrung U1476) belegen, dass es am Übergang von Pliozän zum Pleistozän zu einer Abnahme der Oberflächenwassertemperaturen gekommen ist, die zu einer verstärkten Durchmischung und damit zu einer Zunahme in der Oberflächenwasserproduktivität geführt hat. Diese Produktivitätsänderungen verliefen in zwei Phasen mit einem starken Wechsel um 2,4 Ma, der in etwa mit dem Beginn der Vereisung der nördlichen Hemisphäre zusammenfällt. Ein geringer *F. profunda*-Index sowie größere Häufigkeiten von Arten der oberen photischen Zonen mit Affinität für erhöhte Nährstoffgehalte (*Gephyrocapsa* spp., *Reticulofenestra* spp., *Calcidiscus leptoporus*) deuten auf eine stärker durchmischte obere Wassersäule, die wiederum zu einer Abnahme und dem sukzessiven Verschwinden von Discoasteriden am Übergang Plio-Pleistozän führt.

Insgesamt stimmen die hier ermittelten, auf Coccolithophoriden basierenden Paläoproduktivitätsrekonstruktionen gut mit denen Ergebnissen aus dem östlichen Indischen Ozean überein. Sie lassen auf einen Zustrom warmer, oligotropher pazifischer Wassermassen in den westlichen äquatorialen Indischen Ozean schließen, der auf Schwankungen in der Intensität der Walker-Zirkulation reagiert hat. Die Daten belegen eine auf eine La Niña-ähnliche stärkere Walker-Zirkulation zurückzuführende erhöhte Produktivität von 300 bis 160 ka, während die abnehmende Produktivität von 160 ka bis heutige Folge einer eher El Niño-ähnlichen Phase darstellt. Dieses entspricht jüngsten Modellierungsstudien die auf eine Verlangsamung der Walker-Zirkulation seit dem letzten Jahrhundert deuten, die wiederum zu einem eher El-Niño-ähnlichem Zustand mit einer stärker geschichteten Wassersäule und einer damit verbundenen geringen Produktivität im westlichen Indischen Ozean geführt hat.

CHAPTER 1

General introduction

CHAPTER 1 General introduction

1.1 Coccolithophore biology, morphology and fossil record

Coccolithophores are marine, unicellular flagellate phytoplankton, belonging to phylum Haptophyta and division Prymnesiophyceae (Pienaar, 1994). Together with planktonic foraminifera and pteropods, they are considered the ocean's most important suppliers of calcium carbonate (CaCO_3) in the water column and the seafloor (Bramlette, 1958). They are one of the most abundant phytoplankton groups, holding a vital position at the base of the food chain (Westbroek et al., 1993).

Coccolithophores possess golden-brown chloroplasts, an exoskeleton of calcareous scales (coccoliths) and unique flagella-like structure, the haptonema (Bown, 1998). Their cell surfaces are covered with these coccoliths exhibiting complex morphology (Pienaar, 1994; Young, 1994). The cell is dominated by large chloroplasts responsible for photosynthesis and a nucleus, the location of its genetic material. It is bordered by a multi-layered cell membrane, also identified as the plasmalemma or plasma membrane. Organic scales of haptophytes are distinct, and calcareous scales are unique to them (Young, 1994). These coccoliths offer a variety of possible functions for the coccolithophore cell summarized in **Figure 1.1**.

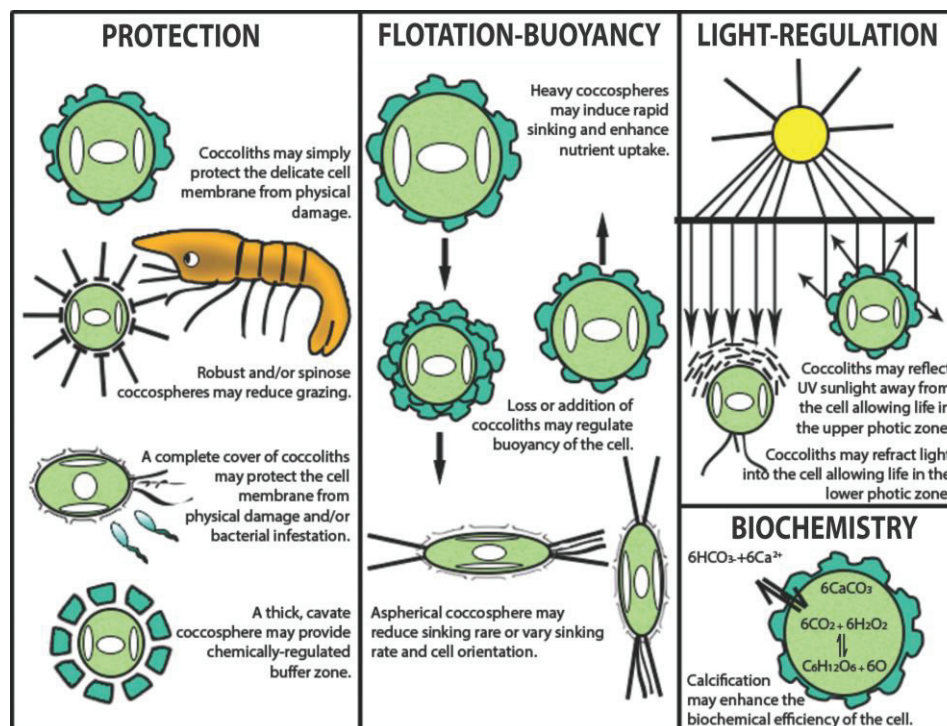


Figure 1.1: Possible functions of coccoliths (redrawn from Bown (1998)).

The highly diverse morphology of coccoliths (and coccospheres) reflects the unique ecological strategies and environmental preferences of different coccolithophore groups (**Figure 1.2**). The particular environment is dominated by characteristic assemblages, which can be distinguished by their coccolith types and coccosphere morphology (Young, 1994). For instance, placolith-bearing species (e.g., *Emiliana huxleyi*) are more often linked to eutrophic conditions in coastal and upwelling environments (**Figure 1.2a**) while umbelliform taxa (e.g., *Umbellosphaera tenuis*) are more adapted to oligotrophic waters of the mid- to low latitude (**Figure 1.2b**). The floriform species *Florisphaera profunda* is typified to dominate assemblage of the deep photic layer whereas the motile group (e.g., *Helicosphaera carteri*) is found in mesotrophic environments (**Figure 1.2c**).

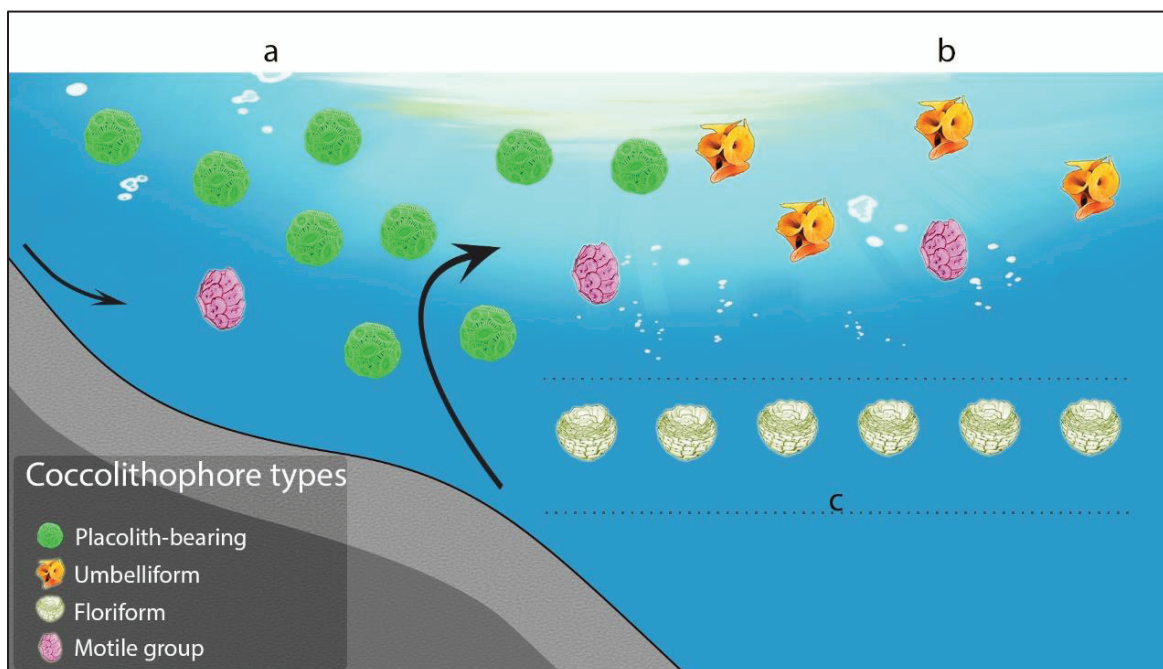


Figure 1.2: Ecological distribution of coccolithophore morphological types (adapted from Young, 1994). Arrows represent the influx of nutrients supplied by river run off and coastal upwelling.

When the coccolithophore organism dies, its calcareous exoskeleton falls to the seafloor as aggregates (i.e., algal aggregates, faecal pellets, marine snow), and preserved in sediments either as disaggregated coccoliths or as partially intact coccosphere. The fossil record of coccolithophores has been remarkably abundant and continuous since their first occurrence in the Late Triassic (230 Ma) (Bralower, 2002), and constituting a major part of deep sea sediments since the Upper Jurassic.

1.2 Coccolithophores and their role in the global biogeochemical cycles

Calcifying haptophytes, such as coccolithophores, play a significant role in the global biogeochemical cycles. These organisms have gained increased attention as they make vital contributions to oceanic primary productivity and play an important role in the carbon dioxide (CO₂)-oxygen exchange between the ocean and the atmosphere. They are peculiar because of their combined effects on both the biological and carbonate pump (e.g., Baumann et al., 1999), playing an important part in the global carbon cycle since the Mesozoic by supplying organic carbon and CaCO₃ to the deep ocean (Hay, 2004) (**Figure 1.3**). For instance, the evolution of pelagic coccolithophores during the Mesozoic era resulted in a shift in global calcification, affecting deep ocean CO₂ budgets, calcite compensation depths and CO₃ turnover rates (Kennett, 1983; Bown, 1998). Moreover, it is estimated that coccolithophores produce approximately 20-60% of marine pelagic carbonate (Winter et al., 1994; Brand, 1994). Baumann et al. (2004) showed that coccolithophore carbonate accounts for 20-80% of biogenic carbonate in the South Atlantic exported from the photic zone to the seafloor, showing that they can be one of the dominant biogenic CO₂ components of deep sea sediments.

Complex relationship between coccolithophores and seawater chemistry exists, and are interconnected via various feedback mechanisms (**Figure 1.3**). In particular, coccolithophores may alter the seawater characteristics through photosynthesis and calcification and in turn, their distribution in the water column is controlled by seawater physical and chemical properties (e.g., Westbroek et al., 1993; Brand, 1994). Large amounts of CO₂ are sequestered by coccolithophores via photosynthesis (particulate organic carbon; POC) and through calcification (particulate inorganic carbon; PIC), the CO₂ is released back to the atmosphere. The ratio between the PIC and POC reflects whether the coccolithophore communities act as a carbon source or as a carbon sink (Rost and Riebesell, 2004).

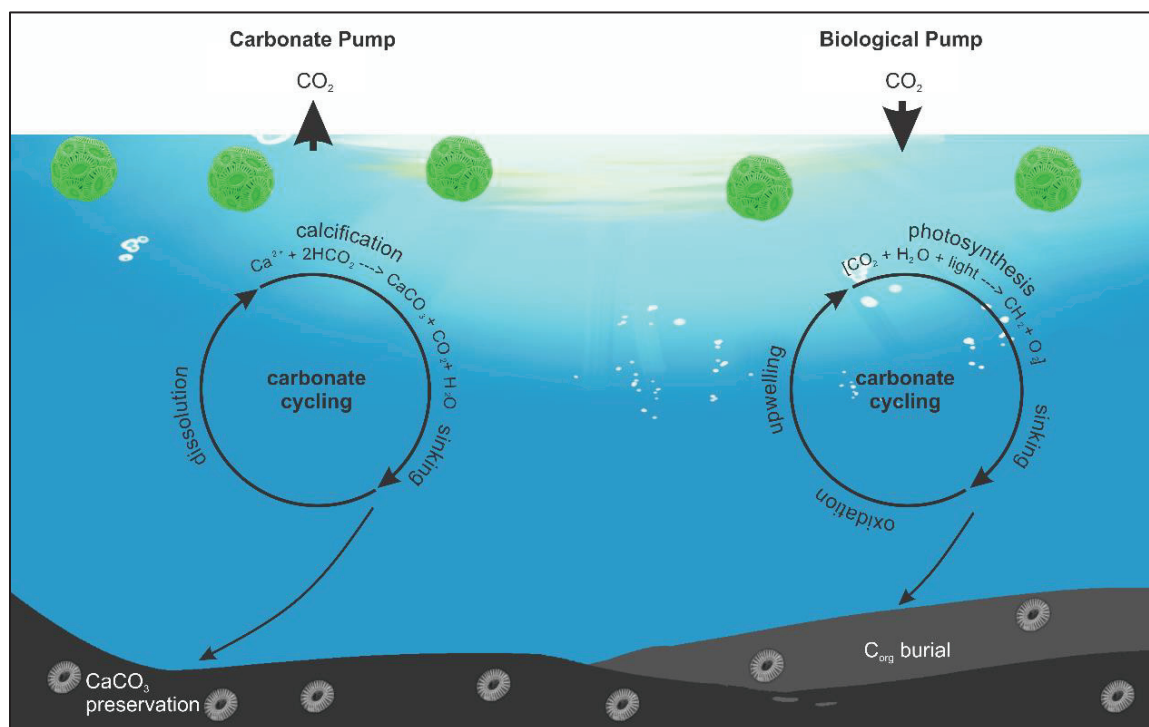


Figure 1.3: Simplified schematic representation of the complex role of coccolithophores in the global carbon cycle, being involved in both biological and carbonate pumps. Figure was modified from Baumann et al. (2004).

1.3 Coccolithophores as paleoenvironmental proxies

Among the components of deep sea sediments, coccolithophores are known to be the most essential organisms providing key floral and biomarker signals for interpreting global change in the geologic record (Baumann et al., 1999; Stoll and Ziveri, 2000). Since coccolithophore distribution in the water column is largely controlled by latitudinal oceanic zonations and frontal system dynamics (McIntyre and Bé, 1967; Bown et al., 2004), their fossil records are useful for understanding the ocean's past environmental and oceanographic conditions. Moreover, their high abundance in deep-sea sediments, widespread distribution, and dynamic evolution make them important proxies for paleoceanographic reconstructions.

Coccolithophores are used as indicators for reconstructing past variations in the nutricline and therefore record productivity changes in the water column. High abundances of LPZ flora are associated with a deeper nutricline while its low abundances indicate enhanced surface water productivity. Three possible scenarios of coccolithophore response to variations in nutricline depth in the investigated area driven by physical

processes in the water column are summarized in **Figure 1.4**. In a stratified water column, surface water is depleted with nutrients; nutricline is deeper, which is favourable for the LPZ taxa (**Figure 1.4a**). On the other hand, the influx of nutrients from a localized source, such as lateral advection of nutrients to a stratified water column (**Figure 1.4b**) and mixing driven by winds (**Figure 1.4c**) could enhance productivity at the surface and increase abundance of the UPZ flora.

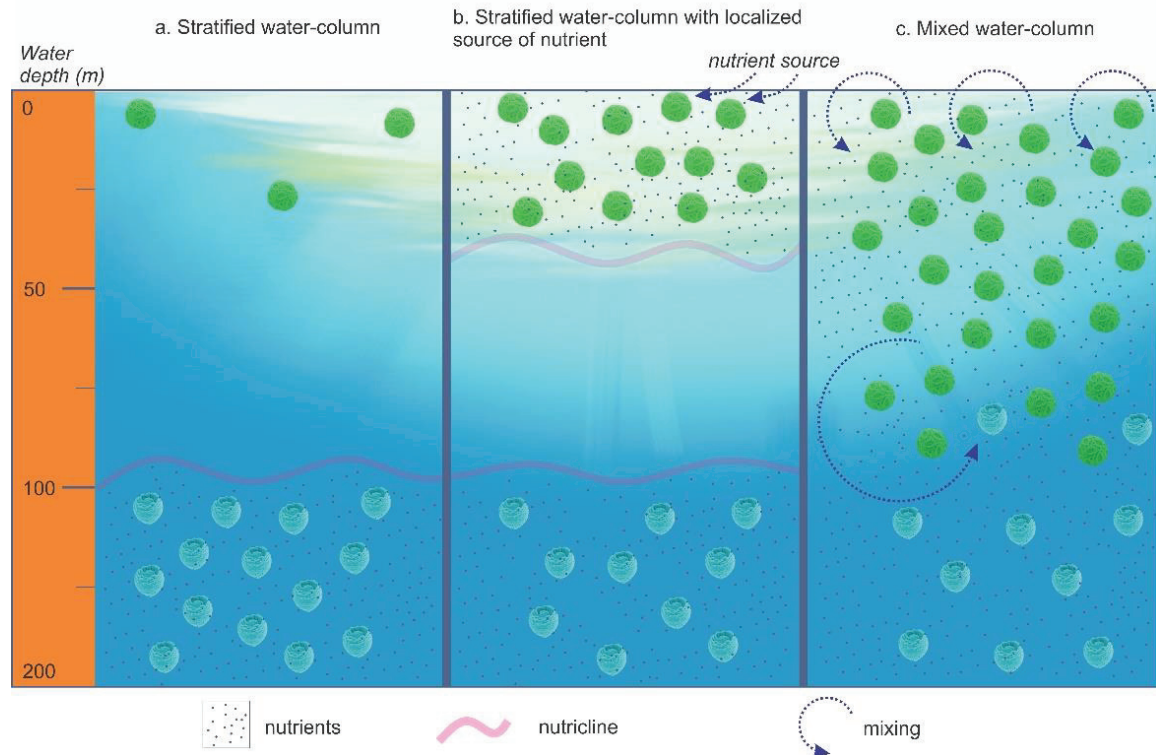


Figure 1.4: Hypothetical scenarios of coccolithophore response to nutrient availability driven by physical processes in a non-upwelling region of the western Indian Ocean.

1.3.1 Coccolithophore assemblage

Previous studies have already proven the utility of coccolithophores in understanding the paleoceanography of the world's oceans (e.g., Winter et al., 1994; Young, 1994; Brand, 1994). In particular, numerous studies relating their abundance to productivity have been conducted (e.g., Okada and Honjo, 1975; Beaufort, 1996; Flores et al., 1999; Mejia et al., 2014). Generally, coccolithophores are known to be well-adapted to oligotrophic conditions, and to proliferate in warm and stable surface waters. However, certain coccolithophore species may have other individual ecological preferences. Their abundance and distribution reflect water column characteristics and processes (**Table 1.1**).

This peculiarity in some species makes them particularly useful for detailed paleoenvironmental reconstructions.

One particular species is the lower photic zone (LPZ)-dwelling taxon *F. profunda*, which thrives in areas where nutrients are comparatively abundant and light is limited (Okada and Honjo, 1975). Its dominance in the water column indicates a deep nutricline, low total primary production (Molfinio and McIntyre, 1990) and less turbid waters (Ahagon et al., 1993). For this reason, this species has been proposed by several authors as an efficient low productivity indicator in Quaternary sediments (e.g., Molfinio and McIntyre, 1990; Ahagon et al., 1993; Beaufort et al., 2003). Alternatively, an increase in the abundance of the upper photic zone (UPZ) species (e.g., *Emiliana huxleyi*, geophyrocapsids) is a characteristic of shallow nutricline and often associated to enhanced productivity.

In the Plio-Pleistocene assemblages, the extinct genus *Discoaster* has been used as an indicator of sea surface temperature (SST; Backman and Pestiaux, 1987) although later studies suggested that those fluctuations were not associated to temperature alone (e.g., nutrients (Chepstow-Lusty et al., 1989; Chapman and Chepstow-Lusty, 1997). Paleorecords of the discoasters also demonstrated orbital cyclicity that are at paced with the 23, 41 and 100 kyr periodicities (e.g., Backman et al., 1986; Backman and Pestiaux, 1987; Chepstow-Lusty et al., 1989; Gibbs et al., 2004). Other coccolithophore taxa that have been suggested to be useful for paleoecological reconstructions of Plio-Pleistocene sediments are *Coccolithus pelagicus* (indicator of cool, high salinity waters), *Helicosphaera* spp. (high productivity, low salinity), *Rhabdosphaera* spp. (warm, low productivity), and *Syracosphaera* spp. (high salinity) (Pujos, 1992).

Table 1.1: Ecological preferences of Pliocene to Recent indicative species recorded in the study area in comparison to other studies conducted in other locations.

Genus/ Species	Warm	Temperate	Cool	Oligotrophic	Meso/eutrophic	This Study
<i>C. leptoporus</i>	7, 14, 18, 22		8		8, 11	warm, meso/eutrophic
<i>C. pelagicus</i>		22	11, 13, 14, 19			inconclusive occurrence (could be nutrient- enrichment or excursion taxa)
<i>Calcosolenia</i> spp.; <i>Oolithothus</i> spp.;	26		26			warm, oligotrophic
<i>R. clavigera</i> ; <i>U. foliosa</i>				24, 27		warm, oligotrophic
<i>Discoaster</i> spp.						
<i>E. huxleyi</i>	7, 18		10, 12	2	10, 11, 12, 14, 15	ubiquitous
<i>F. profunda</i>				6, 9, 11, 15, 21		oligotrophic, stable water column
<i>G. caribbeanica</i>			14	16	22	meso/eutrophic
<i>G. ericsonii</i>	7, 18, 22				11, 15, 14	ubiquitous
<i>G. muelleriae</i>			4, 16, 17, 25			cool, excursion taxa
<i>G. oceanica</i>	7, 8, 11, 18, 22				11	warm, meso/ eutrophic
<i>H. carteri</i>	11,17				8	warm, meso/ eutrophic
<i>R. minuta</i>					11, 15	meso/eutrophic
<i>S. hystrix</i> ; <i>S. pulchra</i>	4, 8, 18, 26		4, 23, 26		11	warm, oligotrophic
<i>U. irregularis</i> ; <i>U. tenuis</i>	26			1, 11, 20, 23, 26		warm, oligotrophic
<i>U. sibogae</i>	7, 18, 22, 26	5	14	8, 26	3, 11	oligotrophic

¹Horjio and Okada, 1974; ²Okada and Honjo, 1975; ³Roth and Berger, 1975; ⁴Jordan et al., 1996; ⁵Okada and McIntyre, 1979; ⁶Molfinio and McIntyre, 1990; ⁷Winter and Martin, 1990; ⁸Giraudeau, 1992; ⁹McIntyre and Molfinio, 1996; ¹⁰Brand, 1994; ¹¹Winter et al., 1994; ¹²Young, 1994; ¹³Samtleben et al., 1995; ¹⁴Wells and Okada, 1996; ¹⁵Beaufort et al., 1997; ¹⁶Bollman, 1997; ¹⁷Okada and Wells, 1997; ¹⁸Flores et al., 1999; ¹⁹Baummann et al., 2000; ²⁰Kinkel et al., 2000; ²¹Beaufort et al., 2001; ²²Baummann and Freitag, 2004; ²³Baummann et al., 2004; ²⁴Gibbs et al., 2004; ²⁵Giraudeau et al., 2010; ²⁶Marino et al., 2014; ²⁷Schuetth and Bralower, 2015.

1.3.3 Coccolithophore-based geochemical proxies

Coccolithophores are among the marine organisms that provide proxies for paleoceanographic reconstructions from both organic and inorganic fossil records (Stoll and Ziveri, 2004 and references therein). Particular organic biomarkers, i.e., alkenones, which are produced by a specific/small-sized group of coccolithophores (e.g., *E. huxleyi* and *Gephyrocapsa oceanica*) has emerged as an important proxy of past SST and productivity (Brassell et al., 1986; Müller et al., 1998), as well as of atmospheric CO₂ concentrations (Jasper and Hayes, 1990). Additionally, elemental chemistry of the inorganic constituent coccoliths offers a unique signal for past variations in coccolithophore productivity (Stoll and Schrag, 2000). In particular, the coccolith fraction (CF; < 20µm) Sr/Ca is a well-developed proxy, which reflects coccolithophore growth rates and therefore documents variations in coccolithophore production independent of any coccolith counting (Stoll et al., 2002a). The increase in CF Sr/Ca was recorded at higher nutrient-regulated growth rates in culture experiments, sediment core tops and sediment trap records and in long climate archives (e.g., Rickaby et al., 2002; Stoll et al., 2002a; Stoll et al., 2007). Furthermore, high CF Sr/Ca ratios have been reported to occur in nutrient-rich conditions where the CF Sr/Ca parallels productivity trend (Stoll and Schrag, 2000; Stoll et al., 2007). Studies from the Indian and the Pacific oceans (Rickaby et al., 2007) and the North Atlantic (Barker et al., 2006) also revealed maximum CF Sr/Ca values coinciding with the overwhelming abundance of *G. caribbeanica* during MIS 11. A recent study by Saavedra-Pellitero et al. (2017) also recorded positive correlation between coccolith accumulation rates and CF Sr/Ca in the Southern Ocean, showing peaks in coccolithophore productivity.

1.4 The study area

Warm and oligotrophic surface waters of the Indonesian Throughflow (ITF) enter the study area in the western tropical Indian Ocean (GeoB12613-1) via the South Equatorial Current (SEC; **Figure 1.5**). The SEC flows westward year-round across the Indian Ocean and splits into two western boundary currents (Northeast and Southeast Madagascar Currents; NEMC and SEMC) off the coast of Madagascar (Schott et al., 2009). The NEMC flows toward the north tip of Madagascar and breaches into northward and southward flows. The northward current feeds the northward-flowing East African Coastal Current (EACC), the

prevailing current off Tanzania (GeoB12613-1). Surface waters off Tanzania are relatively oligotrophic year round although a slight increase in phytoplankton productivity can be observed during summer (Lévy et al., 2007; Koné et al., 2013). Extant coccolithophore assemblages in this location are characterized by the dominance of *G. oceanica* in the Pemba Channel and *U. irregularis* in the open ocean (Stolz et al., 2015). The dominance of *G. oceanica* in the Pemba Channel was attributed to the enhanced nutrient availability in the region supplied by the Pangani River or by the lateral advection of nutrient-rich upwelled water of the Somali Current (SC) during the winter, when SC reverses direction and flows southward. The warm, oligotrophic and stratified water of the open ocean, on the other hand promotes the abundance of *U. irregularis* in the UPZ and *F. profunda* in the LPZ.

The southward flow of the NEMC, on the other hand merges with the Mozambique Channel throughflow to form a set of anticyclonic eddies (Schott and McCreary, 2001; Schouten et al., 2003), affecting Site U1476 (Mozambique Channel). In contrast to the area off Tanzania, the Mozambique Channel is one of the most turbulent areas of the world ocean (Ternon et al., 2014) and characterized by a complex surface water circulation (Hall et al., 2016). The formation of mesoscale anti-cyclonic eddies in the channel (Schouten et al., 2003; Biastoch et al., 2009) and its southward flow may have major implications in the Agulhas Current system.

The Agulhas Current system is the strongest western boundary current, responsible for transporting warm and saline waters to the South Atlantic (Lutjeharms, 2006). It is an integral part of the global thermohaline circulation as it acts as a potential modulator of the Atlantic Meridional Overturning Circulation (AMOC) (e.g., Knorr and Lohmann, 2003; Biastoch et al., 2009). Hence, it has major implications on the climate of the surrounding continents and the global climate system. Two types of extant coccolithophore assemblages were identified by Friedinger and Winter (1987) in this region: the Agulhas Current assemblage, which is dominated by *E. huxleyi* and *G. ericsonii*, and the Agulhas Return Current assemblage, which is characterized by abundant *G. oceanica*. The distribution of the assemblages in the area was interpreted by these authors to be driven by the contrasting oceanographic regimes between the relatively stable Agulhas Current and the more dynamic Agulhas Return Current.

Further downstream, the Natal Valley (MD96-2077) is influenced by the highly dynamic Agulhas Current region and within the influence of the Agulhas Return Current, a component of the Agulhas Current that retroflects and does not leak to the South Atlantic. The Agulhas Current flows around the southern tip of Africa, where warm and saline surface waters are transported to the South Atlantic via shedding of large rings and eddies (Agulhas leakage) from the Agulhas retroflexion area, south of the African continent.

The warm water route of the Agulhas Current continues to the South Atlantic where ODP Sites 1264/1266 are located. Here warm and oligotrophic surface waters from the Indian Ocean and the South Atlantic Gyre are transported to the North Atlantic by the SEC. The two study sites in the South Atlantic could potentially be bathed by the nutrient-rich upwelling waters of the Benguela Current. Previous studies in this region suggested influence of the Benguela Current on the coccolithophore assemblage and distribution (e.g., Giraudeau, 1992; Baumann et al., 2004; Baumann and Freitag, 2004; Boeckel and Baumann, 2004). Enhanced coccolithophore productivity was associated with reduction in upwelling intensity (Baumann et al., 2004), reflecting that coccolithophore communities were dependent on the phase of the upwelling cycle (Giraudeau et al., 1993; Giraudeau and Bailey, 1995). A detailed description of the hydrography of the investigated regions can be found in the respective manuscript chapters.

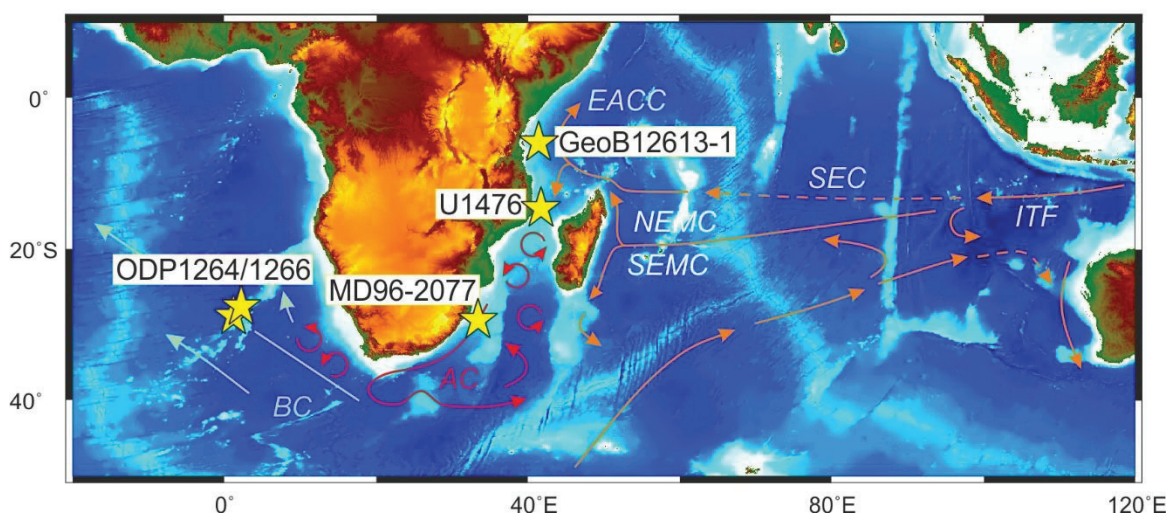


Figure 1.5: Map of the study area showing site locations of the investigated sediments (yellow stars) for this research. The arrows represent the main surface ocean currents adapted from Hall et al. (2016): Indonesian Throughflow (ITF), South Equatorial Current (SEC), East Africa Coastal Current (EACC), North East Madagascar Current (NEMC), South East Madagascar Current (SEMC), Agulhas Current (AC), and Benguela Current (BC).

1.5 Objectives of the thesis

This Ph.D. thesis deals with the investigation of deep sea sediments from the tropical Indian Ocean and the South Atlantic in order to decipher climatic variations and associated changes in productivity, focusing on two time windows, the late Pleistocene to Holocene (500 to 0 kyr) and the Late Pliocene to the early Pleistocene (2.85 to 1.85 Myr) using coccolithophore-based proxies. Knowledge on the coccolith preservation, assemblage composition, distribution patterns of individual coccolithophore species, and stable isotopes and Sr/Ca measured on the coccolith fraction provide a robust groundwork for an accurate productivity reconstruction.

Here we reconstructed and characterized productivity changes in the study area based upon these proxies and relate these parameters to astronomical and orbital variations (insolation, glacial-interglacial, orbital periodicities) and to short term atmospheric and oceanographic variations (monsoons, Walker Circulation, subtropical front migration). Being situated within the reaches of two important current systems, the Agulhas Current and the Benguela Current, the core locations for this research offer an exceptional opportunity for high-resolution climate reconstructions. The strategic position of the study sites (**Figure 1.5**) provides an ideal scenario in tracing the route of the Indonesian Throughflow surface waters, which transport heat and salt to the western Indian Ocean and the South Atlantic. In addition, it is well-suited to obtain a comprehensive paleoproductivity overview of the investigated area.

With this in mind, major emphasis was given to the following research questions, which are addressed in the succeeding manuscripts:

1. Is it possible to identify the inter-annual modes of the Walker Circulation (i.e., Indian Ocean Dipole and El Niño Southern Oscillation) in the coccolithophore paleorecord from the western tropical Indian Ocean (off Tanzania)? What triggered the climatic variability (e.g., monsoon, orbital changes, glacial/interglacial cyclicity)?
2. How did the migration of the subtropical front and/or movement of the Southern Hemisphere westerlies affect the nutricline/thermocline depths off South Africa over the past glacial/interglacial cycles? How did the individual coccolithophore taxa respond to these variations in the nutricline/thermocline depths?

- Discoasters are typified to have an affinity for warm water and oligotrophic conditions. Can their extinction towards the end of the warm Pliocene reveal important environmental scenarios during the Plio-Pleistocene transition? What was the impact of the global climatic cooling to the coccolithophore productivity in the tropical Indian Ocean during the end of the Pliocene?

The above-mentioned research questions were addressed with a calibrated coccolithophore-based productivity reconstruction using long climate archives collected from the western Indian Ocean and the South Atlantic. Results from this study were correlated to existing coccolithophore data from other regions and to other proxies (e.g., planktonic foraminifera, sediment geochemistry, magnetic susceptibility) in order to have a broad overview of the past productivity conditions in the investigated region.

1.6 Materials and analytical techniques

Sediment cores investigated in this study were retrieved from the southwestern Indian Ocean and the southeast Atlantic Ocean during four different oceanographic expeditions (**Table 1.2**).

Table 1.2: Geographic locations and water depths of the sediments used for this study.

Cruise	Core/Site	Location	Coordinates (Lat/Long)	Water depth (m)
Meteor 2008	GeoB12613-1	off Tanzania	05°29'S; 40°56'E	2292
IMAGES-2	MD96-2077	Natal Valley	33°10'S; 31°15'E	3781
ODP Leg 208	ODP 1264	Walvis Ridge	28°32'S; 02°51'E	2505
ODP Leg 208	ODP 1266	Walvis Ridge	28°33'S; 02°21'E	3798
IODP Exp. 361	U1476	Mozambique Channel	15°49'S; 41°46'E	2166

The materials analyzed are described in detail in the respective sections in the manuscripts. Preparation of samples for coccolithophore assemblage analysis followed the combined dilution/filtering technique of Andrleit (1996) for scanning electron microscopy (SEM) and Bordiga et al. (2015) for light microscopy. Coccolith Sr/Ca measurements performed in cores GeoB12613-1 and ODP Site 1264/1266 followed the protocol for

sample cleaning described in Stoll and Ziveri (2002) and Fink et al. (2010). **Figure 1.6** summarizes the workflow of this research, including data analysis. All the data presented in this thesis are available/will be in the PANGAEA database (www.pangaea.de).

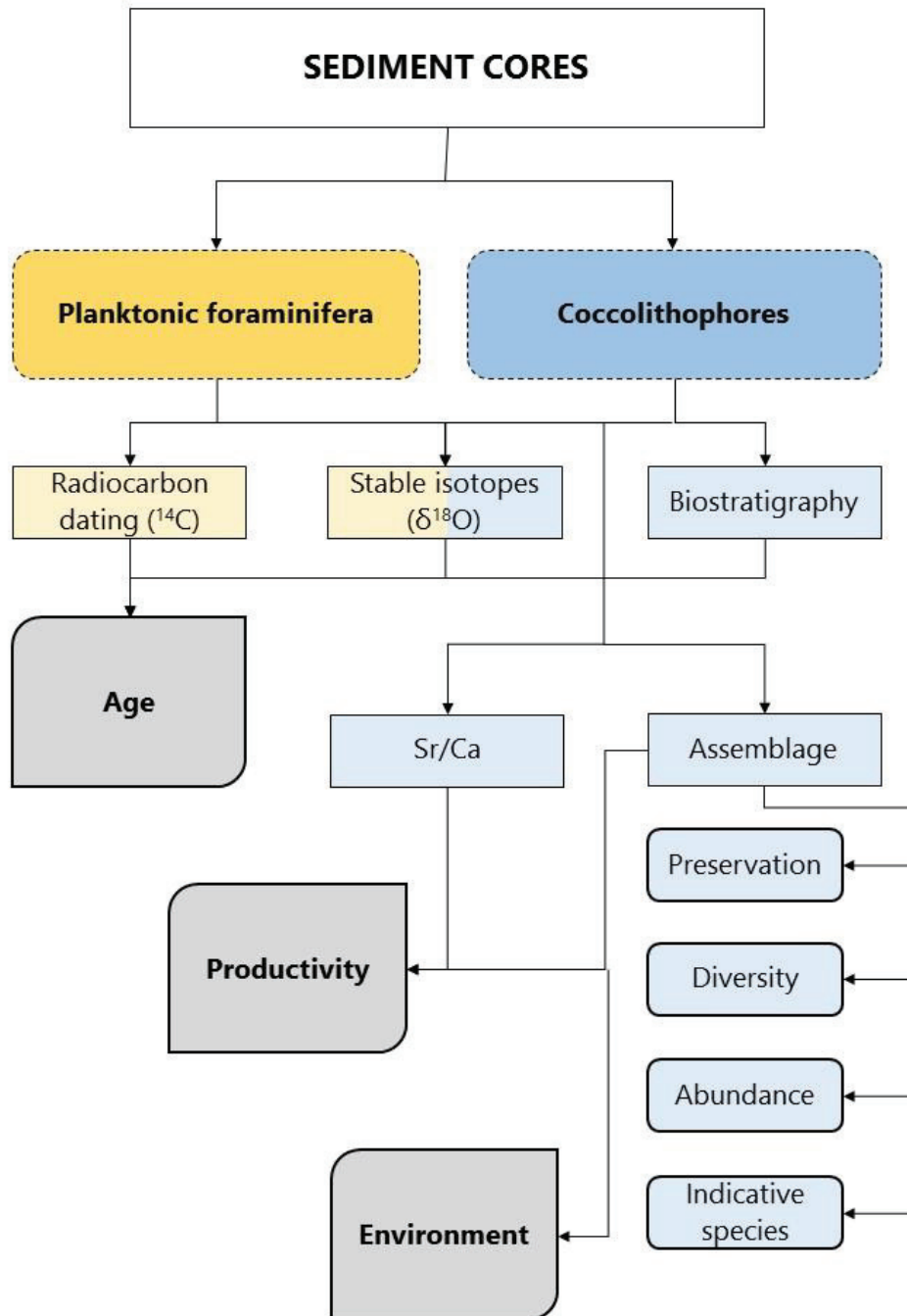


Figure 1.6: Flowchart of all the analyses performed.

1.7 Outline of the thesis

This Ph.D. thesis was carried out from November 2014 to October 2017 at the Faculty of Geosciences, University of Bremen, Germany. The project is part of the MARUM – Center for Marine Environmental Sciences-funded research in the area of micropaleontology and paleoclimate studies in the framework of the project, “Land-ocean interaction and climate variability in low latitudes”. The central theme of this research deals with the investigation of sediment cores from the western Indian Ocean and the South Atlantic to decipher climatic variations and associated changes in productivity from the Late Pliocene to the Holocene by using coccolithophore-based proxies. Results of this thesis are presented in the succeeding three chapters (Chapters 2, 3, and 4), which correspond to manuscripts published in, submitted, or to be submitted to international peer-reviewed journals. To minimize duplication, references have been removed from each manuscript and are cited in a single reference list at the end of this dissertation (see [References](#)), together with references from Chapters 1, 5 and 6.

Below are the three manuscripts from this Ph.D. work:

Manuscript 1. **Insolation forcing of coccolithophore productivity in the western tropical Indian Ocean over the last two glacial/interglacial cycles** (Paleoceanography 32/ <https://doi.org/10.1002/2017PA003102>)

Deborah Tanguan, Karl-Heinz Baumann, Jürgen Pätzold, Rüdiger Henrich, Michal Kucera, Ricardo De Pol-Holz, and Jeroen Groeneveld

Core GeoB12613-1 recovered off the coast of Tanzania, East Africa, retrieved at 2292 m water depth during the 2008 R/V Meteor Cruise was investigated for this manuscript. The paper focused on the drivers of coccolithophore productivity in the study area over the past 300 kyr. Result of the study show that the dominance of the LPZ-dwelling species *F. profunda*, indicate a prevalent regime with deep thermocline and low surface productivity throughout the investigated time period. The existence of an analogous to the present-day El Niño Southern Oscillation and Indian Ocean Dipole events operating on longer timescales is proposed. A La Nina-like state of the Walker Circulation from 300 to 160 kyr and a more El Nino-like state of the Walker Circulation are recorded from 160 kyr to the Holocene. The manuscript is published in *Paleoceanography* journal.

Manuscript 2. **Variations in coccolithophore productivity off South Africa over the last 500 kyr** (submitted to Quaternary Science Reviews)

Deborah Tanguan, Karl-Heinz Baumann, and Christina Fink

Here we present a 500 kyr assemblage- and geochemistry-based coccolithophore productivity record of the southwest Indian Ocean (MD96-2077) and the eastern South Atlantic Ocean (ODP Site 1264/1266) to decipher the role of the subtropical front migration (STF) on the coccolithophore abundance and distribution in both oceans. This study documents how the STF have influenced the Agulhas Current in the Indian Ocean and the Benguela Current in the South Atlantic, and how these affect the coccolithophore communities in the investigated regions. We compared our results with other paleoceanographic data within the region to correlate the coccolithophore-based signals from our record with the widely known paleoceanographic events. Being located near the upper border of the well-established Agulhas Current and within the influence of the Benguela Current, our two study areas are ideal locations for reconstruction of the Agulhas warm-water transport, and its association with the shifts in the subtropical front and the Southern Hemisphere westerlies. The paper was submitted to *Quaternary Science Reviews*.

Manuscript 3. **The last 1 million years of the extinct genus *Discoaster*: Plio – Pleistocene environment and productivity at Site U1476 (Mozambique Channel)** (in preparation for *Palaeogeography, Palaeoclimatology, Palaeoecology*)

Deborah Tanguan, Karl-Heinz Baumann, Janna Just, Stephen Barker, Ian Hall, Sidney Hemming, Leah LeVay and Richard Norris

This paper used Site U1476 sediments collected during the IODP Expedition 361-Southern African Climates, focusing on the Plio-Pleistocene interval (2.85 to 1.85 Myr). New productivity data were obtained from the abundances of the last five *Discoaster* species (*Discoaster brouweri*, *D. triradiatus*, *D. pentaradiatus*, *D. surculus*, and *D. tamalis*), before their complete disappearance from the geologic record. Results were compared to the total assemblage composition, particularly *F. profunda*, a known and widely used productivity proxy and to other coccolithophore taxa with unique ecological preferences. In addition, a detailed late Pliocene-Early Pleistocene nannofossil biostratigraphy was

established. The paper is in preparation and will be submitted to *Palaeogeography*, *Palaeoclimatology*, *Palaeoecology*.

1.8 Declaration of co-author contribution

This cumulative thesis comprises three joint-authorship manuscripts that were/will be published as peer-reviewed articles. The manuscripts were developed in close cooperation with the co-authors.

I confirm that I designed this research and all three manuscripts, with input from my supervisors Rüdiger Henrich and Karl-Heinz Baumann. I performed the microscope work, processed and analyzed all generated data, created all figures and tables, and wrote all sections of the manuscripts, with beneficial reviews and input from all the co-authors. Carbon-14 and $\delta^{18}\text{O}$ planktonic foraminifera isotope data for Manuscript 1 were provided by Jeroen Groeneveld and Jürgen Pätzold, respectively. For manuscript 2, microscopy for ODP Site 1266 was done by Karl-Heinz Baumann while coccolith stable isotope and Sr/Ca data were provided by Christina Fink. I used the Expedition 361 shipboard calcareous nannofossil stratigraphy and paleomagnetic data for Manuscript 3. (*Personal contribution to manuscripts: Manuscript 1 – 80%; Manuscript 2 – 70%; Manuscript 3 – 80%*).

CHAPTER 2

Insolation forcing of coccolithophore productivity in the western tropical Indian Ocean over the last two glacial/interglacial cycles

Paleoceanography (Tangunan et al., 2017)

CHAPTER 2

Insolation forcing of coccolithophore productivity in the western tropical Indian Ocean over the last two glacial/interglacial cycles

Deborah Tanguan¹, Karl-Heinz Baumann^{1,2}, Jürgen Pätzold^{1,2}, Rüdiger Henrich^{1,2}, Michal Kucera¹, Ricardo De Pol-Holz³, Jeroen Groeneveld¹

¹University of Bremen, MARUM - Center for Marine Environmental Sciences, Leobener Straße, 28359 Bremen, Germany; ²University of Bremen, Faculty of Geosciences, Klagenfurter Straße, 28359 Bremen, Germany; ³Universidad de Magallanes, Centro de Investigación GAIA-Antártica, Av. Bulnes 01855, 621-0427 Punta Arenas, Chile

2 Abstract

We present a new coccolithophore productivity reconstruction spanning the last 300 kyr in core Geob12613-1 retrieved from the western tropical Indian Ocean, an area that mainly derives its warm and oligotrophic surface waters from the eastern Indian Ocean. Application of a calibrated assemblage-based productivity index indicates a reduction in estimated primary productivity (EPP) from 300 kyr to the present, with reconstructed EPP values ranging from 91 to 246 g C/m²/yr. Coccolithophore assemblages and coccolith fraction Sr/Ca indicate three main phases of productivity change, with major changes at 160 and 46 kyr. The productivity and water column stratification records show both dominant precession and obliquity periodicities, which appear to control the paleoproductivity in the study area over the last two glacial/interglacial cycles. Shallowing of the thermocline due to strengthening of the trade winds in response to insolation maxima resulted to peaks in EPP. Comparison with the eastern Indian Ocean productivity and stratification coccolithophore data reveals good correspondence with our records, indicating a strong tropical Pacific influence in our study area. Both of these records show high productivity from 300 to 160 kyr, interpreted to be due to stronger Walker Circulation while the declining productivity from 160 kyr to the present day is a consequence of its weakening intensity.

2.1 Introduction

The tropical Indian Ocean (IO) plays an important role in shaping both the regional and global climates as it constitutes the main part of the biggest warm pool on Earth (Schott et al., 2009) and returns warm and saline surface waters to the Atlantic via the Agulhas Current (Piotrowski et al., 2009). Relative to other oceans, such as the Pacific and Atlantic, the IO is situated in a unique geographic location. The Asian continent in the north of the IO blocks the northward heat export, enables weak north thermocline ventilation, and drives the strong Asian Monsoon (Schott et al., 2009). The Indonesian Archipelago located in the east, allows water exchange with the Pacific Ocean, the only inter-ocean passage at modern low latitudes (Naqvi, 2008; Schott et al., 2009). For these reasons, a growing interest on the role of the IO in climate variability has resulted to a significant increase in high-resolution studies of marine records (e.g., Prell and Kutzbach, 1992; Beaufort, 1996; Rogalla and Andruleit, 2005; Andruleit et al., 2008; Bard and Rickaby, 2009; Mohtadi et al., 2010; Bolton et al., 2013; Wang et al., 2013; Rippert et al., 2015). Most of these studies are focused on the monsoon-influenced northern IO, the equatorial IO, and the eastern equatorial upwelling area off Java, Indonesia. So far, the western tropical region, including the present study area is relatively less explored. Moreover, our current understanding of the forcing mechanisms driving the IO circulation is still limited although a number of modelling studies exist (e.g., Xie et al., 2002; Schott et al., 2009), and knowledge about the variability of seasonal winds over the rest of the IO is scarce, especially in areas where seasonal contrasts are less pronounced.

By contrast to the northern IO, characterized by seasonally reversing monsoon winds, the equatorial IO is influenced by the semi-annual inter-monsoon trade winds (Indian Ocean equatorial westerlies; IEW). This feature was particularly exemplified in a study by Beaufort et al. (1997) where they suggested the IEW to be the primary driver of productivity in the equatorial IO and further relating the IEW to the Southern Oscillation. The strong IEW, which blow from May to June generate mixing of the surface water resulting in the shallowing of the thermocline, which enhances the modern primary productivity in the Maldives. In the tropics, the thermocline depth is generally governed by physical processes in the ocean such as the strength of wind-driven mixing, upwelling intensities, and solar radiation power related to seasons and orbital forcing (Bolton et al., 2013). Primary

productivity in the oligotrophic tropical ocean can be dependent on the availability of nutrients from deeper waters (Su et al., 2015). Recently, a study by Rippert et al. (2015) in the western tropical IO (WTIO) using planktonic foraminifera off Tanzania suggested that the depth of the thermocline was shallower during the glacial and deeper during the Holocene. This variation was explained as a result of increased inflow of the Southern Ocean intermediate waters via “ocean tunnels” that appear to cool the thermocline from below. Since such thermocline variations are closely connected to changes in the nutricline, and therefore to productivity variations, phytoplankton productivity reconstructions can be used to entirely independently constrain the hypothesized past thermocline dynamics. Additionally, since productivity in many oceanic areas responds to wind stress, paleoproductivity reconstructions can also provide evidence on the past climatic conditions (e.g., Beaufort, 1996).

A commonly used tool to reconstruct changes in the past productivity are coccolithophores. Coccolithophores are minute marine phytoplankton considered to be important contributors to marine primary productivity (Winter et al., 1994). They play a key role in the oceanic biogeochemical cycles as they are involved in both photosynthesis (biological pump) and biomineralization (carbonate pump) (e.g., Baumann et al., 1999). These organisms are sensitive to changes in temperature, salinity, nutrient availability, among other factors, making them important tools for paleoenvironmental reconstructions (e.g., Kinkel et al., 2000; Baumann et al., 2004; Rogalla and Andruleit, 2005; Andruleit et al., 2008). In equatorial regions, transfer functions based on records of *Florisphaera profunda*, a lower photic zone (LPZ)-dwelling species characteristic of a deep nutricline were successfully used as proxies of past nutricline/thermocline variability (e.g., Molfino and McIntyre, 1990; Ahagon et al., 1993; Flores et al., 1999) and for marine primary production (e.g., Beaufort et al., 1997; Beaufort et al., 2001). Coccolithophores are prominent components of the IO phytoplankton communities and their calcite remains (coccoliths) form a major part of the IO deep-sea sediments (e.g., Beaufort et al., 1997; Beaufort et al., 2001; Rogalla and Andruleit, 2005; Andruleit et al., 2008).

Over the past decades, a number of paleoproductivity reconstructions based on coccolithophore assemblages have been conducted in the eastern tropical IO (ETIO) (e.g., Andruleit, 2007; Andruleit et al., 2008; Bolton et al., 2013) and the northern IO region (e.g., Beaufort, 1996; Beaufort et al., 1997), especially in the Arabian Sea (e.g., Broerse et al., 2000;

Rogalla and Andruleit, 2005) where productivity is controlled by monsoons. Rogalla and Andruleit (2005) showed that coccolithophore productivity variations in the northern Arabian Sea over the last 225 kyr were primarily controlled by changes in the IO summer monsoon and that the winter monsoon played a minor role in the productivity history of the area. On the other hand, productivity was found to be higher during glacial episodes in the more open ocean region of the IO, where the winter monsoon winds drive upwelling or vertical mixing (e.g., Beaufort, 1996; Beaufort et al., 1997). A sediment core taken in the equatorial IO, off the Maldives, for instance showed high amplitude change in primary production based on *F. profunda* relative abundances over the last 910 kyr, suggesting a direct control on productivity in the equatorial oceanic system by insolation forcing (Beaufort et al., 1997).

However, most of these previous productivity reconstructions were mainly based on coccolithophore assemblage composition and abundances of specific productivity indicator species. In addition to these assemblage-based proxies, Stoll and Schrag (2000) introduced the strontium/calcium ratio (Sr/Ca), a proxy that is used to record past changes in coccolith production independent of any coccolith assemblage counts (Stoll et al., 2007). The Sr/Ca is a well-developed proxy reflecting coccolith growth rates and thus interpreted to record variations in coccolith carbonate production (Stoll et al., 2002a). This new method resulted in a number of paleoenvironmental reconstructions in the recent decades, exploring geochemical compositions in the coccolith fraction (e.g., Stoll and Schrag, 2000; Rickaby et al., 2002; Stoll et al., 2002a; Stoll and Ziveri, 2002; Stoll et al., 2007; Bolton and Stoll, 2013; Mejia et al., 2014; Bolton et al., 2016; Saavedra-Pellitero et al., 2017).

In this paper, we present a new 300 kyr paleoproductivity record of the WTIO based on coccolithophores, aiming to assess the dominant factors that control their abundance and distribution. We provide a comprehensive multiproxy productivity overview of the region, including assemblage composition and coccolith fraction (CF) Sr/Ca of the same samples analysed for coccolith assemblage. Being located in a currently oligotrophic setting in the westernmost equatorial region of the IO, core GeoB12613-1 allows us to explore the paleoceanographic potential of coccolithophores in deciphering the paleoproductivity of the area over the last two glacial/interglacial cycles. This location also offers an exceptional opportunity to investigate the changes in productivity with likely links to the Indonesian Throughflow (ITF) development in the ETIO, which could further provide

information on the Indo-Pacific teleconnection and contribute to a better understanding of the ocean-atmosphere interactions across the IO during the late Quaternary, related to the Walker Circulation.

2.2 Atmospheric circulation and oceanographic setting

The surface water circulation of the WTIO is governed by the seasonally reversing monsoon winds (Schott and McCreary, 2001) (**Figure 2.1**). The dominant surface current in the region is the South Equatorial Current (SEC) sourced from the warm and oligotrophic waters of the ITF and from upwelled waters south of the equator that originated from the Sub-Antarctic zone (Sub-Antarctic Mode Water; SAMW). The SEC flows westward year-round across the IO and splits into two western boundary currents (Northeast and Southeast Madagascar Currents; NEMC and SEMC) off the coast of Madagascar (Schott et al., 2009). The NEMC flows toward the north tip of Madagascar and the coast of Tanzania and breaches into northward and southward flows. The northward current feeds the northward-flowing East African Coastal Current (EACC), the prevailing current in the study area while the southward current merges with the Mozambique Channel throughflow forming a set of anticyclonic eddies (Schott and McCreary, 2001; Schouten et al., 2003). The EACC feeds the northward-flowing Somali Current (SC), appearing as a set of eddies and gyres (Schott et al., 2009; Beal et al., 2013). The strongest upwelling phenomenon occurs during the summer monsoon when the SC turns offshore at 4°N causing a strong Ekman transport away from the East African shore (Schott et al., 2009), however the SC does not reach our core location at 5°S. Warm, moist air prevails during this period and a strong southwesterly wind jet traverses obliquely across the Arabian Sea causing a clockwise upper ocean circulation pattern with the SEC and the EACC (Schott and McCreary, 2001). The wind-driven upwelling of nutrient-rich deeper waters leads to the enrichment of the surface waters, which fuels phytoplankton growth, especially off the Somalia coast. This upwelling phenomenon in the IO only occurs in the northern and southern hemispheres while no upwelling occurs in the equatorial region because of the absence of steady equatorial easterlies, which is a result of the rising component of the IO Walker Circulation (Schott et al., 2009). During the winter monsoon, the Arabian Sea surface circulation reverses to a counterclockwise direction, when sustained but weaker winds blow to the southwest (Schott and McCreary, 2001) forming a confluence zone with

the EACC and merges with the South Equatorial Counter Current (SECC) to flow back to the Indonesian waters (Schott et al., 2009; **Figure 2.1**).

A study by Lévy et al. (2007) on the regional characterization of summer and winter phytoplankton blooms in the IO showed that our study area sits between the tropical band region and the Somali bloom during summer and the west equatorial bloom during the winter. However no bloom is detected at our study area for these two monsoon seasons. Surface water productivity in our study area remains relatively low, although a slight increase is observed during summer (Lévy et al., 2007; Koné et al., 2013). Average modern sea surface salinity is 35.0, which ranges from 34.7 (April to June) to 35.2 (October to December) and average sea surface temperature (SST) is 27.2°C, varying from 25°C (August) to 30°C (March) (Antonov et al., 2010). The average depth of the thermocline in the study area is 110 m (Locarnini et al., 2010).

2.3 Material and methods

Gravity core Geob12613-1 was retrieved at 2292 m water depth off the Tanzanian margin in East Africa (05°29'S; 40°56'E) during the R/V Meteor cruise M75/2 in 2008 (Savoie et al., 2013). For this study, we analysed the upper 7.54 m of the 11.7 m core covering the last 300 kyr to investigate the last two glacial/interglacial cycles. Because different coccolithophore species comprise the older assemblage, we focused on the assemblage composition after the first occurrence (FO) of *Emiliana huxleyi* (~270 kyr in the IO) to minimize any species evolutionary bias. A total of 196 samples were collected at 4 cm-intervals representing an average time resolution of 1.5 kyr.

2.3.1 Age model

The age model was based on nine accelerator mass spectrometry ¹⁴C analyses performed on monospecific samples of the planktonic foraminifera *Globigerinoides sacculifer* for the upper part and on the *G. ruber* $\delta^{18}\text{O}$ stratigraphy for the lower part of the core (**Table 2.1**). All ¹⁴C ages were converted into calendar year before present (BP) using Calib 7.0.2 (Stuiver et al., 1993) with Marine13 calibration curve (Reimer et al., 2013). A reservoir age correction of 150 yr (± 40 yr) was estimated from the closest calibration points (Southon et al., 2002) in accordance with previous studies in this area (e.g., Kuhnert et al., 2014; Rippert et al., 2015). The $\delta^{18}\text{O}$ values were tied with the benthic foraminiferal $\delta^{18}\text{O}$

stack (Lisiecki and Raymo, 2005) using Analyseries 1.1 (Paillard et al., 1996; **Figures 2.2a** and **2.2b**).

Table 2.1: Radiocarbon dates and calibrated ages for Geob12613-1.

Laboratory ID	Core depth (cm)	¹⁴ C age yr BP	Error ±	Calibrated ¹⁴ C age yr BP	¹⁴ C age model (ka)
UCIAMS-123494	2	3445	20	3137	3.1
UCIAMS-123495	14	8815	25	9337	9.3
UCIAMS-123496	18	10100	25	10902	10.9
UCIAMS-123504	30	12960	45	14536	14.5
UCIAMS-123497	46	16740	60	19202	19.2
UCIAMS-123498	66	23590	110	27986	28.0
UCIAMS-123499	78	26720	160	30843	30.8
UCIAMS-123500	106	35930	450	40343	40.3
UCIAMS-123501	114	36790	500	41241	41.2

2.3.2 Coccolithophore analysis, assemblage composition and diversity

Samples for coccolithophore analysis were prepared using a combined dilution/filtering technique described by (Andruleit, 1996) and analysed with a Zeiss DSM940A scanning electron microscope (SEM) at 3000X magnification. At least 500 specimens were identified and counted on measured transects for each sample. Species identification was based on Young et al. (2003) and the electronic guide to the biodiversity and taxonomy of coccolithophores (Nannotax 3; <http://www.mikrotax.org/Nannotax3/>). Species diversity (Shannon index; H) was calculated using the paleontological statistical software (PAST) (Hammer et al., 2009). Coccolithophore concentrations were expressed as number of coccoliths per gram of sediment (CC/g sed.) calculated using the equation: Coccolith concentration = $(F \cdot C \cdot S) / (A \cdot W)$, where F = effective filtration area (mm^2), C = number of counted coccoliths, S = split factor, A = investigated filter area (mm^2) and W = weight of sample (g).

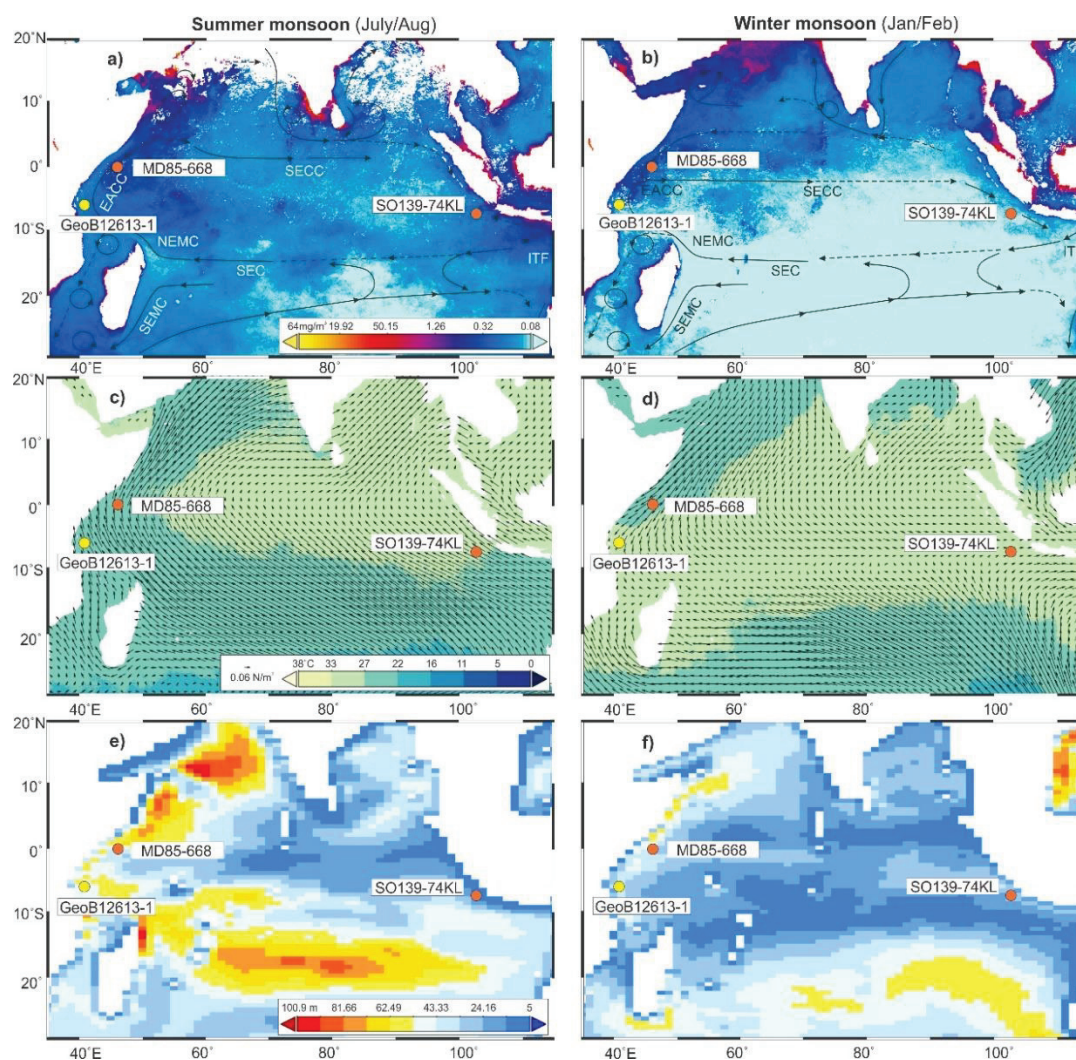


Figure 2.1: Schematic illustration of surface water hydrography of the equatorial IO. Average chlorophyll-*a* concentrations (mg/m^3) for July-August 2015 (summer; **a**) and January-February 2016 (winter; **b**) with the sea surface currents affecting the study area: East African Coastal Current (EACC), Northeast and Southeast Madagascar Current (NEMC, SEMC); South Equatorial Current (SEC); South Equatorial Countercurrent (SECC); and Indonesian Throughflow (ITF). Average sea surface temperatures ($^{\circ}\text{C}$) and wind stress direction (N/m^2) for July-August 2007 (summer; **c**) and January-February 2008 (winter; **d**). Average mixed layer depths (m) for July-August 2011 (summer; **e**) and January-February 2012 (winter; **f**). Our core location is indicated by yellow circle while the two study sites mentioned in the text, SO139-74KL (Andruleit et al., 2008) and MD85-668 (Rickaby et al., 2007) are represented by orange circles. Maps were generated from <http://giovanni.gsfc.nasa.gov/giovanni/>. Surface water circulation was redrawn from (Schott and McCreary, 2001).

2.3.3 Estimated primary productivity, *Florisphaera profunda* index and indicative species

Estimated primary productivity (EPP) expressed in grams of carbon ($\text{g C}/\text{m}^2/\text{yr}$) was calculated from the relative abundance of *F. profunda* using the formula of Beaufort (1996):

$EPP = 617 - [279 * \log (\% F. profunda + 3)]$. This equation was derived from comparison of coccolith numbers from the IO core top samples with the modern primary productivity generated from satellite chlorophyll data in Antoine and Morel (1996). Water column stratification was estimated using the *F. profunda* index (Beaufort et al., 1997; Beaufort et al., 2001). Here we modified the *F. profunda* index formula and included the relative abundance of *Gephyrocapsa ericsonii* because of the similar behavior of this species and *E. huxleyi* as well as the recorded shift in dominance of these two species in the record. The modified formula is: *F. profunda* index = $F. profunda / (F. profunda + E. huxleyi + G. ericsonii)$.

Florisphaera profunda is a LPZ-dweller, dominating the assemblage when thermocline is deep and productivity is low (Molfinio and McIntyre, 1990) while *E. huxleyi* and *G. ericsonii* are representative species of the upper photic zone (UPZ). Thus low values of *F. profunda* index suggest a mixed water column while values closer to 1 indicate a stratified water column (Beaufort et al., 1997; Beaufort et al., 2001). As opposed to the EPP equation that is based on the ratio of *F. profunda* to all other species in the assemblage, the *F. profunda* index is based on the ratio between the LPZ species *F. profunda* and the UPZ taxa *E. huxleyi* and *G. ericsonii*. In addition to these parameters, we also used the relative abundances of *Umbellosphaera* spp. (*U. irregularis* and *U. tenuis*), coccolithophore taxa with affinity for oligotrophic environments to assess surface water productivity in the location.

2.3.4 Sr/Ca measurements on coccolith fraction

We measured the Sr/Ca ratio of multi-species CF (< 20 μm -fraction) from the same samples analysed for coccolithophore assemblages. A small amount (lentil size) of sediment was suspended in 2% ammonia solution to prevent carbonate dissolution and then sieved with a 20 μm -mesh to obtain a polyspecific CF with minimal contamination from other carbonate components. A small amount of the sieved fraction was systematically prepared and observed at 3000x SEM to guarantee the absence of foraminifera fragments in the samples. The solution was then compensated with 2% ammonia. After the tubes were centrifuged at 750 rpm for 5 min, the supernatant was extracted using a pipette. The supernatant was cleaned following three different cleaning protocols by Stoll and Ziveri (2002) but without the oxidation step because test run of

selected samples that we conducted prior to the analysis revealed no significant difference on the oxidized and non-oxidized samples: 1) addition of 15 mL MNX reagent (25 g of hydroxylamine hydrochloride, 200 mL of concentrated ammonia and 300 mL of ultrapure water) to reduce Fe and Mn oxyhydroxides that scavenge metals from the sea water and contain non-carbonate Sr; 2) addition of 15 mL of 2% ammonia solution to remove any non-carbonate Sr (e.g., from clays), by ion exchange with ammonium; and 3) the subsamples were rinsed once with distilled water and twice with ultrapure water to remove any previously released Sr from the preceding methods. After cleaning, the coccoliths were dissolved with weak buffered acid (6 g glacial acetic acid, 7 g ammonium acetate in 1 L ultrapure water) for 12 hours to minimize ion contribution from non-carbonates phases.

Measurements were performed using a simultaneous axial Inductively Coupled Plasma Optical Emission Spectrometry (ICP-OES, Agilent 720) using a microflow nebulizer. All samples were diluted to a common Ca concentration, looking for the highest possible value within the range of standard calibration solutions (Ca = 10, 50, 100 ppm). Element/Ca ratios were determined as a mean of three replicates per sample. The relative standard deviation of the Sr/Ca measurement was better than 0.3%.

The influence of temperature on Sr/Ca was corrected in previous studies using the equation based on (Stoll et al., 2002a) and from independent temperature proxies such as Mg/Ca of planktonic foraminifera (e.g., Mejia et al., 2014; Saavedra-Pellitero et al., 2017). For this study, we used the raw Sr/Ca ratios to measure coccolithophore productivity because a study by Rippert et al. (2015) suggested that the temperature difference in the tropical IO from the Last Glacial Maximum to the Holocene is ~ 2 to 4°C in maximum. Moreover, temperature-corrected and raw Sr/Ca data attributed to productivity from the Agulhas Bank showed similar variations, which indicated only a small contribution of temperature to the Sr/Ca record (Mejia et al., 2014). We also calculated the relative carbonate contribution of the individual species to the total assemblage by multiplying the coccolith concentration (species CC/g of sed.) with the CaCO₃ content of each species listed in Young and Ziveri (2000), taking into account the shape of a coccolith type, average length, and calcite density. This coccolith carbonate calculation has a substantial error of up to 50% but was nevertheless performed to obtain a quantitative estimate of the carbonate contribution of the dominant species in the assemblage.

2.3.5 Time-series analysis

Spectral analysis to determine orbital forcing imprinted on the coccolithophore data was performed using the REDFIT software (Schulz and Mudelsee, 2002).

2.4 Results

2.4.1 Age model and sedimentation rate

The upper 7.54 m of sediment core GeoB12613-1 represents a continuously deposited record of the last 300 kyr (**Figure 2.2**). Based on the age model used here, the FO of *E. huxleyi* is recorded at 698 cm, with an age of 278 kyr. The exact FO of this species in the Pacific and Atlantic oceans was placed at 290 kyr and found to be slightly younger in the Mediterranean at 270 kyr (Gradstein et al., 2012). This FO at 270 kyr was also previously reported by Thierstein et al. (1977) for the IO; however this datum was used with caution and cannot be constrained in this core due to the occurrence of intergradational forms between *E. huxleyi* and *G. protohuxleyi*.

Average sedimentation rate in the core is 2.6 cm/kyr, with values ranging from 2 to 2.9 cm/kyr (**Figure 2.2c**). Lower sedimentation rates occur from 300 kyr to marine isotope stage (MIS) 4 and higher sedimentation rates from MIS 4 to the present day.

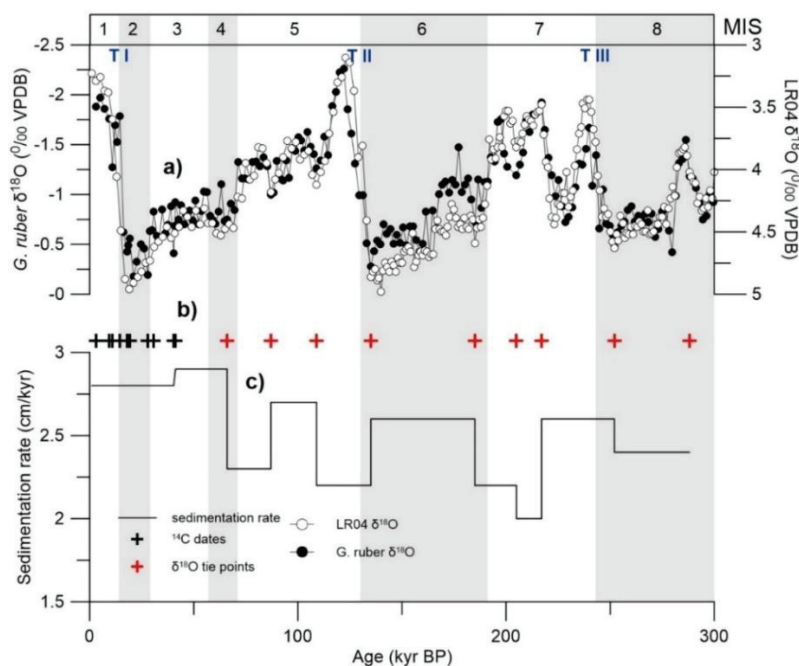


Figure 2.2: Age model and sedimentation rates of GeoB12613-1: **a)** *Globigerinoides ruber* $\delta^{18}\text{O}$ record of GeoB12613-1 and LR04 benthic foraminiferal $\delta^{18}\text{O}$ stack (Lisiecki and Raymo, 2005); **b)** ^{14}C and $\delta^{18}\text{O}$ tie-points used for tuning; and **c)** sedimentation rates.

2.4.2 Species composition, diversity and coccolith abundances

A total of 34 species and species groups entirely composed of tropical assemblage was identified in the core but the assemblage is dominated by four species (*F. profunda*, *G. ericsonii*, *E. huxleyi*, *G. oceanica*). The coccoliths are generally well- to moderately-preserved, with only minor fragmentation and/or dissolution. Species that are considered to be susceptible to dissolution, such as *Discosphaera tubifera*, *Rhabdosphaera clavigera*, and *U. irregularis* are well- to moderately-preserved in the core. This good preservation is also shown by the occasional occurrences of *Gephyrocapsa* coccospheres from the bottom of the core until ~250 kyr. Here consistently high and relatively stable diversity is observed, with the highest diversity close to Termination (T III) and then gradually declining until the middle of MIS 7 (**Figure 2.3a**). For the latter half of MIS 7, coccolith diversity recovers but reaches a minimum during the transition to MIS 6. Relatively high diversity is recorded in the early part of MIS 6, decreases toward the middle, and obtains another peak during T II. A noticeable low diversity is observed during MIS 4 and 5. Diversity increases during MIS 3 until T I, then significantly declines after this deglaciation, and increases again during the Holocene. The relatively high species diversity and the good preservation potential of the study area shows that the coccolith record is not biased by dissolution. As such, changes in total abundances of coccolithophores and abundances of individual species are assumed to reflect reliable productivity signals and reveals true paleoceanographic variations.

The most abundant species in the core is *F. profunda*, with a relative mean of 42%, followed by *G. ericsonii* (31.3%), *E. huxleyi* (14.9%), and *G. oceanica* (6.7%), comprising 60 to 80% of the total assemblage (**Figure 2.3f**). In general, increasing relative percentages of *F. profunda* and decreasing *G. ericsonii* is observed. Other significant contributors to the assemblage are *Calcidiscus leptoporus*, *Calciosolenia brasiliensis*, *Helicosphaera carteri*, *Oolithotus antillarum*, *O. fragilis*, *Syracosphaera* spp., small *Reticulofenestra*, *Umbilicosphaera foliosa*, *U. sibogae*, *U. irregularis*, and *U. tenuis*. Species with relative abundances of < 5% were grouped together as other species (others).

Florisphaera profunda absolute numbers range from 388 to 2200 x10⁷ CC/g sed., with high amplitude variability throughout the record (**Figure 2.3b**). Distinct peaks are observed during glacial terminations and highest abundances are recorded during MIS 7 (197 kyr),

MIS 5 (103 kyr), and MIS 4 (64 kyr). After 64 kyr, *F. profunda* concentration decreased and stayed at this level, gradually regained dominance during T I, and continued to increase until the Holocene. This taxon is the most abundant throughout the 300-kyr record except during MIS 7 when an increase in *G. ericsonii* concentrations is observed, reaching abundances of up to 2295×10^7 CC/g sed. (**Figure 2.3c**).

A general declining trend toward the Holocene is recorded for *G. ericsonii* absolute numbers, with peaks during interglacial periods (MIS 7, 5 and 3) and low abundances during glacial stages (MIS 6, 4 and 2), although an interval of high abundance is also seen during MIS 8. The absolute numbers of this species declined from MIS 7 toward the end of this interglacial stage and recovered at MIS 5 with another peak, reaching abundances of up to 1738×10^7 CC/g sed. During MIS 5 to 4 transition, *G. ericsonii* is replaced by *E. huxleyi* in terms of dominance at ~90 kyr, with gradually decreasing abundances toward the Holocene (**Figures 2.3c** and **2.3d**). Consequently, a progressive increase of *E. huxleyi* from MIS 4 to the Holocene is observed; however, *E. huxleyi* absolute concentrations are still lower compared to *G. ericsonii* in the lower part of the core (**Figure 2.3d**). We believe that this distinct reversal in our core between *G. ericsonii* and *E. huxleyi* is coincident with the *G. caribbeanica* and *E. huxleyi* reversal event of Thierstein et al. (1977) in the cores from the Atlantic Ocean recorded at 85 to 73 kyr. The similarity of our record to data from other areas (e.g., Thierstein et al., 1977; Flores et al., 1999; Andruleit et al., 2008) suggests the validity of this data at the regional scale. *Emiliania huxleyi* abundances range between 85 and 622×10^7 CC/g sed., with highest absolute numbers during MIS 4 to 3 transition, MIS 3 (40 kyr), and MIS 2 to 1 transition.

Gephyrocapsa oceanica is an important component of the assemblage during MIS 8, with abundance of up to 1173×10^7 CC/g sed. (**Figure 2.3e**). High abundances of this species are recorded until MIS 7, decreasing to more than half and remain on relatively similar level until the Holocene.

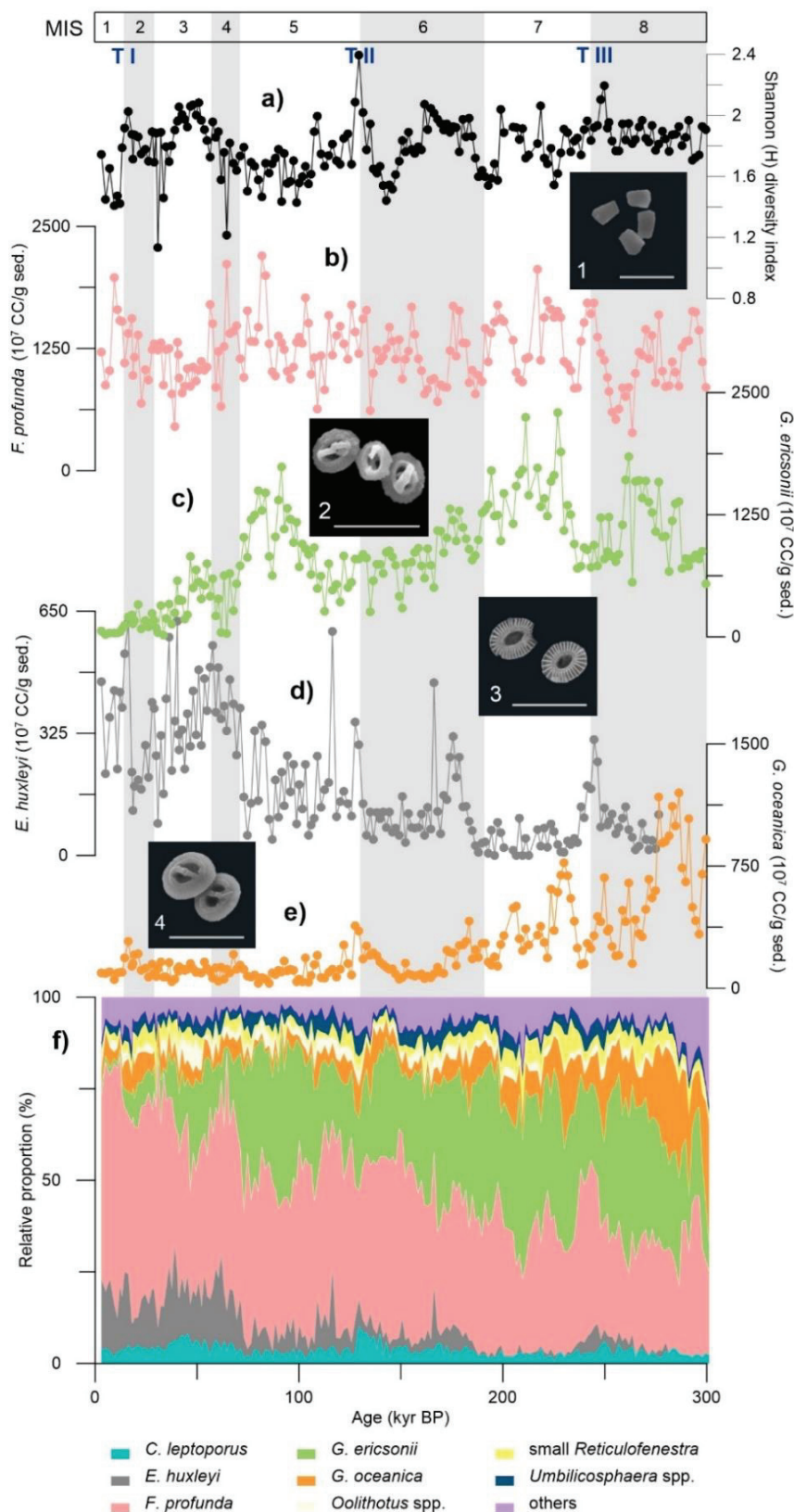


Figure 2.3: Coccolithophore assemblage and abundance records of GeoB12613-1: **a)** Shannon diversity index (H); absolute and relative abundances of **(b, 1)** *Florisphaera profunda*, **(c, 2)** *Gephyrocapsa ericsonii*, **(d, 3)** *Emiliana huxleyi*, and **(e, 4)** *G. oceanica*; **f)** stack of all coccolithophore species. Glacial stages are indicated by grey bands with glacial terminations (T). Scale bar in photomicrographs = 5µm.

2.4.3 Coccolith carbonate contribution

The relative CaCO_3 contribution of the coccolithophore species to the carbonate content shows an absolute dominance of *C. leptoporus* and *Oolithotus* spp. (*O. antillarum* and *O. fragilis*), both having a mean contribution of $\sim 30\%$ and peak values of 56 and 55%, respectively (**Figure 2.4f**). During MIS 8, *G. oceanica* is the main coccolith carbonate producer with a maximum share of 40%. Additionally, *G. ericsonii* is a consistent contributor to the coccolith carbonate fraction until MIS 4, with maximum value of 24% and declines to almost nothing thereafter. Other species with significant shares in the coccolith carbonate fraction are *Helicosphaera* spp. and *Umbilicosphaera* spp.

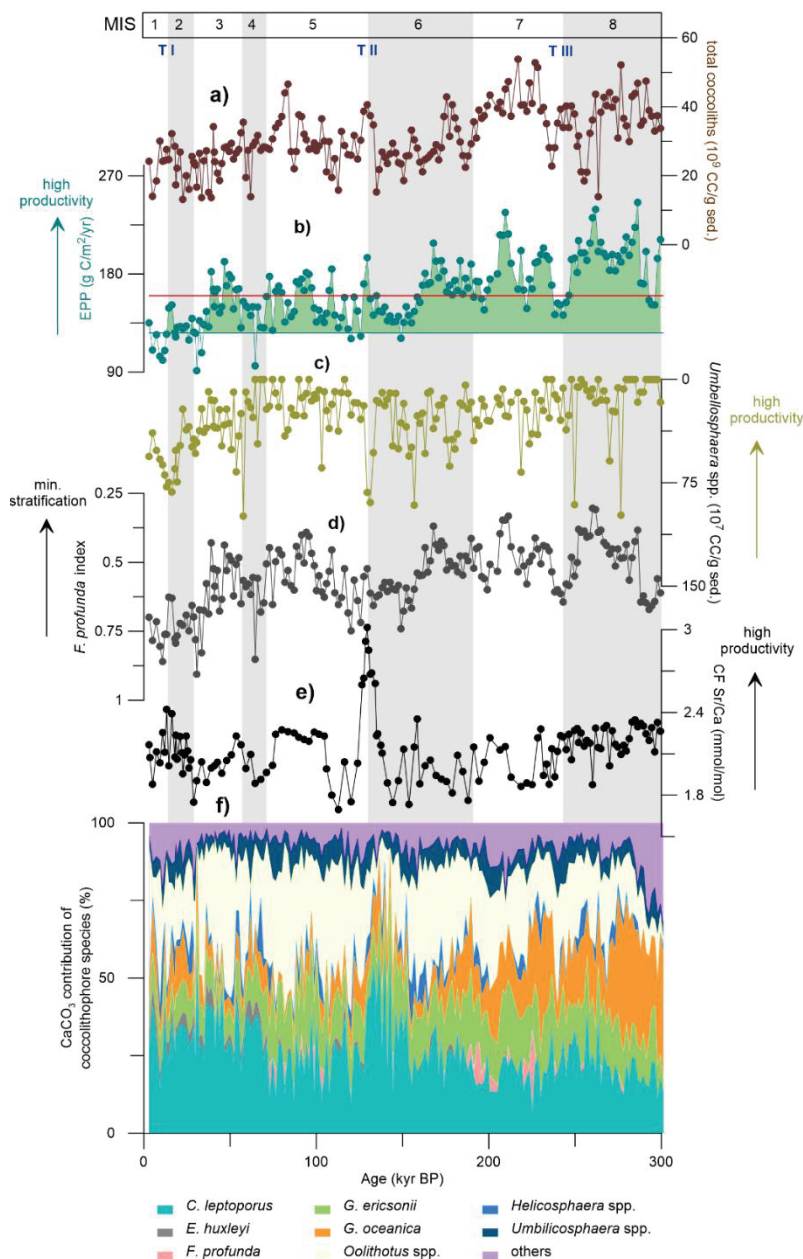


Figure 2.4: Core GeoB12613-1 productivity records over the last 300 kyr: **a)** total coccolith concentrations; **b)** estimated primary productivity (EPP); **c)** *Umbellosphaera* spp. absolute concentration; **d)** *Florisphaera profunda* index **e)** coccolith fraction (CF) Sr/Ca; **f)** relative CaCO_3 contribution of the coccolith fraction. Solid lines are calculated five-point running average of the raw data to highlight general trends. Green solid fill in the EPP record indicates increase in primary productivity relative to the present-day average value of $126 \text{ g C/m}^2/\text{yr}$ (Antoine and Morel, 1996) in the location while the red line is the calculated average value in the core. Glacial stages are indicated by grey bands with glacial terminations (T).

2.4.4 Productivity proxies

A general declining trend in the total coccolith concentrations is observed, with high concentrations (5385×10^7 CC/g sed.) recorded from 300 to 200 kyr (MIS 8 to 7) and declining to the present day, with minimum value of 1300×10^7 CC/g sed. (**Figure 2.4a**). Prominent peaks in the total coccolith concentrations are observed during terminations, with maxima during glacial to interglacial transitions and distinct minima during transition from interglacial to glacial periods. High total coccolith abundances occur during interglacial stages while low abundances are observed during glacial episodes, except for MIS 8. In contrast, the oligotrophic taxa *Umbellosphaera* spp. records high abundances during glacial stages (MIS 8, 6, 4, 2) and low abundances during interglacial periods (MIS 7, 5, 3, 1; **Figure 2.4c**). During the Holocene, total coccolith concentrations dropped to another minimum and slowly started to recover toward the present day.

The declining pattern in total coccolith concentrations is also shown in the estimated EPP calculated from the relative proportions of the LPZ-dwelling taxon *F. profunda*, hence declining productivity toward the present day (**Figure 2.4b**). Productivity values over the last 300 kyr range from 90 to 250 g C/m²/yr, with an average value of 160 g C/m²/yr. This estimate is higher than the average modern value of 126 g C/m²/yr (Antoine and Morel, 1996) in the area but is still low compared to other more productive areas in the IO (e.g., e.g., maximum of 390 g C/m²/yr in Beaufort et al., 1997). Here a decreasing three-step change in paleoproductivity is observed: 1) the interval from MIS 8 to MIS 7/6 transition (300 to 191 kyr) characterized by highest EPP (mean of 188 g C/m²/yr); 2) a period of high amplitude productivity change with lower EPP values (mean of 156 g C/m²/yr) from MIS 6 to MIS 3/2 transition (191 to 46 kyr); and 3) a period of lowest productivity starting at ~45 kyr toward the Holocene (mean of 133 g C/m²/yr). This step-wise reduction in EPP also occurs in the total coccolith record, although the period with the lowest coccolith numbers started earlier at MIS 4/3 transition (71 kyr; **Figure 2.4a**).

The CF Sr/Ca values, which is a proxy for coccolithophore productivity range from 1.70 to 3.02 mmol/mol, exhibiting high frequency variability (**Figure 2.4e**). The three-step productivity change shown by the EPP and total coccolith records is not apparent in the CF Sr/Ca ratios. Here maxima are recorded during terminations, with an interestingly

extreme peak at T II (130 kyr). Moreover, a distinct period of consistently high ratios is observed during MIS 5.

Spectral analysis performed on the productivity proxy records indicates significant orbital frequencies at 41, 23 and 19-kyr cycles (**Figures 2.5a to 2.5d**). *Umbellosphaera* spp. and total coccolith concentrations display a pronounced 23-kyr orbital periodicity with strong spectral powers at 99% and 90% confidence intervals (CI), respectively. Strong spectral peaks are shown by the EPP and CF Sr/Ca both at the obliquity (41 kyr; 95% CI) and the precession (23 kyr; 90% CI) bands, with the EPP showing another significant power at 19-kyr cycle (90%).

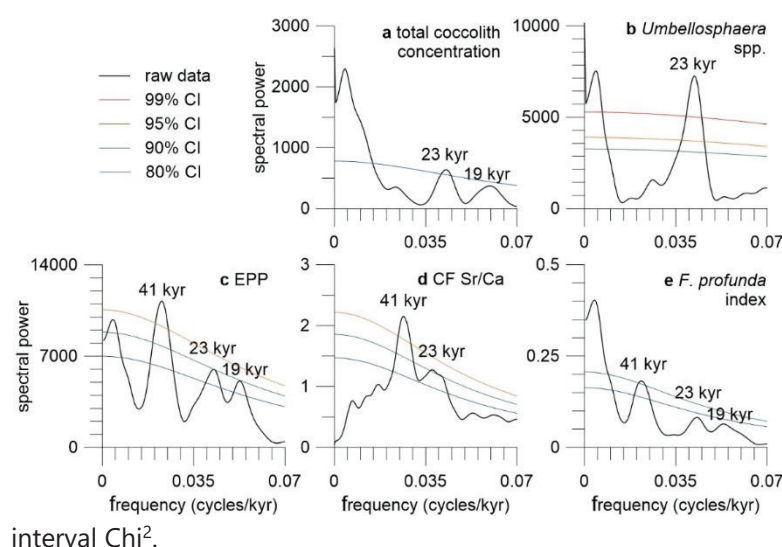


Figure 2.5: Spectral power versus frequency plots of coccolithophore-derived parameter: **a**) total coccolith concentrations; **b**) *Umbellosphaera* spp. (*U. irregularis*, *U. tenuis*) absolute concentration; **c**) estimated primary productivity (EPP); **d**) coccolith fraction (CF) Sr/Ca; and **e**) *Florisphaera profunda* index. Significant orbital frequencies are highlighted. CI- confidence interval χ^2 .

2.4.5 Water column stratification

The stepwise change similar to the EPP trend and timing is reflected in the *F. profunda* index (**Figure 2.4b** and **2.4d**). A distinct strong stratification is recorded during MIS 8, commencing at 288 kyr, with a drastic change and ending at 253 kyr (**Figure 2.4d**). This is followed by a progressive increase in stratification reaching a maximum during T III. Generally lower values of the *F. profunda* index are observed during MIS 7 until the middle of MIS 6, although distinct peaks are also observed between 225 and 209 kyr. From 160 kyr, a gradual enhancement in stratification is indicated by the high values of *F. profunda* index. A well-mixed water column during the remaining period of MIS 5 and part of MIS 3 is recorded while a more stratified surface water conditions occurred during MIS 4 and 2. From MIS 3 toward the Holocene, *F. profunda* index shows a more stratified water column

conditions. Spectral analysis of this proxy displays distinct spectral peaks at 41, 23 and 19-kyr periodicities although only the obliquity band shows significant power (90% CI).

2.5 Discussion

2.5.1 Coccolithophore species as paleoproductivity proxies

Species abundance and coccolith composition at GeoB12613-1 are in good agreement with other studies conducted in the tropical IO (e.g., Beaufort, 1996; Beaufort et al., 1997; Takahashi and Okada, 2000; Rogalla and Andruleit, 2005; Andruleit et al., 2008), with *F. profunda* and/or *Gephyrocapsa* spp. dominating the assemblage. *Florisphaera profunda* is the dominant taxon for the majority of the studied time period. It has been proposed by several authors as an effective indicator of low surface water productivity in Quaternary sediments (e.g., Molino and McIntyre, 1990; Ahagon et al., 1993; Beaufort, 1996), inhabiting the LPZ where light is rare and nutrients are comparatively abundant (Okada and Honjo, 1975). Its overall high abundances in the study area suggest that a relatively stable and stratified water column prevailed over the last 300 kyr. The dominance of this species in the water column reflects a deep nutricline, low total primary production (Molino and McIntyre, 1990) and less turbid waters (Ahagon et al., 1993).

Gephyrocapsa oceanica is significant in numbers from 300 to 160 kyr, coinciding with the highest EPP in the location, which reflects the preference of this species for relatively high surface water productivity conditions (**Figure 2.3e**). Recent study by Stolz et al. (2015) on the modern coccolithophore assemblage distribution in the WTIO showed highest relative abundance of *G. oceanica* in near-shore sediments and in the Pemba Channel, an area with stratified waters but with localized source of nutrients. This is contrary to the open ocean samples, which includes the present study area, where the authors found increased abundances of *U. irregularis* and *D. tubifera*, coccolithophore taxa that are typical of oligotrophic stratified warm water. In the highly productive upwelling cell in the Arabian Sea, *G. oceanica* was found to also dominate the assemblages (e.g., Broerse et al., 2000; Andruleit et al., 2005; Andruleit et al., 2008). The abundance of this species in the Benguela Current area was also tied to relatively warm, high nutrient content surface waters and was scarce in cold fertile waters (Giraudeau, 1992). Additionally, *G. oceanica* peaks in the sediments from the Agulhas Current region were linked to high productivity pulses (Winter

and Martin, 1990). Thus the decline in the abundance of this species toward the Holocene in the study area suggests a decrease in productivity and a diminishing source of nutrients.

On the contrary, *G. ericsonii* is not considered as an indicator of upwelling processes in low latitudes, but is more typical of stable regimes with increased nutrient availability (Andrulleit and Rogalla, 2002; Rogalla and Andrulleit, 2005) in the surface. This species reveals a parallel trend with *G. oceanica*, although with higher concentrations in the record. At the beginning of MIS 4, *E. huxleyi*, a taxon also typified to prefer a stable water column with a local nutrient source, shifted dominance with *G. ericsonii*. Rogalla and Andrulleit (2005) combined the abundances of these two species in the record based on the assumption that they had similar ecological preferences and that the increase in *E. huxleyi* was due to the evolutionary replacement of *G. ericsonii*. *Emiliana huxleyi* belongs to the Noelaerhabdaceae family, a group that have undergone a considerable phylogenetic development since the early Pliocene (Thierstein et al., 1977). Thus the abundance shift between *G. ericsonii* and *E. huxleyi* at ~90 kyr in our study area is proposed to be evolutionary steered.

2.5.2 Orbital and atmospheric forcing of coccolithophore productivity

Productivity and water column stratification proxies suggest that dynamic productivity conditions prevailed in the investigated area over the last two glacial/interglacial cycles. The generated time series of independent coccolithophore productivity (EPP, *Umbellosphaera* spp., CF Sr/Ca) and water column stratification (*F. profunda* index) proxies reveal dominant periodicities at 41, 23, and 19 kyr, corresponding to the earth's orbital periods of obliquity and precession (**Figure 2.5**). This suggests that productivity in the study area is influenced by obliquity and precession through atmospheric processes such as insolation intensity, the Southern Oscillations or monsoons (Su et al., 2015). **Figure 2.6** shows that productivity in the WTIO is responding to the December insolation maxima at the equator except during T II, when the high productivity peak is coincident with the June insolation maximum. Precession forcing appears to be also driving the surface water conditions in the tropical IO, influencing coccolithophore productivity changes in the eastern IO (Andrulleit et al., 2008) and the equatorial IO (Beaufort, 1996; Beaufort et al., 1997), with the latter demonstrating obliquity forcing in the

record as well. Although obliquity is known to have little effect on low latitude insolation, 41 kyr cyclicity has been imprinted in several marine records from the Indo-Pacific region (e.g., Clemens et al., 1991; Beaufort et al., 1997; Beaufort et al., 2001; Su et al., 2015). In Beaufort et al. (2001), obliquity oscillation is rarely linked to the increase in the intensity of the zonal winds since an increase in thermocline slope was not observed in their record. Nevertheless, the increase in nutrients in the equatorial IO during glacial periods was associated with the global decrease in SST that consequently led to weakened stratification and shoaling of the thermocline (Beaufort, 1996; Fedorov and Philander, 2000). A stronger NH summer monsoon and strengthening of the IEW during insolation maxima subsequently led to an intensified surface water circulation in the study area. This mechanism could potentially have shoaled the thermocline, bringing nutrients to the surface, and thus increasing productivity. Accordingly, a stronger NEMC could have pushed the surface waters as it flows northward and merges with the EACC, causing possible mixing and shallowing of the mixed layer depth (**Figure 2.1c** and **2.1d**). Another possible mechanism of nutrient delivery to the site is via a local perpetuation of the SC that reverts direction during the winter monsoon period, carrying with it nutrient-enriched upwelled water off Somalia, located north of the study area (e.g., Stolz et al., 2015). However, modern day records show no evidence of surface water nutrient enrichment in the study area during the winter monsoon period (e.g., Lévy et al., 2007) as observed from the chlorophyll (**Figure 2.1a** and **2.1b**) and water chemistry (e.g., phosphate and nitrate, not shown in figure).

2.5.3 Paleoproductivity over terminations

There is no clear glacial/interglacial pattern observed in the individual coccolith species records (**Figure 2.3**). Increased abundances are observed during the glacial stages but peaks are also recorded during interglacial periods. This observation suggests that the coccolithophore community in the study area is not dependent on temperature but rather on nutrient availability (Andruleit et al., 2008). The assemblage is entirely composed of tropical species suggesting that warm conditions with SSTs of at least 20°C prevailed in the WTIO throughout the studied time interval. An overall correlation between CF Sr/Ca, EPP and *F. profunda* index, reflecting increase in productivity coincident with the weakening of

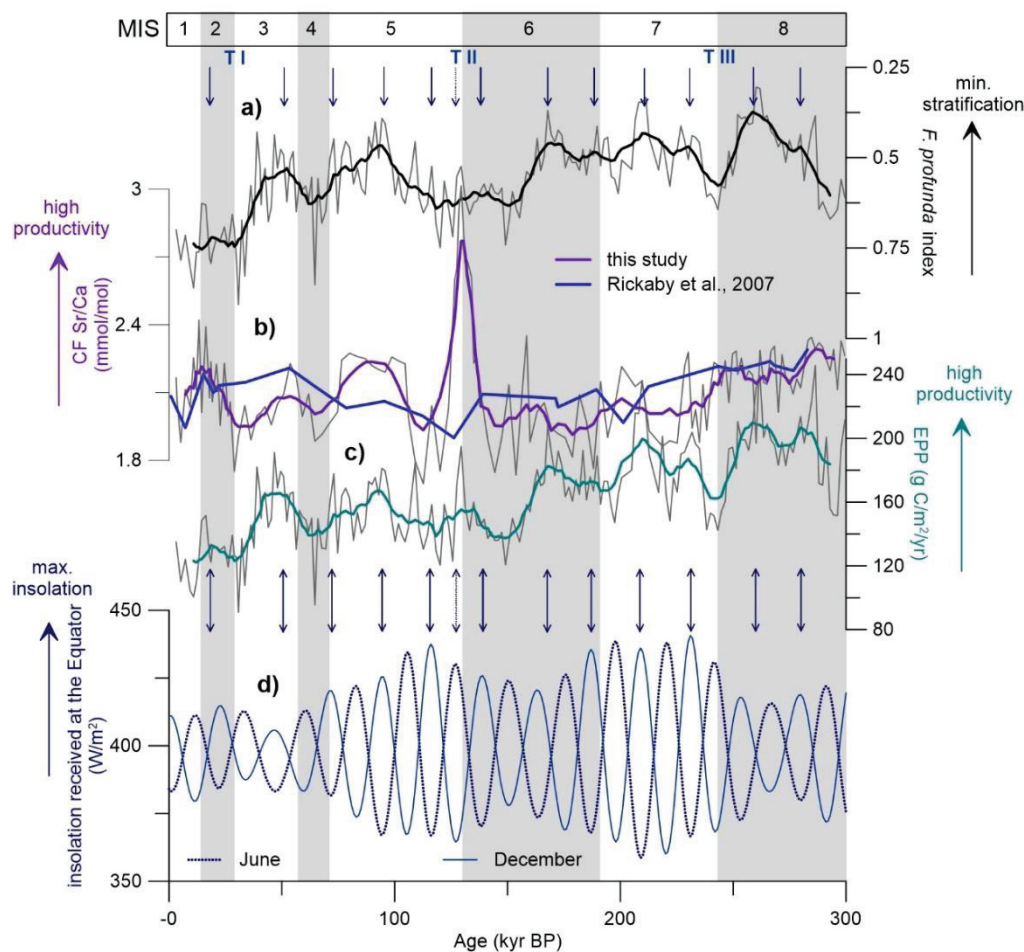


Figure 2.6: Geob12613-1 stratification and productivity records (**a to c**) compared to the insolation received at the equator during summer (June, dotted) and winter (December, solid) from Berger (1992) (**d**). coccolith fraction (CF) Sr/Ca data of MD85-668 in Rickaby et al. (2007) located north of the study area is shown in comparison to the CF Sr/Ca record in the present study. The arrows represent the coincidence between our records (high productivity and minimum stratification) and insolation maxima during summer (dotted) and winter (solid). Solid lines are calculated five-point running average of the raw data (faint background lines) to highlight general trends. Glacial stages are indicated by grey bands with glacial terminations (T).

stratification during the three terminations is observed (**Figure 2.6**). However, EPP values during these terminations are on a similar scale, which are still comparably low (**Figure 2.6c**). This low productivity trend was also observed during T II in the Agulhas Corridor, south of the study area, where an abrupt warm and saline episode during T II did not coincide with a productivity peak (Mejia et al., 2014). A study by Rickaby et al. (2007) shows similar trend in CF Sr/Ca values and suggested the influence of day length and light intensity, in addition to insolation in coccolithophore productivity (**Figure 2.6b**). Productivity as shown from the CF Sr/Ca ratio is increased during terminations, with a

prominent peak during T II, coincident with the increased total coccolith concentration, higher diversity, and weak stratification. We compared this extreme maximum to the coccolith carbonate contribution of individual coccolithophore species in the record and found that this high peak matches the peak in coccolith carbonate of the large species *C. leptoporus* and *Oolithotus* spp., which together contributed more than 60% of the total coccolith carbonate (**Figure 2.4f**). These medium to large coccoliths (5-15 μm) have higher Sr/Ca ratios compared to smaller species (< 5 μm) (Stoll et al., 2007; Fink et al., 2010), hence despite their low abundance (**Figure 2.3f**), can influence the CF Sr/Ca and coccolith productivity records.

2.5.4 Paleoproductivity history over the past 300 kyr

The interval from MIS 8 to MIS 6 (300 to 191 kyr) is characterized by relatively high productivity conditions as recorded by the indicative coccolithophore taxa and CF Sr/Ca. This high productivity is interrupted by a period of low productivity during T III. Here highly stratified waters occurred at our site as observed from the high *F. profunda* index values. Consequently, an increase in the low productivity species umbellosphaerids is observed (**Figure 2.4c**). High total coccolith concentrations, dominated by *F. profunda* are also recorded during T III, reflecting a deeper nutricline. After T III, higher productivity is recorded as shown by higher CF Sr/Ca than before the termination, a peak in *G. ericsonii* concentration, high *G. oceanica* abundance, an increase in total coccolith concentrations, and high EPP values. Interestingly, a peak in *E. huxleyi* abundance is observed during T III. It is consistently low during the entire MIS 7, when *G. ericsonii* is proliferating in the water column. The *F. profunda* index shows minimum stratification, suggesting mixing caused by strong winds. This weakening of stratification led to low abundances of deep-dwelling species *F. profunda*. The prevalence of oligotrophic surface water conditions during the middle of MIS 6 (160 kyr) led to a decline in the UPZ-dwelling species. During this time, productivity is still generally high but there is larger amplitude in variability. After TII, MIS 5 commenced with a highly stratified water column and decreasing productivity. A decline in relative abundances of all species, except *F. profunda* is observed. The rest of MIS 5 is characterized by weakening of stratification accompanied by an increase in nutrient concentrations in the surface waters as reflected in the EPP values. This is succeeded by an

increase in productivity observed in the total coccolith concentrations with increased diversity. Marine isotope stage 4 is characterized by low CF Sr/Ca, extreme drop in the EPP, and low total coccoliths due to a more stratified water column observed from high values of *F. profunda* index. After MIS 4 (46 kyr), stratification weakened and an increase in productivity is recorded.

Strong stratification and relatively low surface water productivity, except during T I characterizes the interval from MIS 3 toward the Holocene. Here distinct peaks are observed in CF Sr/Ca, EPP, and total coccoliths with maximum *E. huxleyi* absolute concentrations. Together with *F. profunda*, *E. huxleyi* is a significant component of the Holocene sediments in the study area. The period from the LGM to the present is characterized by low EPP with stable water column conditions. The modern-day oligotrophic surface water condition with pronounced stratification in the WTIO is suggested to have started after T I, which led to the dominance of *F. profunda*, a decline in diversity, and an increase in the abundance of the oligotrophic species *Umbellosphaera* spp.

2.5.5 Comparison with the tropical eastern Indian Ocean

In order to better understand the productivity dynamics of the WTIO, we compared our results with the eastern IO, the area where the western tropical surface waters are mainly sourced (**Figure 2.7**). We compared our results with SO139-74KL from an upwelling region off the southern tip of Sumatra (**Figure 2.1**) (Andruleit et al., 2008), allowing us to determine the productivity and water column dynamics between the two regions.

At present, the IO climate is mainly controlled by the El Niño Southern Oscillation (ENSO), the IO Dipole (IOD), and monsoon systems, which are inter-annual modes of the Walker Circulation. The Walker Circulation is a prominent feature of the tropical climate (Tokinaga et al., 2012), revealing a number of east-west patterns across all tropical oceans and even in higher latitudes. However, current knowledge on the Walker Circulation is tied to these short-term events or features (e.g., ENSO and IOD) and the long-term variations in the Walker Circulation is still a subject of intense debate (e.g., Power and Kociuba, 2011; Meng et al., 2012; Tokinaga et al., 2012).

The two parameters calculated from the relative abundance of *F. profunda* (*F. profunda* index and EPP) of our core and SO139-74KL show the same long-term trend in paleoproductivity for the studied time period, i.e. an increase in stratification and reducing productivity toward the Holocene (**Figure 2.7**). Andruleit et al. (2008) found a periodical recurrence at 20 to 25 kyr in the total coccolith concentrations and *U. irregularis* and suggested an insolation-driven paleoproductivity in the SO139-74KL retrieved off Sumatra. In this present study, we observed similar cyclicity not only at the precession but at the obliquity band as well. This indicates that productivity variations in the ETIO and WTIO are tightly coupled independently from sea level changes during the late Quaternary, which one might expect due to sea level dependent changes in the ITF (e.g., Song and Gordon, 2004; Lückge et al., 2009) and possibly related to changes in the Walker Circulation. Moreover, strong similarities exist in the EPP and stratification records between the ETIO and the WTIO (**Figures 2.7a** and **2.7b**), implying the potential teleconnection between these two regions. However, despite these similarities, we also observed opposing patterns during certain intervals (MIS 7, MIS 5 and MIS 3). In particular, during the interglacial periods, minimum stratification and therefore higher productivity is observed in the WTIO while this pattern occurred during the glacial stages in the ETIO. This suggests, for the first time, the possible existence of an analogous to the present-day IOD operating on longer timescales. In contrast, we point that the current view of the paleo-IOD-like conditions is so far based only on the Holocene timescales (e.g., Abram et al., 2007; Niedermeyer et al., 2014; Kwiatkowski et al., 2015) and is defined as the difference in SST gradients between the two regions. Rippert et al. (2015) observed similar thermocline temperature between the ETIO and WTIO, except during the last deglaciation, when the thermocline was warmer in the western and cooler on the eastern side. Mohtadi et al. (2010) explained this event to be related to the northward migration of the Southern Hemisphere frontal system during the glacial, which shifted the formation area of the SAMW to the lower latitudes that brought warmer thermocline waters in the IO.

Overall, EPP record shows a more La Niña-like state of the Walker Circulation from 300 kyr to the end of MIS 6 (T II) while a more El Niño-like is observed from T II toward the present day (**Figure 2.7b**). A stronger Walker Circulation leads to La Niña and intensifies surface water mixing, which further leads to high productivity while a weaker Walker Circulation causes El Niño, hence a more stratified water column and low productivity. A

weaker Walker Circulation is more prominent at the beginning of MIS 2 and continues to the present day as shown from the low EPP values. The parallel change in stratification and productivity between the ETIO and the WTIO over the past 300 kyr may provide a hint on the dynamics and varying intensity of the Walker Circulation in the past.

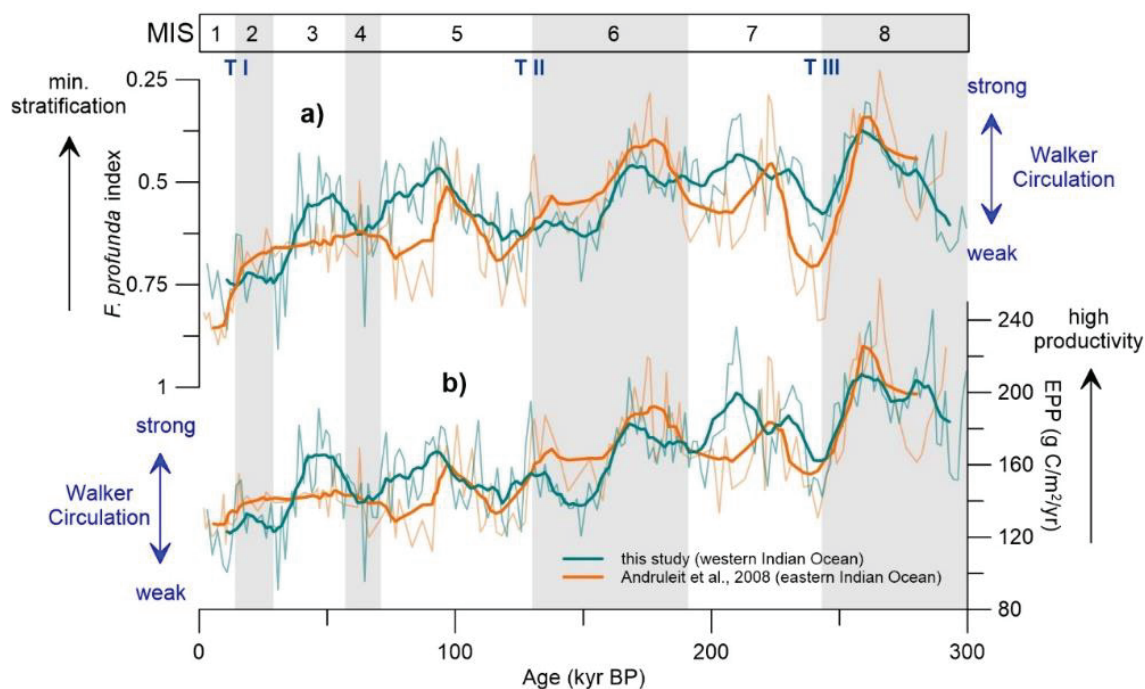


Figure 2.7: GeoB12613-1 stratification and productivity records in comparison to the eastern tropical Indian Ocean records of Andruleit et al. (2008; SO139-74KL). Solid lines are calculated five-point running average of the raw data (faint background lines) and used to highlight general trends. Glacial stages are indicated by grey bands with glacial terminations (T).

2.6 Conclusions

A wide range of taxa composed of 34 species and species groups were identified in the WTIO. In particular, coccolithophore assemblages are characterized by relatively moderate to high diversity of tropical species but were only dominated by four taxa: *F. profunda*, *G. ericsonii*, *E. huxleyi*, *G. oceanica*. These species altogether comprise 60 to 80 % of the total assemblage, with the deep-dwelling species *F. profunda* dominating the assemblage, reflecting a relatively oligotrophic environment prevailing throughout the studied time period. In general, high productivity and weak stratification in the study area over the last two glacial/interglacial cycles is coincident with the insolation maxima at the equator. Average EPP based on the relative abundance of *F. profunda* is 160 g C/m²/yr, a

value which is in the same scale as the modern average value of 126 g C/m²/yr in the location.

Water column stratification index (*F. profunda* index) and productivity proxies (assemblage, CF Sr/Ca) indicate a changing paleoproductivity primarily governed by shoaling of the thermocline caused by stronger NH summer monsoon and strengthening of the IEW in response to maximum insolation. Spectral analysis of the generated proxy records show periodicities both at the obliquity and precession cycles, corresponding with other studies conducted in the tropical oceans. This suggests a long-term glacial/interglacial climatic trends over the past 300 kyr, with patterns possibly related to the Walker Circulation. Comparison with the ETIO coccolithophore productivity record indicates strong correspondence, suggesting a strong teleconnection of the driving mechanisms of climatic conditions between the two regions. Higher productivity from MIS 8 to the middle of MIS 6 in the eastern and western IO is interpreted to be the result of stronger Walker Circulation. Weakening of the Walker Circulation from T II toward the present day resulted in a more El Niño-like state, leading to a more stratified water column, and thus low productivity. This result is consistent with recent studies suggesting that the Walker Circulation has been slowing for the past century due to global warming (e.g., Vecchi et al., 2006; Vecchi and Soden, 2007; Luo et al., 2012; Tokinaga et al., 2012). The rapid warming of the IO, particularly the WTIO was recently suggested and predicted by a number of these modelling studies (e.g., Roxy et al., 2014; Roxy et al., 2016) and showed that this phenomenon is causing a reduction in phytoplankton production over the recent decades (Roxy et al., 2016). With the projected global warming over the coming decades, understanding the long-term trend of the Walker Circulation through the study of biological responses in longer timescale sediment records is therefore an important step in determining patterns that will allow us to advance our capability in modeling the present and even future climate change.

Acknowledgments

We are thankful to the scientists and crew of R/V Meteor Expedition M75-2. We are grateful to Jeremy Young and Tom Dunkley Jones for their comments and suggestions, which have substantially improved the original manuscript. We also thank Mariem Saavedra-Pellitero and Catarina Guerreiro for their input during the initial preparation of

this manuscript, and David De Vleeschouwer and Manfred Mudelsee for their help in the time series analysis. Consultation and discussions with Clara Bolton and Catarina Cavaleiro on the Sr/Ca method and laboratory assistance from Nele Vollmar, Martin Kölling, and Silvana Pape are also greatly appreciated. The analyses were performed at the Keck Carbon Cycle Accelerator Mass Spectrometry Facility at the University of California, Irvine, USA (radiocarbon dating) and Isotope ($\delta^{18}\text{O}$) and Sediment Geochemistry laboratories (Sr/Ca) of the MARUM-Center for Marine Environmental Sciences, University of Bremen, Germany. Jeroen Groeneveld thanks the German Science Foundation (DFG) for funding grant (GR 3528/3-1). This research is part of the project Ocean and Climate 2: Land-ocean interaction and climate variability in low latitudes funded thru the DFG Research Center/Cluster of Excellence "The Ocean in the Earth System" MARUM. Data are available in the PANGAEA database (<https://doi.pangaea.de/10.1594/PANGAEA.875239>).

CHAPTER 3

Variations in coccolithophore productivity off South Africa over the last 500 kyr

Quaternary Science Reviews (Tangunan et al., submitted)

CHAPTER 3

Variations in coccolithophore productivity off South Africa over the last 500 kyr

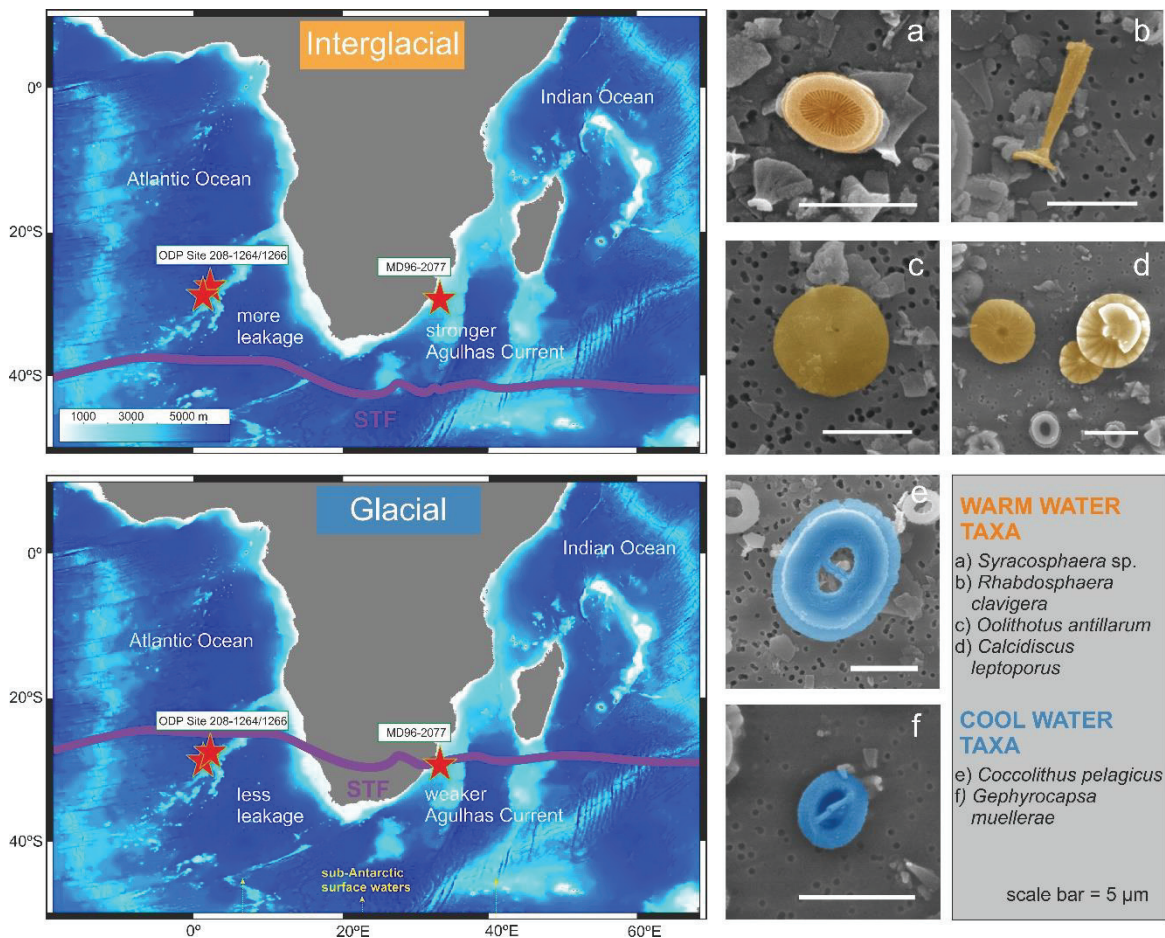
Deborah Tanguan^a, Karl-Heinz Baumann^{a,b}, Christina Fink^b

^aUniversity of Bremen, MARUM - Center for Marine Environmental Sciences, Bremen, Germany; ^bUniversity of Bremen, Faculty of Geosciences, Bremen, Germany

3 Abstract

Here we present a 500 kyr coccolithophore productivity reconstruction of the Indian-Atlantic Ocean gateway from assemblage composition and geochemistry of sediment cores retrieved from the southwestern Indian Ocean (MD96-2077) and the eastern South Atlantic Ocean (ODP Sites 1264/1266). Our multiproxy reconstruction highlights how hydrographic and orbital processes controlled the glacial/interglacial variability in coccolithophore productivity as triggered by the migration of the subtropical front (STF). Fluctuations in the records show prominent glacial/interglacial variations at 100 kyr orbital periodicity. Here two assemblage groups are recognized: cooler water dominated by *Gephyrocapsa muelleriae* suggestive of the northward shift of the STF and warm water taxa including *Syracosphaera pulchra*, *Rhabdosphaera clavigera*, *Umbilicosphaera foliosa*, *U. sibogae*, *Calciosolenia* spp., *Oolithotus fragilis*, *Umbellosphaera tenuis* and *Calcidiscus leptoporus*, indicative of the Agulhas Current warm water transport to the South Atlantic. We propose that the frontal shifts have modulated the Agulhas Current in the Indian Ocean and the Benguela Current upwelling in the South Atlantic, and played a critical role in the water column characteristics of these regions. The equatorward migration of the STF during the glacial periods resulted to a reduced intensity of the Agulhas Current and a stronger Benguela Current upwelling, as revealed by similar long-term productivity patterns between the Natal Valley (MD96-2077) and the area off Namibia (ODP Site 1082), showing enhanced surface water productivity during the glacial periods. By contrast, productivity in the Walvis Ridge (ODP Site 1266), show opposite patterns, i.e., enhanced productivity during the interglacial periods indicating that the cold and nutrient-rich upwelled waters could be transported via seaward lateral advection towards the cessation of the coastal upwelling process.

Graphical abstract



3.1 Introduction

The latitudinal migration of the subtropical front (STF) in the Southern Hemisphere (SH) emerged as a key phenomenon influencing the surface water hydrography of the Indian-Atlantic Ocean gateway (Orsi et al., 1995; Lutjeharms, 1996), which were proposed to have implications for regional and global climate variability over a period of long timescales (e.g., Peeters et al., 2004; Bard and Rickaby, 2009; Martínez-Méndez et al., 2010; Simon et al., 2013). These frontal shifts create a region of dynamic oceanographic conditions, with complex surface water biogeochemistry (Orsi et al., 1995), which drive changes in plankton distribution and surface water productivity (Read et al., 2000), as well as influence variations in the global thermohaline circulation (Bard and Rickaby, 2009; Beal et al., 2011). In the recent decades, the STF migration has been suggested to modulate the Agulhas Current, the largest western boundary current of the SH, transporting ~70 Sv of saline tropical waters (Lutjeharms, 2006) from the Indian Ocean to the South Atlantic

(Gordon et al., 1992; De Boer et al., 2013). This heat and salt transfer, termed as the Agulhas leakage, which occurs via shedding of large eddies and rings at the southern tip of Africa (Lutjeharms, 2006) is thought to have triggered the Atlantic Meridional Overturning Circulation (AMOC) (e.g., Reason and Mulenga, 1999; Schonten et al., 2000; Knorr and Lohmann, 2003; Bard and Rickaby, 2009; Biastoch et al., 2009; Beal et al., 2011). The increased influx of salt into the South Atlantic during a stronger Agulhas leakage could have potentially strengthened the AMOC at the beginning of the interglacial intervals (Bard and Rickaby, 2009; Caley et al., 2012; Caley et al., 2014). Indeed, the Indian-Atlantic Ocean gateway is a region where complex interaction of oceanic processes occur, with the Indian Ocean being the origin of the Agulhas Current, and the South Atlantic situated along the Agulhas Current warm water path (Knorr and Lohmann, 2003; Caley et al., 2014; Petrick et al., 2015) and location of the Benguela Current, a highly productive region (Shannon et al., 1989; Peterson and Stramma, 1991).

Interest in the long-term response of these two major current systems on the STF shifts resulted in a number of studies. In particular, the northward shift of the STF during the glacial intervals was associated with a weaker Agulhas leakage (Bard and Rickaby, 2009; Martínez-Méndez et al., 2010), cooler sea surface temperature (SST), and increase in surface water productivity (Bard and Rickaby, 2009). Alternatively, the poleward migration of the STF permitted stronger Agulhas leakage, which consequently led to a stronger AMOC (e.g., Bard and Rickaby, 2009; De Boer et al., 2013). The strengthening of the Agulhas leakage was evidenced by high abundances of the Agulhas leakage fauna based on planktonic foraminifera abundances (Peeters et al., 2004; Caley et al., 2014). So far, the "gatekeeper" hypothesis of Bard and Rickaby (2009) on the heat and salt leakage from the Indian Ocean to the South Atlantic is one of the widely used concepts on the interpretation of frontal migrations. At least for the long climate archives, there is a general agreement that the equatorward movement of the STF has modulated the Agulhas leakage (e.g., Peeters et al., 2004; Bard and Rickaby, 2009; Caley et al., 2012; Caley et al., 2014). However, recent modeling studies showed a stronger link of the strength of Agulhas leakage to the SH westerlies (Durgadoo et al., 2013) and that decoupling between the STF position and the westerly wind belt exists (e.g., De Boer et al., 2013; Graham and De Boer, 2013). Nevertheless, the factors that determine the changing position of the STF in the Indian Ocean is up until today remain controversial. This controversy thus raises questions about

the importance of latitudinal positions of the STF and the westerly wind belts on the strength and variability of the Agulhas Current and the Benguela Current.

Several studies have already demonstrated the long-term response of marine organisms to the variations in the Agulhas Current (e.g., Flores et al., 1999; Peeters et al., 2004; Bard and Rickaby, 2009; Martínez-Méndez et al., 2010; Caley et al., 2012; Kohfeld et al., 2013; Caley et al., 2014; Petrick et al., 2015; Romero et al., 2015) and the Benguela Current (e.g., Summerhayes et al., 1995; Little et al., 1997; Baumann and Freitag, 2004; Krammer et al., 2006). These studies suggested the influence of meridional shifts in the STF position to plankton assemblage composition in the Agulhas Current region (e.g., Peeters et al., 2004; Bard and Rickaby, 2009; Kohfeld et al., 2013; Caley et al., 2014; Romero et al., 2015). Consequently, the STF migration that modulates the Agulhas Current, transports Agulhas Current waters to the Benguela Current region and allows entrance of the sub-Antarctic surface waters (SASW) (Shannon et al., 1989) derived from the south.

Most of the previously mentioned studies on the Agulhas Current are based on planktonic foraminifera and diatoms, whereas studies using coccolithophores as proxies in longer sediment record are scarce (e.g., Winter and Martin, 1990; Flores et al., 1999; Mejia et al., 2014), although there exist papers on modern coccolithophore assemblage of the Agulhas Current region (e.g., Friedinger and Winter, 1987; Flores et al., 1999). While the Benguela Current region is relatively well-studied when it comes to coccolithophore assemblages, the areas outside the direct influence of this current are so far under represented.

Coccolithophores (coccoliths) are unicellular flagellate marine phytoplankton, which are directly dependent on variations in temperature, salinity, nutrient availability and light intensity in the water column, making them valuable tools for paleoclimate and paleoceanographic reconstructions (e.g., Giraudeau, 1992; Winter et al., 1994). Its distribution has been suggested to be controlled by latitudinal zonation and frontal system dynamics (McIntyre and Bé, 1967; Findlay and Flores, 2000; Ziveri et al., 2004), with some indicative species having unique ecological preferences. From these previous studies, coccolithophores were among the significant components of marine phytoplankton communities of the Indian Ocean and the South Atlantic, showing temporal and latitudinal variations in distribution and assemblage composition. Furthermore, such reconstructions have also been based on geochemical analysis of the coccolith fraction (CF; <20 μ m), which

indicates variations in past ocean chemistry, SST, and coccolithophore productivity (e.g., Stoll and Ziveri, 2004; Fink et al., 2010; Mejia et al., 2014; Saavedra-Pellitero et al., 2017; Tangunan et al., 2017). In particular, the CF strontium/calcium (Sr/Ca) is used to record coccolithophore growth rates and thus reflects changes in coccolithophore production independent of any coccolith counting (Stoll et al., 2002b). These studies have suggested the direct relationship between Sr/Ca in coccoliths and coccolith productivity (Stoll and Schrag, 2000; Rickaby et al., 2007) and that high CF Sr/Ca values occur in conditions of high productivity (Stoll et al., 2007).

Here we present a 500 kyr assemblage- and geochemistry-based coccolithophore productivity record of the southwest Indian Ocean (Natal Valley; MD96-2077) and the eastern South Atlantic Ocean (Walvis Ridge; Ocean Discovery Program; ODP Site 1266) to decipher the role of the STF migration on coccolithophore abundance and distribution (**Figure 3.1**). We aim to compare how STF migration has affected the intensity of the Agulhas Current in the Indian Ocean and the Benguela Current in the South Atlantic, and how these marine phytoplankton communities have responded to variations in water column properties over the past glacial/interglacial cycles. Our two study sites are situated in two different oceanographic regimes: one located near the upper border of the well-established Agulhas Current and the other within the influence of the Benguela Current. Owing to its locations, our two study sites are ideal locations for paleoproductivity reconstruction associated with the shifts of the STF, which provides information on how hydrographic mechanisms (e.g., upwelling intensity, wind-mixing, etc.) and atmospheric processes have shaped surface water productivity in the Indian-Atlantic Ocean gateway.

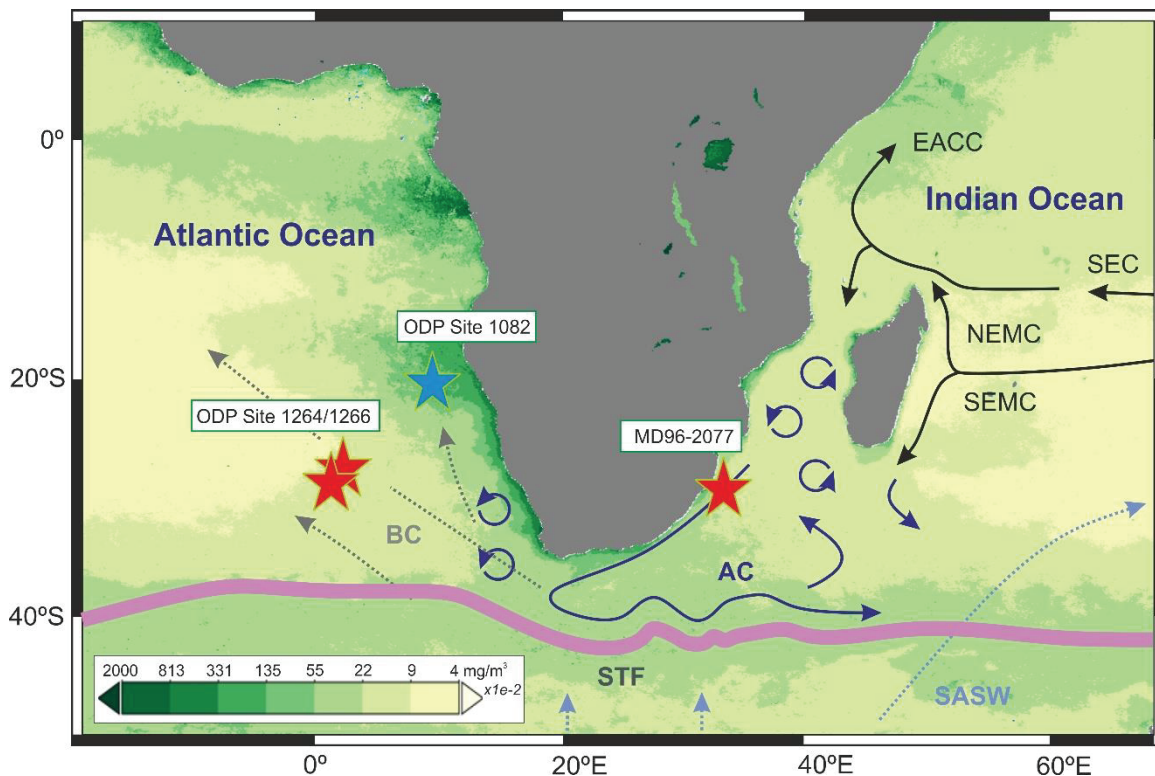


Figure 3.1: Mean chlorophyll map of the study area for 2010 generated using the Giovanni online data system developed and maintained by the NASA GES DISC (Acker and Leptoukh, 2007). Positions of the studied cores are marked with red stars. ODP Site 1082 mentioned in text is indicated by blue star. Black arrows represent the main surface ocean currents adapted from Beal et al. (2011): South Equatorial Current (SEC), East Africa Coastal Current (EACC), North East Madagascar Current (NEMC) and South East Madagascar Current (SEMC), with the Agulhas Current (AC; blue), Benguela Current (BC; gray) and Sub-Antarctic surface water (SASW; light blue). Present day position of the subtropical front (STF) is represented by the thick pink line.

3.2 Study sites and oceanographic settings

Sediment cores selected for this study, located on almost similar latitude offer a comparison between the southwestern sector of the Indian Ocean and the eastern South Atlantic Ocean. The Calypso giant piston core MD96-2077 was retrieved in the Natal Valley (33°10'S; 31°15'E) at 3781 m water depth, within the Agulhas Current headwaters during the IMAGES II Campaign "NAUSICAA" (Bertrand and al., 1997). The Natal Valley surface waters are sourced from the southward flowing Eastern Madagascar Current that merges with the Mozambique Channel throughflow, and forms the Agulhas Current (Lutjeharms, 2006; Hall et al., 2016). It was retrieved from the highly dynamic Agulhas Current region and within the influence of the Agulhas Return Current, a component of the Agulhas Current that retroflects and does not leak to the South Atlantic.

On the other hand, sediment cores from Sites 1264 and 1266 were collected from the Walvis Ridge (28°32'S; 02°51'E/28°33'S; 02°21'E) at 2505 and 3798 m, respectively during the ODP Leg 208 Expedition, and located within the reaches of the Benguela Current. The warm water route of the Agulhas Current continues to the South Atlantic where Sites 1264/1266 are located. Here warm and oligotrophic surface waters from the Indian Ocean and the South Atlantic Gyre are transported to the North Atlantic by the SEC. The Benguela Current can also receive the Agulhas Current water and southern sourced sub-Antarctic surface waters due to changes in the STF (Shannon et al., 1989).

3.3 Materials and methods

3.3.1 Coccolithophore assemblage analysis

For coccolithophore analysis, the upper 20.94 m of sediment core MD96-2077 and the upper 3 m at Site 1266, covering the last ~500 kyrs were sampled. A total of 208 samples were collected at 10 cm-interval in MD96-2077, representing an average time resolution of 2.3 kyr while 59 samples were taken from Site 1266, between 2.5 and 7.5 cm, with an average time resolution of 3.5 to 10.5 kyr.

Samples for coccolith identification and counting were prepared using a combined dilution/filtering technique (Andruleit, 1996) and analyzed with a Zeiss DSM940A scanning electron microscope (SEM) under 3000x magnification. Abundances were determined by counting at least 500 coccoliths on measured transects. Coccolith taxonomic identification was based upon Young et al. (2003) and the electronic guide to the biodiversity and taxonomy of coccolithophores (Nannotax 3; <http://www.mikrotax.org/Nannotax3/>). The conversion of coccolith counts into number of coccoliths per gram of sediment (CC/g. sed.) was calculated using the equation: $CC = (F * N * S) / (A * W)$, where *CC* = coccolith concentration; *F* = effective filtration area (mm²); *N* = number of coccoliths counted; *S* = split factor; *A* = investigated filter area (mm²); *W* = weight of bulk dry sediment (g). Species diversity (Shannon index; *H*) was calculated using the paleontological statistical software (PAST; Hammer et al., 2009).

3.3.2 Coccolith fraction Sr/Ca measurements

For sediment core MD96-2077, we used the CF Sr/Ca record published in Bard and Rickaby (2009). Sites 1264/1266 were analyzed for Sr/Ca of multi-species CF (< 20 µm-fraction) following the procedure described in detail in Fink et al. (2010). Sample cleaning was based on a combined mechanical and chemical treatments by Bairbakhish et al. (2010): 1) a small amount (~0.8 g) of sediment was wet-sieved at 20 µm-mesh with buffered water; 2) sodium hypochloride (NaClO) and hydrogen peroxide was added to the solution, disaggregated by ultrasonication, and filtered using 0.45 µm cellulose to get rid of the organic matter component of the sediments; 3) the sediments from the filter were transferred to a tube and brought into suspension with 50 mL hydroxyl ammonia chloride (MNX solution) to reduce Fe and Mn oxyhydroxides that scavenge metals from sea water and contain non-carbonate Sr; and 4) after 24 hr in a mechanical shaker, the MNX solution was then removed and the sample was cleaned by repeated filtration using buffered water.

After cleaning, a portion of the sample (0.3 mg) was used for elemental analysis. Measurement was performed using a simultaneous axial inductively coupled plasma optical emission spectrometry (ICP-OES) at the MARUM, University of Bremen. A defined standard solution was analyzed every five samples. The deviations between each standard measurement were used as a correction factor, allowing a precision better than 2%.

3.3.3 Preservation and productivity estimations

The influence of carbonate dissolution to the coccolith assemblage was assessed following the dissolution index (CEX') by Dittert et al. (1999) using the relative abundances of selected taxa. Here we modified the equation to include *Gephyrocapsa ericsonii*, another small and fragile taxon. The original CEX' index was based upon the differential preservation behavior between *Emiliana huxleyi*, a coccolithophore species exhibiting delicate coccoliths with fragile t-shaped elements and the dissolution-resistant *Calcidiscus leptoporus*, a species that makes larger strongly calcified coccoliths. This modified equation was already used in Boeckel and Baumann (2004) in a core from the South Atlantic, where a shift in the abundances between *G. ericsonii* and *E. huxleyi* at 70 kyr was recorded. The modified formula that we used is: $CEX' = (E. huxleyi + G. ericsonii) / (E. huxleyi + G. ericsonii + C. leptoporus)$.

Estimated primary productivity (EPP) expressed in grams of carbon ($\text{g C/m}^2/\text{yr}$) was calculated from the relative abundance of *Florisphaera profunda*, a species known to have an affinity for oligotrophic surface water and deeper nutricline (Beaufort, 1996): $\text{EPP} = 617 - [279 * \log (F. profunda) + 3]$. Because of the overwhelming abundance of *G. caribbeanica* in the lower part of the South Atlantic core (Site 1266), we have excluded the contribution of this species and recalculated the relative abundances of the other taxa accordingly. The dominance of *G. caribbeanica* can potentially mask the contribution of other species in the record, hence could lead to anomalous EPP values.

3.3.4 Coccolithophore indicative species

The cumulative abundance of minor coccolithophore taxa *Syracosphaera pulchra*, *Rhabdosphaera clavigera*, *Umbilicosphaera* spp. (*U. foliosa*, *U. sibogae*), *Calciosolenia* spp., *Oolithotus fragilis*, and *Umbellosphaera tenuis* at Site 1266 was used here as Agulhas Current taxa. In Marino et al. (2014), the sum of these species was considered warm water proxy, indicating warmer and oligotrophic surface waters and presence of tropical to subtropical waters in the South Atlantic. The Agulhas Current is a large water mass of warm and saline water from the southern tip of South Africa, and the abundance of the warm-water taxa at Site 1266, situated within the Agulhas leakage path can theoretically reveal influence of the Agulhas Current. Moreover, the above-mentioned species are found in oligotrophic tropical to subtropical waters (e.g., Winter et al., 1994; Baumann et al., 2004; Boeckel and Baumann, 2004; Marino et al., 2014). Additionally, *C. leptoporus* (small + intermediate) is used here as warm-water proxy while the oligotrophic species *Umbellosphaera* spp. is indicative of low surface water productivity conditions in the studied regions.

3.4 Results

3.4.1 Age model and site correlation

We used the age model constructed by Rickaby et al. (2007) for MD96-2077, which was based upon the last three geomagnetic reversals and tuning of the foraminiferal $\delta^{18}\text{O}$ record (Rau et al., 2006) to the benthic foraminiferal $\delta^{18}\text{O}$ stack (Lisiecki and Raymo, 2005). The chronologies at Sites 1264/1266, on the other hand were established by correlating

the coccolith fraction (CF; 20 μm) $\delta^{18}\text{O}$ curves of these cores obtained for this study, with the benthic foraminiferal $\delta^{18}\text{O}$ stack (Lisiecki and Raymo, 2005) and to the CF $\delta^{18}\text{O}$ record of MD96-2077 (Rickaby et al., 2007), using Analyseries 1.1 (Paillard et al., 1996).

The measured CF $\delta^{18}\text{O}$ values reveal 3.0 to -1‰ excursions from the base to the top of the records, reflecting short-term fluctuations at the glacial/interglacial variability, with the MD96-2077 core showing slightly heavier CF $\delta^{18}\text{O}$ values than the two ODP sites from the South Atlantic (**Figure 3.2a**). The generated age model (**Figure 3.2**) shows a continuous sedimentary succession of the uppermost 3 m of cores from Sites 1264/1266 spanning the last ~500 kyr, covering marine isotope stage (MIS) 12 to MIS 1. The South Atlantic Ocean sites record low sedimentation rates, with values ranging from 0.25 to 2 cm/kyr (**Figure 3.2c**).

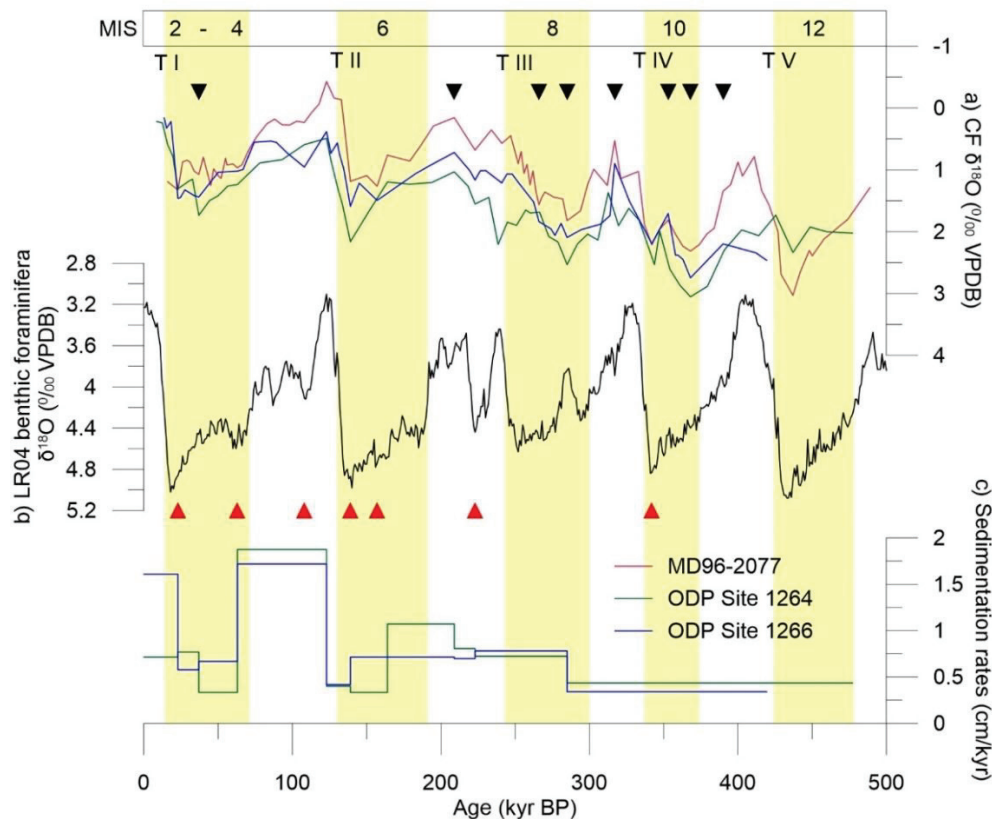


Figure 3.2: Age model and sedimentation rates of the investigated cores: **(a)** plots of coccolith fraction (CF) $\delta^{18}\text{O}$ of Site 1264 (green) and Site 1266 (blue) tied to CF $\delta^{18}\text{O}$ of MD96-2077 (Bard and Rickaby, 2009; pink); **(b)** benthic foraminiferal $\delta^{18}\text{O}$ stack (Lisiecki and Raymo, 2005; LR04); and **(c)** calculated sedimentation rates of Sites 1264 and 1266. Tie-points used for tuning are shown by triangles: black (Site 1266 vs MD96-2077) and red (Site 1266 vs LR04). Glacial stages are marked by yellow bands with Terminations (T).

3.4.2 Coccolith total concentration, preservation and diversity

The total coccolith concentrations in the two study sites show similar trend, with highest concentrations and greater amplitude from MIS 12 to MIS 8, and lower from MIS 7 to MIS 1 (**Figure 3.3a**). A general decrease in the total concentrations is observed during glacial terminations for both sites while maxima are recorded during interglacial episodes, although peaks are also observed during the glacial periods for MD96-2077 (MIS 12, 10, 8). Highest concentrations of 8648×10^7 CC/g. sed. and 6434×10^7 CC/g. sed. are recorded for the MD96-2077 core at ~400 kyr and for Site 1266 at ~300 kyr, respectively.

Species diversity at MD96-2077 core is highly variable throughout the studied time interval, with highest diversity during MIS 8, 6 and 4 (**Figure 3.3b**). Lowest coccolith diversity for this location is observed during interglacial periods (MIS 9, 7 and 1) and Terminations (T) V and T II. These episodes are coincident with a general poor preservation as shown by low CEX' values, especially during T II, and persisting through the middle of MIS 5 at the MD96-2077 core (**Figure 3.3c**). However, better preservation is recorded in this area compared to Site 1266, although with similar preservation degree recorded during MIS 11 and MIS 5.

An increase in the overall low coccolith diversity is documented at Site 1266 during MIS 8, when diversity reaches maximum peak and continues toward the Holocene, but interrupted by a minimum at the transition to MIS 7 (**Figure 3.3a**). The coccolith diversity at this site appears to be anti-correlated to the total coccolith concentrations, having low diversity with high coccolith concentration and high diversity with low coccolith concentration, while it parallels with the CEX' pattern (**Figures 3.3b** and **3.3c**).

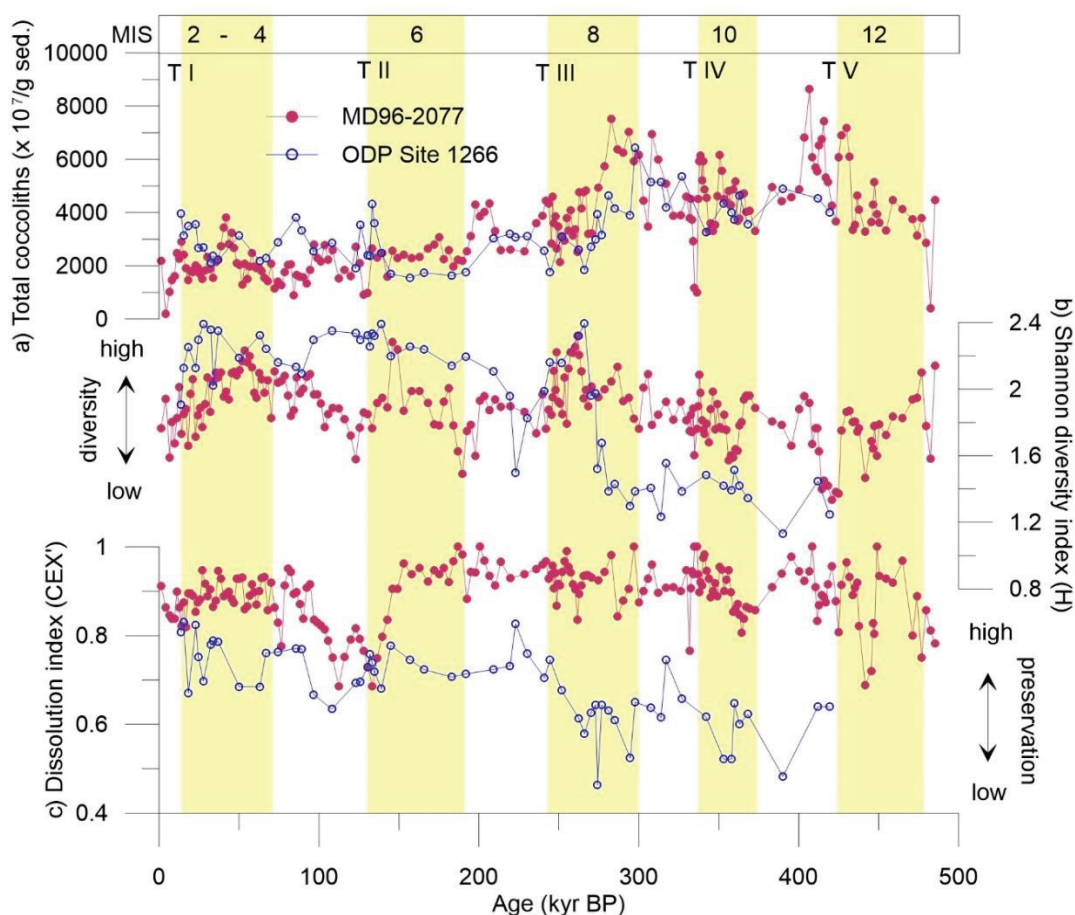


Figure 3.3: Total coccolith concentrations, diversity and preservation in sediment cores MD96-2077 and Site 1266: **(a)** total coccolith concentrations, **(b)** Shannon diversity index (H) and **(c)** coccolith dissolution index (CEX'). Glacial stages are marked by yellow bands with Terminations (T).

3.4.3 Coccolith relative abundances and absolute concentrations

A total of at least 27 (MD96-2077) and 25 (Site 1266) species and species groups were identified in the investigated areas comprising of taxa typical of tropical to subtropical setting. The assemblages contain rich biota characteristic of the tropical environment such as *C. leptopus*, *F. profunda*, *G. oceanica*, *Helicosphaera carteri*, *Umbilicosphaera* spp. and *Umbellosphaera* spp., and abundance of subtropical taxa typified by *G. muelleriae* and common occurrences of *Coccolithus pelagicus* in the records.

Differences in the species dominance for the two sites are recorded (**Figure 3.4a** and **3.4b**), given the different hydrographic settings of the studied cores. The most abundant species in the Indian Ocean core (MD96-2077) are *F. profunda* (mean relative abundance of 31%) and *G. oceanica*, (mean 17%) comprising of up to 55% and 63% of the total assemblage, respectively. On the other hand, *G. caribbeanica* is the dominant species at

Site 1266 (mean 24%), with highest relative abundance of 72%. *Florisphaera profunda* is the second dominant species in the MD96-2077 core but was found to only comprise up to 14% at Site 1266. Other dominant species at MD96-2077 core are *G. caribbeanica* (up to 54%), small *Gephyrocapsa* (up to 50%) and *E. huxleyi* (up to 41%) while small *Gephyrocapsa* (up to 65%), *E. huxleyi* (up to 52%), *C. leptoporus* (up to 24%) and *G. muelleriae* (up to 19%) are the major contributors at Site 1266.

Gephyrocapsa oceanica is the most abundant species in terms of coccolith concentrations in MD96-2077 core, with maximum of 4561×10^7 CC/g. sed. (**Figure 3.4c**). This species is only abundant from 300 (MIS 12) to 250 kyr (MIS 8) and is considered a minor species from MIS 7 to MIS 1. High coccolith numbers are recorded during interglacial periods (MIS 11 and 9) and low abundances are observed during glacial episodes (MIS 12 and 10). At Site 1266, *G. oceanica* absolute numbers are far lower than in the Indian Ocean core, with concentrations from 9 to 108×10^7 CC/g. sed. (mean 43×10^7 CC/g. sed.). This species registers a relatively stable abundance throughout the record, with increased concentrations during terminations and interglacial periods at this site.

Likewise, *G. caribbeanica* shows significant contribution to the coccolith numbers from MIS 12 to 8, with a mean relative abundance of 281×10^7 CC/g. sed. at MD96-2077 core (**Figure 3.4d**). Increased concentrations of this species are recorded during glacial stages with consistent high abundances during the entire MIS 12 and reaching maximum of 1967×10^7 CC/g. sed. at 447 kyr. Higher concentrations of this species are recorded at Site 1266, with mean relative concentrations of 1563×10^7 CC/g. sed. Peak abundances are recorded during the onset of glaciation at MIS 10 (390 kyr) and MIS 8 (298 kyr), with highest concentrations of 3533×10^7 CC/g. sed. and 4553×10^7 CC/g. sed., respectively. The reversal of this species with *E. huxleyi*, which was observed by Thierstein et al. (1977) in the Atlantic Ocean at 85 to 73 kyr is not found in the record. Nevertheless, we found the start of the continuous decline of this species during T III (250 kyr) both for the Indian Ocean and South Atlantic sites.

Three stages in abundance shift of the cool water species *G. muelleriae* can be recognized at both locations, with higher concentrations at Site 1266 (**Figure 3.4e**). From the bottom of the core to the end of MIS 8, higher concentrations are recorded for both sites with mean absolute concentrations of 236×10^7 CC/g. sed. and 401×10^7 CC/g. sed., at core MD96-2077 and Site 1266, respectively. This high concentration is followed by an

evident decline in *G. muelleriae* concentrations from mid-MIS 8 to mid-MIS 6, reaching lowest abundances in both locations. *Gephyrocapsa muelleriae* recovers and starts to gradually increase for the latter half of MIS 6 to the Holocene, although interrupted by another distinct low abundance during MIS 5.

A general opposing pattern is observed in the abundances of small *Gephyrocapsa* between MD96-2077 and Site 1266 cores from MIS 12 to MIS 5 (**Figure 3.4f**). Higher concentrations of this species group, with decreased abundances during glaciations and terminations are recorded in MD96-2077 (mean 840×10^7 CC/g. sed.) from MIS 12 to 5 compared to Site 1266 core (mean 23×10^7 CC/g. sed.). On the contrary, small *Gephyrocapsa* abundance at Site 1266 shows peak during interglacial stages, with highest concentrations of 1997×10^7 CC/g. sed. at 223 kyr (MIS 7) and 1490×10^7 CC/g. sed. at 86 kyr (MIS 5). During MIS 5 to MIS 4 transition, this species is replaced by *E. huxleyi* in both records, registering lowest abundances and almost entirely disappearing in the record toward the present day. This reversal is also recorded in the Indian Ocean sediment cores (e.g., Flores et al., 1999; Andruleit et al., 2008; Tanguan et al., 2017) and can be coincident with the *G. caribbeanica* - *E. huxleyi* reversal event recorded by Thierstein et al. (1977).

At ~290 kyr, *E. huxleyi* was first recorded at MD96-2077 core and Site 1266, with absolute numbers ranging from 17 to 915×10^7 CC/g. sed. (mean 282×10^7 CC/g. sed.) for MD96-2077 core and 5 to 2063×10^7 CC/g. sed. (mean 443×10^7 CC/g. sed.) for Site 1266 core (**Figure 3.4g**). In both locations, *E. huxleyi* abundances gradually increase toward the present, with the highest concentrations starting from 70 kyr, although with higher abundances at Site 1266.

Another species with higher concentrations at Site 1266 is *C. leptoporus* (mostly small and intermediate forms), with absolute concentrations ranging from 172 to 701×10^7 CC/g. sed. (mean 390×10^7 CC/g. sed.) (**Figure 3.4h**). A notable decline in the concentration of this species during the glacial periods is observed at this location, especially during MIS 6 and 4, when it interrupts the high concentrations from 260 to 209 kyr and from 139 kyr to the Holocene. This species displays high variability in terms of absolute concentrations at MD96-2077 core (mean 83×10^7 CC/g. sed.), with abundances that are consistently lower than at Site 1266. Similarly, low concentrations of this species are recorded during MS 6 and 4 at MD96-2077 core.

The deep-photoc zone species *F. profunda* registers high absolute concentrations at MD96-2077 core, ranging from 81 to 1939 x 10⁷ CC/g. sed. (mean 933 x 10⁷ CC/g. sed.) and with high amplitude change in abundance (**Figure 3.4i**). *F. profunda* consistently records maxima during interglacial stages while a distinct decline in its abundance is recorded during the glacial periods (MIS 10, 8, 6 and 4). Although much lower in concentration, *F. profunda* at Site 1266 is found to be increasing toward the Holocene, with concentrations ranging from 45 to 518 x 10⁷ CC/g. sed. (mean 208 x 10⁷ CC/g. sed.). A gradual increase in the abundance of this species is observed toward the end of MIS 5, and reaching maximum during TII.

Umbilicosphaera sibogae mean absolute abundance at MD96-2077 core is 55 x 10⁷ CC/g. sed., showing highest concentrations during interglacial periods (MIS 11, 7, 5, 3) (**Figure 3.4j**). The concentration of this species at this location is highly variable and almost similar in magnitude all throughout the studied interval. At Site 1266, this species displays lower concentrations from 419 to 145 kyr and higher concentrations from 139 kyr toward to Holocene. Peak abundances of this species are recorded during deglaciations and interglacial stages, with highest abundance during T II and T I, reaching maxima of 281 x 10⁷ CC/g. sed. and 256 x 10⁷ CC/g. sed., respectively.

3.5 Discussion

3.5.1 Fluctuations in coccolithophore productivity

Comparison of coccolithophore fluctuations between the study sites situated within two different oceanographic regions reveals regional characteristics distinct to each other, as well as similarities within the records. The abundances of tropical species, such as *F. profunda*, *G. oceanica* and *Umbellosphaera* spp. reflect warm tropical conditions with temperature higher than 17°C in both regions (**Figure 3.4**). The tropical Agulhas Current can be distinguished from the subtropical water by the latter, having temperature of less than 17°C (Hutson, 1980). Thus, the incursions of cool water species such as *G. muellerae* and *C. pelagicus* at certain intervals, specifically during the glacial intervals suggest influence of cooler subtropical surface waters in the two locations. Overall, the species compositions in core MD96-2077 (Natal Valley) and Site 1266 (Walvis Ridge) are in good correspondence with other studies conducted in the Indian Ocean (e.g., Flores et al., 1999;

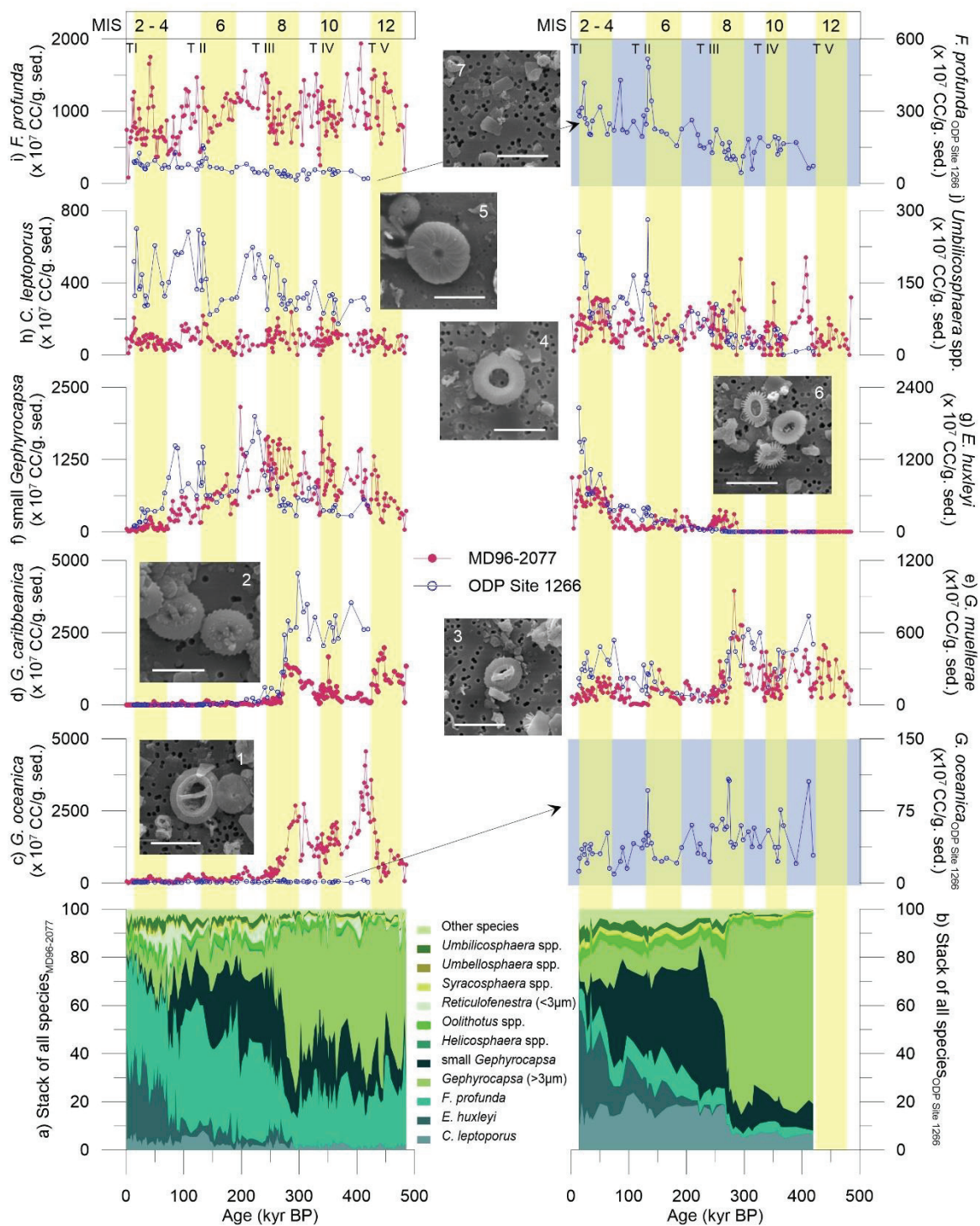


Figure 3.4: Coccolithophore relative abundance (shades of green) and absolute concentration records of MD96-2077 (pink) and Site 1266 (blue): (a) stack of all species in core MD96-2077; (b) stack of all species at Site 1266; (c, 1) *Gephyrocapsa oceanica*; (d, 2) *G. caribbeanica*; (e, 3) *G. muelleriae*; (f) small *Gephyrocapsa*; (g, 6) *Emiliania huxleyi*; (h, 5) *Calcidiscus leptoporus*; (i, 7) *Florisphaera profunda*; and (j, 4) *Umbilicosphaera* spp. Glacial stages are marked by yellow bands with Terminations (T).

Andruleit et al., 2008; Mejia et al., 2014; Tangunan et al., 2017) and the South Atlantic (e.g., Giraudeau, 1992; Baumann et al., 2004; Baumann and Freitag, 2004; Boeckel and Baumann, 2004). Limited coccolithophore studies in surface and downcore sediments associated with the Agulhas Current showed dominance of *E. huxleyi*, *G. oceanica*, *C. leptoporus* and *U. sibogae* (Fincham and Winter, 1989; Winter and Martin, 1990; Flores et al., 1999). Abundances of these species were also observed by Friedinger and Winter (1987) in the living coccolithophore assemblage of the Agulhas Current. The abundance of *F. profunda* in core MD96-2077 indicates a deeper nutricline/thermocline with a more oligotrophic surface water conditions in the subtropical Indian Ocean in comparison to the more productive and well-mixed water column conditions in the South Atlantic, as evidenced by much lower abundance of this species at Site 1266. The Walvis Ridge is not directly affected by the Benguela upwelling but it could be that the intensified upwelling in the coastal region has widened the filamentous zone of high nutrients (Lutjeharms and Stockton, 1987), reaching our study site and enhancing the surface water productivity. This is shown by increased abundances of coccolithophore taxa with affinity for enriched surface water conditions such as *G. caribbeanica*, *G. muelleriae* and small *Gephyrocapsa*. These species were found in high abundances and typical of the Benguela upwelling region (Giraudeau, 1992; Boeckel and Baumann, 2004; Baumann et al., 2008). However, despite of the higher concentrations of these species in the Walvis Ridge than in the Natal Valley, these concentrations are still lower compared to the more productive regions directly within the influence of the Benguela upwelling system (e.g., Baumann and Freitag, 2004; Boeckel and Baumann, 2004; Boeckel et al., 2006) (**Figure 3.5c**).

These records also show synchronous pattern with the 100-kyr cyclicity, which corresponds to the glacial/interglacial orbital eccentricity (**Figure 3.5b**). A study by Bard and Rickaby (2009) on the same core from the Indian Ocean (MD96-2077) suggested similar cyclicity in the SST record reconstructed from coccolithophore alkenones, which the authors linked to the migration of the STF (**Figure 3.5a**).

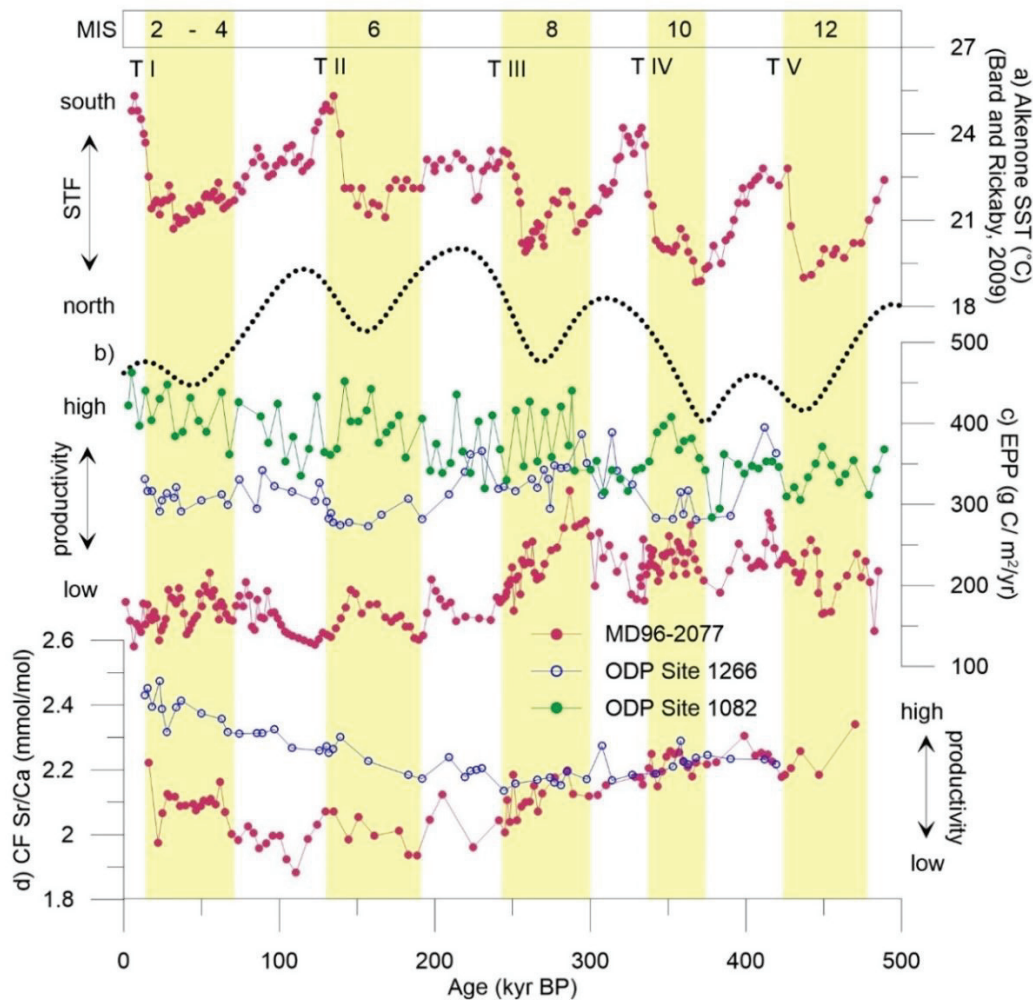


Figure 3.5: Productivity records of sediment cores off South Africa: (a) sea surface temperature reconstructed from alkenones at MD96-2077 indicating the position of the subtropical front (Bard and Rickaby, 2009); (b) orbital eccentricity (Berger, 1992); (c) estimated primary productivity (EPP) calculated from % *Florisphaera profunda* of the investigated sites with EPP values at ODP Site 1082 (Baumann and Freitag, 2004); (d) Coccolith fraction (CF) Sr/Ca records at Site 1266 correlated with data from MD96-2077 by Rickaby et al. (2007). Glacial stages are marked by yellow bands with Terminations (T).

3.5.2 Northward migration of the subtropical front enhances glacial coccolithophore productivity

Previous studies suggested that the migration of the STF, which is controlled by the strength and position of the atmospheric winds (Bard and Rickaby, 2009), plays a critical role in marine plankton communities by altering the physical and chemical properties of water masses (e.g., Findlay and Flores, 2000; Bard and Rickaby, 2009; Mejia et al., 2014; Romero et al., 2015) (Figure 3.5a). Our study areas in the Indian-Atlantic Ocean gateway are both in positions affected by this migrating front, which we suggest to have modulated

the strengths of the Agulhas Current and the Benguela Current, and played a critical role in nutricline/thermocline depths and nutrient availability in both regions. Here we therefore postulate that the fluctuations in coccolithophore productivity over the last 500 kyr are driven by the movement of the STF and associated changes in the water column characteristics.

The long-term productivity variations in the two study sites shown by the estimated primary productivity (EPP) and coccolith fraction (CF) Sr/Ca show substantially higher values at Site 1266 (Walvis Ridge) than in core MD96-2077 (Natal Valley), indicating that higher productivity conditions have prevailed in the South Atlantic than in the Indian Ocean over the last 500 kyr (**Figures 3.5c** and **3.5d**). However, the Walvis Ridge is still comparatively low, in contrast to the highly productive region of the South Atlantic where coastal upwelling occurs (ODP Site 1082; Baumann and Freitag; 2004) (**Figure 3.4b**). Moreover, the Natal Valley core reveal similar productivity pattern to the ODP Site 1082 (off Namibia), i.e., enhanced surface water productivity during the glacial intervals and reduced productivity during the interglacial periods (**Figure 3.5c**). Particularly, in the Natal Valley, two distinct phases of productivity change based on the EPP values are recognized (**Figure 3.5c**): the interval from MIS 12 to the end of MIS 8 (T III) and the interval from MIS 7 to the Holocene. We observed productivity peaks during the glacial periods, with maxima during stages 8 and 10, which is in accordance with the CF Sr/Ca record of the same sediment core in Bard and Rickaby (2009). The authors interpreted this result as a productivity signal driven by the northward migration of the STF during the glacial periods. The cooler SSTs and high surface water productivity conditions during this time (Bard and Rickaby, 2009) could have resulted from the shallowing of the nutricline/thermocline, which was further enhanced by the inflow of the cold, nutrient rich surface water of the sub-Antarctic surface waters (SASW). These cold conditions have led to the increased abundances of the cooler water species *G. muelleriae* in the record (**Figure 3.4e**).

Similarly, we found peak abundances of *G. caribbeanica* during the glacial stages 12, 10 and 8 in the Natal Valley core (**Figure 3.4d**), in agreement with the findings of Flores et al. (1999) from a core recovered off Cape Town. Although there was an overall understanding that the dominance of *G. caribbeanica* in records up to ~280 kyr was due to phylogenetic evolution of this species (e.g., Bollmann et al., 1998; Flores et al., 1999; Baumann and Freitag, 2004), its ecological preference is still poorly understood. In our

record, the pronounced increase of this species during stages 12, 10 and 8 is proposed to be associated to higher productivity conditions during the glacial periods, as also shown by the increased EPP values. Compared to other glacial intervals, higher productivity conditions occurred in the Indian Ocean site during MIS 10 and 8 and in some periods of MIS 12. According to Bard and Rickaby (2009), the extreme glacial stages 12 and 10 was 6°C cooler than the Holocene, and characterized by enhanced productivity as shown by foraminiferal and coccolithophore assemblages. During this period, the STF was suggested to be at its northernmost position, migrating by at least 7° latitude and almost completely interrupting the transport of warm Agulhas Current waters into the South Atlantic (Peeters et al., 2004; Bard and Rickaby, 2009). However, during this interval, our results show increased abundances of coccolithophore taxa indicative of warm water conditions (*G. oceanica*, small *Gephyrocapsa*) in the Natal Valley and Walvis Ridge cores, which we regarded as influence of the Agulhas Current warm water transport. Interestingly, the enhancement of surface water productivity during the glacial periods is evidenced by greater productivity gradient between a core retrieved off Tanzania, an area that is outside the influence of the STF migration (Tangunan et al., 2017), and the Natal Valley (off Tanzania EPP-Natal Valley EPP; **Figure 3.6a**). Here consistently higher EPP values are registered in the Natal Valley during the glacial stages, with widest gradient during MIS 8 and 6.

The two productivity phases recorded in the Natal Valley can also be observed in the Walvis Ridge record, with high amplitude change during the first phase and relatively lower amplitude change toward the present (**Figure 3.5c** and **3.5d**). Here we observe an opposing productivity pattern with the Natal Valley core, i.e., lower productivity is registered during the glacial periods and higher during the interglacial stages. In particular, maxima in the EPP values are observed during stages 9, 7 and 5 while lower values are observed during stages 10, 8, 6 and 2-4 (**Figure 3.5c**). Furthermore, consistently higher productivity occurs in the Walvis Ridge than in the Natal Valley all throughout the investigated interval (**Figure 3.6b**). The productivity gradient between the two locations (Walvis Ridge EPP-Natal Valley EPP) show larger differences during the interglacial periods, and smaller gradient during the glacial intervals, which further supports the high productivity regime in the Natal Valley during these intervals.

In the South Atlantic, the northward STF shift could have intensified the Benguela Current, leading to higher productivity off Namibia compared to the Walvis Ridge (**Figure 3.6c**). This is shown by greater productivity gradient (ODP Site 1082 EPP-Site 1266), favoring productivity in the core off Namibia almost throughout the studied interval, except during interglacial stages 11, 9 and 7, which shows higher productivity in the Walvis Ridge. The higher productivity in the Walvis Ridge during the interglacial periods could be due to seaward lateral advection of nutrient-rich upwelled waters of the Benguela Current during the cessation of the coastal upwelling process (Giraudeau et al., 1993; Baumann and Freitag, 2004). The subtropical South Atlantic also receives the nutrient-enhanced SASW during the equatorward movement of the STF (Shannon et al., 1989), resulting to higher productivity in the region. The intensified Agulhas leakage during the interglacial periods on the other hand, could have created a more favorable conditions for the coccolithophores in the Walvis Ridge, leading to increased coccolithophore productivity in the location during these intervals (**Figure 3.6c**).

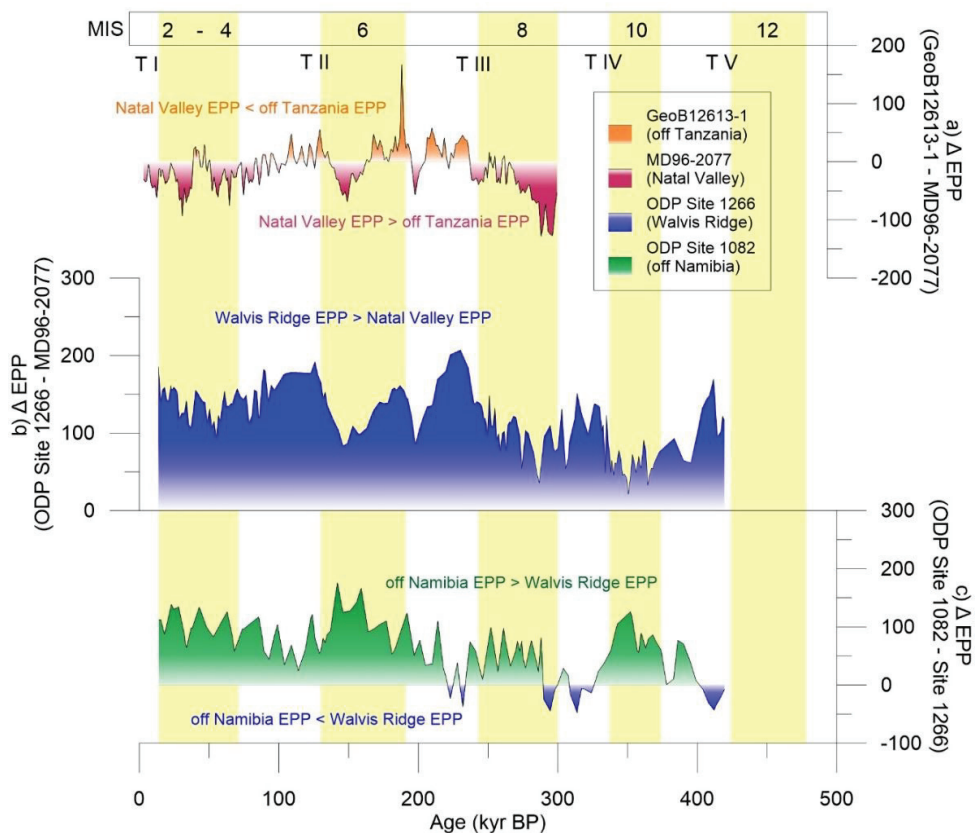


Figure 3.6: Differences in estimated primary productivity (EPP): (a) ODP Site 1255 and MD96-2077; (b) ODP Site 1082 data by Baumann and Freitag (2004) and MD96-2077; and (c) ODP Site 1082 and Site 1266. Glacial stages are marked by yellow bands with Terminations (T).

3.5.3 Timing and variability of warm-water leakage to the South Atlantic

The Agulhas Current has been a general feature of the south Indian Ocean since the mid-Tertiary (Martin et al., 1982), with the Agulhas leakage documented since the last 1.3 Myr (Peeters et al., 2004; Caley et al., 2012; Petrick et al., 2015). Maximum leakage is observed during glacial terminations based on the increased concentrations of warm water taxa, composed of *S. pulchra*, *R. clavigera*, *Umbilicosphaera* spp. (*U. foliosa*, *U. sibogae*), *Calciosolenia* spp., *Oolithotus fragilis*, and *U. tenuis* and *C. leptoporus* (small + medium) from Site 1266, which we used as indicators of the Agulhas warm water transport to the South Atlantic (**Figures 3.7c** and **3.7d**). Additionally, higher leakage is recorded during interglacial periods in our study site compared to full glacial episodes, consistent with the Agulhas leakage proxies of Caley et al. (2014) (**Figure 3.7a**), Peeters et al. (2004) (**Figure 3.7b**), and Petrick et al. (2015), showing greater leakage during interglacial periods and maxima at glacial terminations. A slight difference in the trends of the two coccolithophore groups indicative of the warm tropical Agulhas Current are also observed, especially during MIS 11 and the beginning of MIS 5, indicating that different environmental parameters other than temperature (e.g., nutrients), have controlled the coccolithophore distribution during these interglacial periods. A study by Dickson et al. (2010) at Site 1085, located close to the South African margin in the southeast Atlantic, suggested a stronger Agulhas leakage at the end of MIS 11 and further related this to the AMOC activity and wind forcing. A stronger Agulhas leakage during this time could have promoted more mixing in the water column, bringing nutrients to the surface that consequently led to a decline in the abundances of the warm water species, which are more adapted to oligotrophic water column (e.g., *Umbellosphaera* spp.). The relatively high concentrations of warm water taxa in the Natal Valley during the glacial periods indicate that the northward migration of the STF did not completely obstruct the Agulhas Current and transport of warm water to the South Atlantic. However, the northward shift could have reduced the Agulhas leakage, leading to a decline in warm water species abundances in the eastern South Atlantic site (ODP Site 1266) (**Figure 3.7c**). Nevertheless, the consistent occurrences of these warm water taxa in the study areas indicate that the Agulhas Current is a prevalent feature of the past 500 kyr, with reduced magnitude and leakage during the glacial intervals.

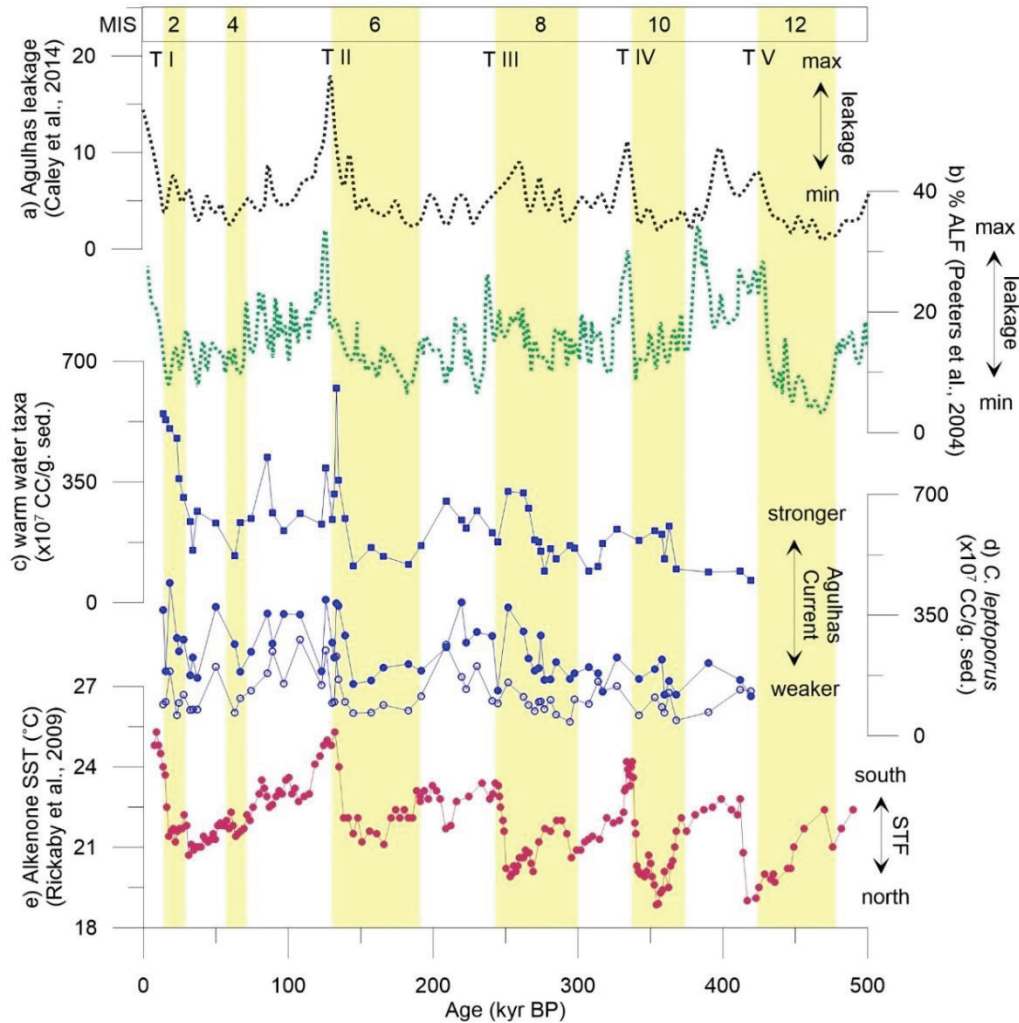


Figure 3.7: Paleoclimatological records of the southwest Indian Ocean and the eastern South Atlantic Ocean: **(a)** Agulhas leakage (Sv) variability based on model regression (Caley et al., 2014); **(b)** percent abundance of the Agulhas leakage fauna (Peeters et al., 2004); **(c)** Site 1266 warm water taxa composed of *Syracosphaera pulchra*, *Rhabdosphaera clavigera*, *Umbilicosphaera* spp. (*U. foliosa*, *U. sibogae*), *Calciosolenia* spp., *Oolithotus fragilis*, and *Umbellosphaera tenuis*; **(d)** Absolute concentrations of small and intermediate *Calcidiscus leptoporus*; **(e)** Sea surface temperature reconstructed from alkenones at MD96-2077 (Bard and Rickaby, 2009). Glacial stages are marked by yellow bands with Terminations (T).

3.6 Conclusions

Our coccolithophore-derived productivity reconstruction indicates that the latitudinal shifts of the subtropical front (STF) played a critical role in the nutricline/thermocline depths and nutrient availability in the Indian-Atlantic Ocean gateway over the last 500 kyr. Based on the coccolithophore-based proxies, we propose that the movement of the STF has modulated the strengths and magnitude of the Agulhas Current in the Indian Ocean and the Benguela Current upwelling in the South Atlantic, and

controlled coccolithophore productivity changes in the water column. As such, three major conclusions are drawn out of this study:

1. Higher concentrations of the deep-dwelling species *F. profunda* in the Natal Valley (MD96-2077) than in the Walvis Ridge (ODP Site 1266) suggest a deeper nutricline/thermocline with a more oligotrophic surface water conditions in the southwestern Indian Ocean than in the eastern South Atlantic.
2. Coccolithophore productivity in the investigated areas show glacial/interglacial variability, which is concurrent with the 100-kyr orbital eccentricity. The productivity fluctuations in the Natal Valley resembled variations in the Benguela upwelling region (ODP Site 1082), i.e., enhanced surface water productivity during the glacial episodes. This indicates that the northward shift of the STF during the glacial periods resulted to a weaker Agulhas Current and a more intense Benguela Current upwelling. The equatorward movement of the STF also allowed entrance of cold nutrient-rich SASW coming from the south, which have promoted higher surface water productivity that favored the abundance of the upper photic zone coccolithophore species. By contrast, higher productivity at the Walvis Ridge occurred during the interglacial periods, which could be a result of the seaward lateral advection of nutrient-rich upwelled waters of the Benguela Current during the weakening of the coastal upwelling process or by a localized upwelling event at the location.
3. The abundances of cooler water species (*G. muelleriae*) and warm water taxa (*S. pulchra*, *R. clavigera*, *U. foliosa*, *U. sibogae*, *Calciosolenia* spp., *Oolithotus fragilis*, *U. tenuis* and small + medium *C. leptoporus*) offered significant clues for understanding the dynamics of the Agulhas Current over the past 500 kyrs. In the Natal Valley, the increased abundances of *G. muelleriae* during the glacial periods reflect cooler surface water conditions driven by the northward STF migration. In the Walvis Ridge, greater abundances of the warm water taxa indicated warm water influx by the Agulhas Current. The consistent occurrences of the warm water taxa in both locations indicate that the Agulhas Current is a persistent feature of the past 500 kyr, although with reduced magnitude and leakage during the glacial intervals.

Acknowledgments

We are thankful to Jacques Giraudeau and Xavier Costa of EPOC UMR-CNRS, University of Bordeaux for providing us with the MD96-2077 samples. We thank Rüdiger Henrich and Mariem Pellitero-Saavedra for their constructive comments on the earlier drafts that have improved this manuscript. This work is part of the project Ocean and Climate 2: Land-ocean interaction and climate variability in low latitudes funded thru the DFG Research Center/Cluster of Excellence "The Ocean in the Earth System" MARUM. Data will be archived in the PANGAEA database (www.pangaea.de).

CHAPTER 4

The last 1 million years of the extinct genus *Discoaster*: Plio-Pleistocene environment and productivity at Site U1476 (Mozambique Channel)

Palaeogeography, Palaeoclimatology, Palaeoecology
(Tangunan et al., in preparation)

CHAPTER 4

The last 1 million years of the extinct genus *Discoaster*: Plio–Pleistocene environment and productivity at Site U1476 (Mozambique Channel)

Deborah Tanguan^a, Karl-Heinz Baumann^{a,b}, Janna Just^b, Stephen Barker^c, Ian Hall^c, Sidney Hemming^d, Leah LeVay^e and Richard Norris^f

^aUniversity of Bremen, MARUM - Center for Marine Environmental Sciences, 28359 Bremen, Germany; ^bUniversity of Bremen, Department of Geosciences, 28359 Bremen, Germany; ^dSchool of Earth and Ocean Sciences, Cardiff University Main Building, Park Place Cardiff Wales CF10 3AT, United Kingdom; ^dLamont-Doherty Earth Observatory, Columbia University, 61 Route 9W, Palisades NY 10964, USA; ^eInternational Ocean Discovery Program, Texas A&M University, 1000 Discovery Drive College Station, TX 77845, USA; ^fScripps Institution of Oceanography, University of California, San Diego, 9500 Gilman Drive, La Jolla CA 92093-0244, USA

4 Abstract

A detailed paleoenvironment reconstruction based on calcareous nannoplankton assemblage was conducted for the interval between 2.85 and 1.85 Myr, covering the period when successive extinction of the last five species of discoasters occurred. New productivity data obtained from the abundances of the *Discoaster* species (*Discoaster brouweri*, *D. triradiatus*, *D. pentaradiatus*, *D. surculus*, and *D. tamalis*) and other indicative calcareous nannoplankton taxa showed variations in frequencies, which were paced with the 100, 41, and 23 kyr orbital periodicities. Two stages of productivity change are observed, with major change at 2.4 Myr. This shift at 2.4 Myr could be correlated to the extreme climatic variability during the Pliocene that have initiated the onset of the Northern Hemisphere glaciation. Here we propose tropical Pacific forcing at Site U1476 as shown by the consistent occurrence of warm water taxa (*Calcidiscus leptoporus*, *Oolithotus* spp., *Rhabdosphaera clavigera*, *Syracosphaera* spp., *Umbellosphaera* spp.), typical of the Indonesian Throughflow surface waters. On the other hand, the occurrence of *C. pelagicus* and *C. braarudii* indicates influence of cold, nutrient-rich sub-Antarctic surface water. A more mixed water column that have initiated at 2.4 Myr, and consequent productivity increase led to the gradual reduction of the *Discoaster* species until extinction as shown by

the low values of the *F. profunda* index and high abundances of UPZ flora indicative of nutrient-rich surface waters conditions. High productivity at the location during this period could have been also amplified by a localized upwelling event driven by the Mozambique Channel eddies.

4.1 Introduction

Major climatic variability during the middle part of the Pliocene was first proposed by Shackleton et al. (1984) to have triggered the onset of the Northern Hemisphere (NH) glaciation. Succeeding studies have corroborated this claim on the basis of paleontological, sedimentological and geochemical records of long climate archives. Much of the evidence for this consensus came from the $\delta^{18}\text{O}$ and $\delta^{13}\text{C}$ of foraminifera (e.g., Raymo et al., 1992; Clemens et al., 1996; Ravelo et al., 2004), suggesting the significance of this phenomenon in the evolution of the Plio-Pleistocene climate. This extreme climatic variability was coupled by global-scale variations in the sea surface temperature (SST) (Clemens et al., 1996), which could have created a complex oceanographic regime, which in turn controlled changes in plankton distribution in the photic layer.

Calcareous nannoplankton (nannofossils) are single-celled, marine haptophyte algae that are one of the dominant calcifying plankton groups in the Indian Ocean (e.g., Friedinger and Winter, 1987; Stolz et al., 2015) and form a major part of its deep-sea sediments (e.g., Flores et al., 1999; Beaufort et al., 2001; Rogalla and Andruleit, 2005; Tangunan et al., 2017). These organisms commonly live in the photic layer where light intensity is strong enough to carry out photosynthesis and the nutrient levels are preferable for its growth. Their temporal and spatial distributions are controlled by latitude, ocean currents, and the characteristic nutrients, salinity and temperature profiles of the underlying water masses (Winter et al., 1994). They are sensitive to variations in water column characteristics, making them recorders of past environmental conditions.

The late Pliocene to the early Pleistocene is a significant time interval in calcareous nannoplankton evolution history due to a recorded decrease in diversity during this period (Bown et al., 2004; Aubry, 2007). High frequency variability in glacial/interglacial temperatures occurred during this interval, with the Pleistocene exhibiting greater variance compared to the late Pliocene (Ravelo et al., 2004; Lisiecki and Raymo, 2005). The gradual

cooling during the transition from the warm Pliocene to the cold Pleistocene (Ravelo et al., 2004) was proposed by Aubry (2007) to have driven the Pliocene nannoplankton turnover and subsequent extinction events.

The extinct genus *Discoaster* is one of the nannoplankton groups that were affected by these climatic fluctuations. This group exhibited a fairly continuous evolutionary development since the first occurrence of this genus during the late Paleocene (~60 Myr) to the extinction of the last species toward the end of the Gelasian stage (1.93 Myr). Previous works suggested that the inception of the NH glaciation during the Pliocene (Shackleton et al., 1984; Raymo et al., 1992; Clemens et al., 1996) led to the successive disappearance of *Discoaster* species (e.g., Backman and Pestiaux, 1987; Chapman and Chepstow-Lusty, 1997). While these extinction events are widely documented (e.g., Bukry, 1971; Chepstow-Lusty et al., 1989; Chapman and Chepstow-Lusty, 1997; Raffi et al., 2006), our knowledge of the ecological preference of the *Discoaster* species and the environment that they lived in before they disappeared from the geologic record is still limited (e.g., Bukry, 1971; Haq and Lohmann, 1976; Aubry, 1998; Schueth and Bralower, 2015). Furthermore, the reported diachronous occurrences (Raffi et al., 2006; Schueth and Bralower, 2015) of its member taxa at different regions suggest that *Discoaster* extinction could not be explained by SST variations alone (e.g., Chepstow-Lusty et al., 1989; Chapman and Chepstow-Lusty, 1997), but by a combination of complex environmental parameters (Schueth and Bralower, 2015). Discoasters are typified to have an affinity for warm water and oligotrophic conditions (Aubry, 1998; Bralower, 2002; Schueth and Bralower, 2015) and their extinction toward the end of the warm Pliocene can tell us about the magnitude of the global climatic change that happened during the Plio-Pleistocene transition.

Here we investigated the temporal distribution of the last five species of *Discoaster* (*D. tamalis*, *D. surculus*, *D. pentaradiatus*, *D. triradiatus*, *D. brouweri*) in the western Indian Ocean using materials from Site U1476 (Mozambique Channel) collected during the International Ocean Discovery Program (IODP) Expedition 361 – Southern African Climates (**Figure 4.1**) to reconstruct past changes in the environmental and productivity conditions that have led to the extinction of these species. Owing to its location, Site U1476 offers an exceptional opportunity for high-resolution paleoenvironmental and productivity reconstructions. The study area derives its warm and oligotrophic surface waters from the eastern Indian Ocean supplied by the Indonesian Throughflow (ITF) and is linked to the

Agulhas Current, the largest western boundary current that transports warm and saline surface waters to the Atlantic Ocean (Lutjeharms, 2006). We present here new records of productivity from the abundances of *Discoaster* species and compared our results with the downcore record of *Florisphaera profunda*, a widely used productivity proxy, and to other calcareous nannoplankton taxa with unique ecological preferences.

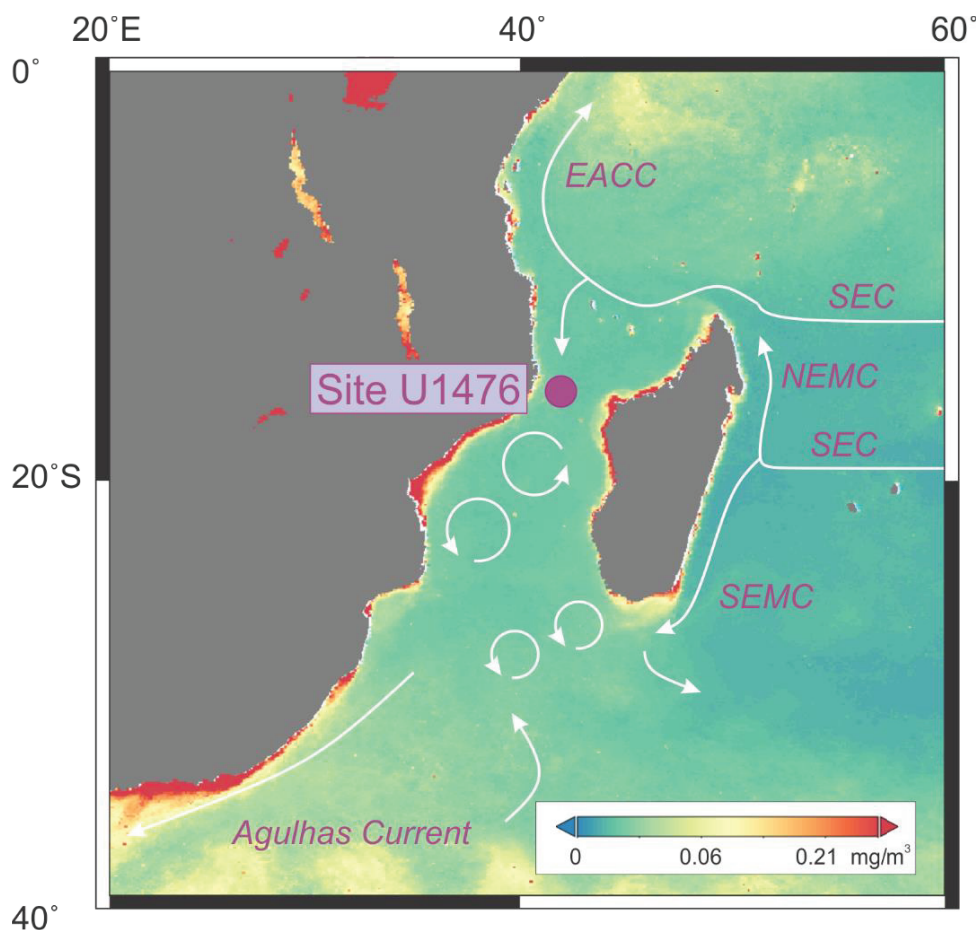


Figure 4.1: Location of IODP Site U1476 in the Mozambique Channel plotted on the 2010 average chlorophyll map, with the schematic illustration of surface water circulation: East African Coastal Current (EACC), Northeast and Southeast Madagascar Current (NEMC, SEMC); South Equatorial Current (SEC); and South Equatorial Countercurrent (SECC). Surface water circulation was redrawn from Beal et al. (2011). The chlorophyll map was generated using the Giovanni online data system developed and maintained by the NASA GES DISC (Acker and Leptoukh, 2007).

4.2 Site U1476 and oceanographic setting

Site U1476 lies on the Davie Ridge, a bathymetric high rise in the Mozambique Channel, between the African continent and Madagascar. The site is located at the northern entrance of the Mozambique Channel (15°49.25'S; 41°46.12'E; **Figure 4.1**) at a water depth

of 2165 m (Hall et al., 2016). The study area is presently influenced by seasonally reversing monsoon winds (boreal summer and winter), induced by the migration of the Intertropical Convergence Zone, with rainfall maxima during the boreal winter (Hastenrath et al., 1993). The sea surface current in the western Indian Ocean is in turn driven by the monsoon and semi-annual inter-monsoon trade winds (Indian Ocean equatorial westerlies).

The surface water at Site U1476 is being fed by the South Equatorial Current (SEC) that flows westward year-round across the Indian Ocean, carrying warm and oligotrophic surface water of the ITF (Schott et al., 2009; **Figure 4.1**). The SEC splits into two western boundary currents off the coast of Madagascar (Northeast and Southeast Madagascar Currents; NEMC and SEMC), with the NEMC breaching into northward and southward flows at the northern tip of Madagascar. The southward branch merges with the Mozambique Channel throughflow forming a set of anticyclonic eddies (Schott and McCreary, 2001; Schouten et al., 2003), affecting Site U1476. This southward flowing water mass was suggested to have major implications in the Agulhas Current, the largest western boundary current that transports salt and heat into the South Atlantic (Lutjeharms, 2006).

4.3 Material and methods

4.3.1 Sampling and age model construction

Samples were selected between 40 and 80 m depth on the stratigraphic splice, covering the Plio-Pleistocene boundary (calcareous nannofossil biozones NN15 to NN19; 2.85 to 1.85 Ma), focusing on the interval of *Discoaster* extinction. Using the shipboard chronology, a total of 269 samples were collected every ~15 cm, representing an average time resolution of ~5 kyr. The age model was established based on the refined biochronology of five *Discoaster* species (**Figure 4.2**).

Calcareous nannofossil assessment during the expedition showed abundant and well-preserved Plio-Pleistocene specimens, which offer reliable basis for precise chronological approximations of these *Discoaster* datum events. Additionally, three shipboard calcareous nannofossil bioevents were used to constrain the top and bottom of the selected interval: the top occurrence (T) of *Calcidiscus macintyre* (1.60 Myr), base (B) of *Gephyrocapsa* (>4 µm; 1.73 Myr), and the T of *Sphenolithus* spp. (3.54 Myr). The refined age model yielded sedimentation rates between 2.5 to 4 cm/kyr. This estimate agrees well

with the average sedimentation rate of ~ 2.5 cm/kyr at DSDP Site 242 (Simpson and Schlich, 1974), located ~ 5 km southeast of the study area, and with the shipboard estimate based on combined planktonic foraminifera and calcareous nannofossil stratigraphy (2.3 to 3.5 cm/kyr; Hall et al., 2016).

The uncertainty of this age model comes from the recorded global diachronous occurrences of some of the marker taxa. Only the top occurrences of *D. brouweri* and *D. triradiatus* are by far accepted as globally synchronous events (Bukry, 1971; Chepstow-Lusty et al., 1989; Chapman and Chepstow-Lusty, 1997; Raffi et al., 2006). Nevertheless, *Discoaster* extinction is a widely documented event of the Plio-Pleistocene, and thus provide age constraints on the investigated time interval. A detailed list of the identified calcareous nannofossil biostratigraphic events encountered at Site U1476 can be found in the [supplementary information](#).

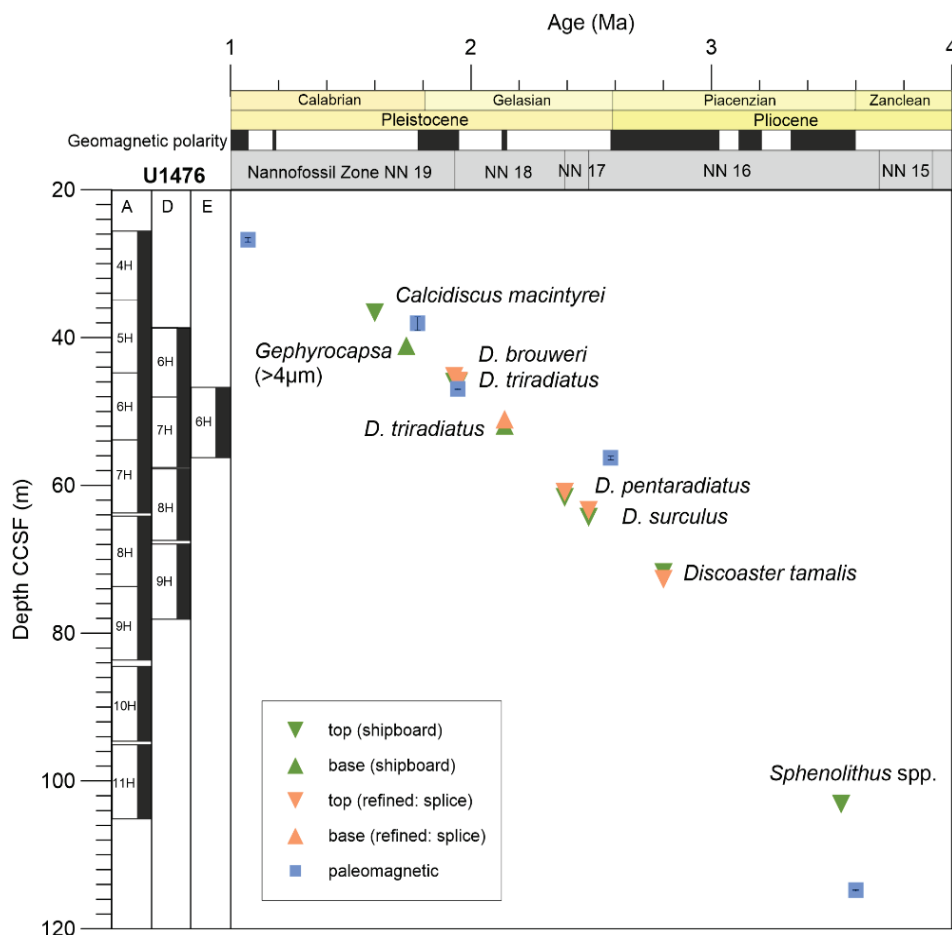


Figure 4.2: Age-depth relationships at Site U1476 showing the shipboard and refined calcareous nannofossil biochronology. Because of strong remagnetization during coring, depths of paleomagnetic data are approximately indicated but not considered in the age model construction. The five *Discoaster* datums occurred between the late Gauss and Olduvai. Only the base of Olduvai at 1.95 Myr corresponds to the calcareous nannofossil datum.

4.3.2 Species identification, abundance and biostratigraphy

Slides for calcareous nannofossil analysis were prepared following the drop technique by Bordiga et al. (2015). Quantitative analysis was performed with a Leica polarized light microscope under 1000 x magnification. Abundances were determined by counting at least 300 species per sample. Additional 10 to 20 fields of view (FOV) were counted to document uncommon and rare taxa. Minor reworking was observed, but when present, reworked specimens were counted separately. In each sample, the entire slide was scanned after counting to detect index taxa for refining the biostratigraphy. Supplementary smear slides were prepared for selected intervals to confirm biostratigraphic boundaries. The zonation schemes of Martini (1971; Codes NN) and Okada and Bukry (1980; Codes CN) were adopted for this study. Calcareous nannofossil datum events followed Gradstein et al. (2012). Preservation of species was assessed while counting using the criteria described in (Hall et al., 2017a).

Species taxonomic identification was based on Bolli et al. (1989), Bown (1998) and the electronic guide to the biodiversity and taxonomy of calcareous nanoplankton (Nannotax 3; <http://www.mikrotax.org/Nannotax3/>). The conversion of nannofossil counts into absolute number of nannofossils per gram of sediment (N/g. sed.) was calculated using the equation: $\text{Nannofossil concentration} = (N \cdot A) / (f \times n \times W)$, where N = total nannofossil counts; A = area of the coverslip (mm^2); f = area of FOV (mm^2); n = number of FOV counted; and W = weight of bulk dry sediment (g). Species diversity (Shannon index; H) was calculated using the paleontological statistical software (PAST). The Shannon index varies between 0 for populations with one species and high values for populations consisting of several taxa, each having few individuals (Hammer et al., 2009).

4.3.3 Indicative taxa for productivity and temperature

The genus *Discoaster* has been used as a warm water and low surface water productivity proxy (Backman and Pestiaux, 1987). This group is known to have an affinity for warm, oligotrophic and stratified water column conditions (Bukry, 1971; Haq and Lohmann, 1976; Aubry, 2007; Schueth and Bralower, 2015) and their extinction toward the end of the Pliocene is thought to be due to the intensified NH glaciation (Chapman and Chepstow-Lusty, 1997). In addition, cyclic patterns in the records of the Pliocene *Discoaster*

taxa were observed (e.g., Backman and Pestiaux, 1987; Chepstow-Lusty et al., 1989; Gibbs et al., 2004). Here we will use the abundances of these species as both productivity and sea surface temperature proxies.

Transfer functions based upon the abundance of the LPZ-dwelling taxon *F. profunda* were effectively used as proxies of past changes in the nutricline/thermocline depths in Quaternary sediments (e.g., Molfino and McIntyre, 1990; Ahagon et al., 1993; Flores et al., 1999) and in estimation of marine primary production (Beaufort et al., 1997; Beaufort et al., 2001). For this study, the estimated primary productivity (EPP) expressed in grams of carbon (g C/m²/yr) was calculated from the relative abundance of this taxon using the formula: $EPP = 617 - [279 * \log (\% F. profunda + 3)]$. This equation was calibrated by (Beaufort, 1996) using calcareous nannofossils from the Indian Ocean core top samples and modern primary productivity generated from satellite chlorophyll data by Antoine and Morel (1996). The EPP is used as a proxy for primary productivity because in contrast to other taxa, *F. profunda* prefer to thrive in the deep photic zone, where nutrients are comparatively abundant and light is rare (Molfino and McIntyre, 1990). Hence, high abundances of *F. profunda* indicate deeper nutricline/thermocline and low abundances of this species suggest otherwise. The ratio of this species to small placolith-bearing taxa (*F. profunda* index) was also used as water column stratification proxy (*F. profunda* index; Beaufort et al., 1997; Beaufort et al., 2001): $F. profunda \text{ index} = F. profunda / (F. profunda + \text{small } Gephyrocapsa + \text{small } Reticulofenestra)$. Low values of *F. profunda* index suggest a more mixed water column whereas values closer to 1 indicate a more stratified water column.

Two different morphotypes of the species *Coccolithus pelagicus* (*C. pelagicus pelagicus* and *C. braarudii*) were recognized and counted separately due to the reported differences in their ecological preferences. *Coccolithus pelagicus* is the small cold water type found in subarctic environments (Baumann et al., 2000) and used as an indicator of cool surface water (e.g., Marino et al., 2014). Parente et al. (2004) found this species together with high abundances of the planktonic foraminifera species *Neogloboquadrina pachyderma* (sinistral), another cold-water proxy and interpreted their joint occurrence to be linked to the influx of subpolar waters off western Iberia during Heinrich events. This species also registered distinct abrupt glacial peaks during the mid-Pleistocene transition in north Atlantic sediments (Marino et al., 2011). On the other hand, the large temperate

species *C. braarudii* was found in high productivity and upwelling region of the South Atlantic (Baumann et al., 2000).

4.4 Results

4.4.1 Plio-Pleistocene calcareous nannofossil stratigraphy

The age model used for this study is based on the refined shipboard calcareous nannofossil biostratigraphy. Six Plio-Pleistocene nannofossil datum events (Gradstein et al., 2012) were recognized at Site U1476 and the shipboard chronology of the five *Discoaster* taxa was refined (**Figure 4.2**). Index taxa are common in all the samples and are well-preserved, which allowed precise estimation of the calcareous nannofossil events.

Upper Pliocene (2.85 to 2.58 Myr)

The T of *D. tamalis* (2.8 Myr) in Sample U1476D-9H-4W, 6 cm (72.72 m CCSF) marks the CN12b/CN12a boundary within Biozone NN16. Other species such as *D. surculus*, *D. pentaradiatus* and *D. brouweri* are also present. *Discoaster asymmetricus* is recorded co-occurring with these taxa and disappeared at 2.54 Myr.

Lower Pleistocene (2.58 to 1.85 Myr)

The earliest Pleistocene event is recognized in Sample U1476A-8H-4W, 125 cm (63.42 m CCSF) based on the T of *D. surculus* (2.49 Ma), which marks the CN12c/CN12b boundary and the NN17/NN16 transition. The top of NN17 and CN12c are found in Sample U1476A-7H-5W, 108 cm (60.97 m CCSF), where the T of *Discoaster pentaradiatus* (2.39 Myr) occurs. The base common (Bc) occurrence of *D. triradiatus* (2.14 Myr) in Biozones NN18 and CN12d is identified in Sample U1476E-6H-3W, 147 cm (51.08 m CCSF) and its T (1.95 Myr) is recorded in Sample U1476D-6H-5W, 141 cm (45.89 m CCSF). The NN19/18 and CN13a/CN12d boundaries are determined by the T of *Discoaster brouweri* (1.93 Myr) in Samples U1476D-6H-5W, 81 cm (45.29 m CCSF).

4.4.2 Nannofossil assemblage composition, preservation and diversity

A total of 35 species and species groups comprising of tropical to subtropical taxa and occurrences of cold water species were identified. The Plio-Pleistocene assemblage is

generally well-preserved, with all the species identifiable at the species level. The assemblage at Site U1476 is dominated by the *Reticulofenestra* species (13 to 63%) and *F. profunda* (2 to 59%), with alternating dominance in the record (**Figure 4.3a**). This is followed by *Gephyrocapsa* spp. (up to 24%), *Discoasters* spp. (up to 17%), and *Pseudoemiliana lacunosa* (up to 15%). Other species that made significant contribution to the total assemblage are *Helicosphaera* spp., *Oolithotus* spp., *Umbilicosphaera* spp. and *Rhabdosphaera clavigera*.

Total calcareous nannofossil absolute concentrations show highly variable pattern throughout the studied time interval, with total concentrations ranging from 1729×10^9 to 7287×10^9 N/g sed. (**Figure 4.3b**). The Plio-Pleistocene transition (2.58 Myr) is characterized by reduction in both the total nannofossil concentration and species diversity (**Figures 4.3b** and **4.3c**). During the Pliocene, total concentrations strongly correspond to species diversity until transition to Pleistocene. The interval between 2.31 and 2.17 Myr is characterized by consistently low total nannofossil concentrations accompanied by increased diversity. Total nannofossils stayed at relatively similar level after the Plio-Pleistocene transition while species diversity immediately recovered.

4.4.3 Variations in *Discoaster* abundance

The oldest discoasters in the record, *D. tamalis* and *D. asymmetricus* show lowest concentrations, with maximum abundances of only up to 110×10^9 N/g sed. and 50×10^9 N/g sed., respectively (**Figures 4.4a** and **4.4b**). *Discoaster surculus* display a relatively constant abundance from 2.85 to 2.6 Myr, gradually increased at the beginning of MIS 103 and registering maximum concentration (289×10^9 N/g sed.) (**Figure 4.4c**). Its abundance then progressively decreased until it completely disappeared from the record at 2.49 Myr. Pattern of *D. pentaradiatus* matches *D. surculus* showing highest concentrations during the interglacial stages G11 (431×10^9 N/g sed.) and MIS 103 (386×10^9 N/g sed.) (**Figure 4.4d**). This species is the most abundant species in the investigated time interval. After 2.39 Myr, when the extinction of *D. pentaradiatus* occurred, only two members of this genus were left. *Discoaster triradiatus*, a short-lived species has evolved, with its base common occurrence placed at 2.14 Myr. Maxima in abundance of this species are recorded at MIS 81 (95×10^9 N/g sed.), MIS 78 (146×10^9 N/g sed.) and MIS 74 (131×10^9 N/g sed.) (**Figure**

4.4e). The second most abundant species in the record is *D. brouweri*, with highly variable abundance throughout the record (**Figure 4.4f**). Lower concentrations of this species is recorded until 2.58 Myr, when abundance is shared with other *Discoaster* taxa (*D. pentaradiatus*, *D. surculus*, *D. asymmetricus*, and *D. tamalis*). After the extinction of *D. surculus*, *D. brouweri* dominated the *Discoaster* assemblage. All these species show declining trends toward their respective demise from the record.

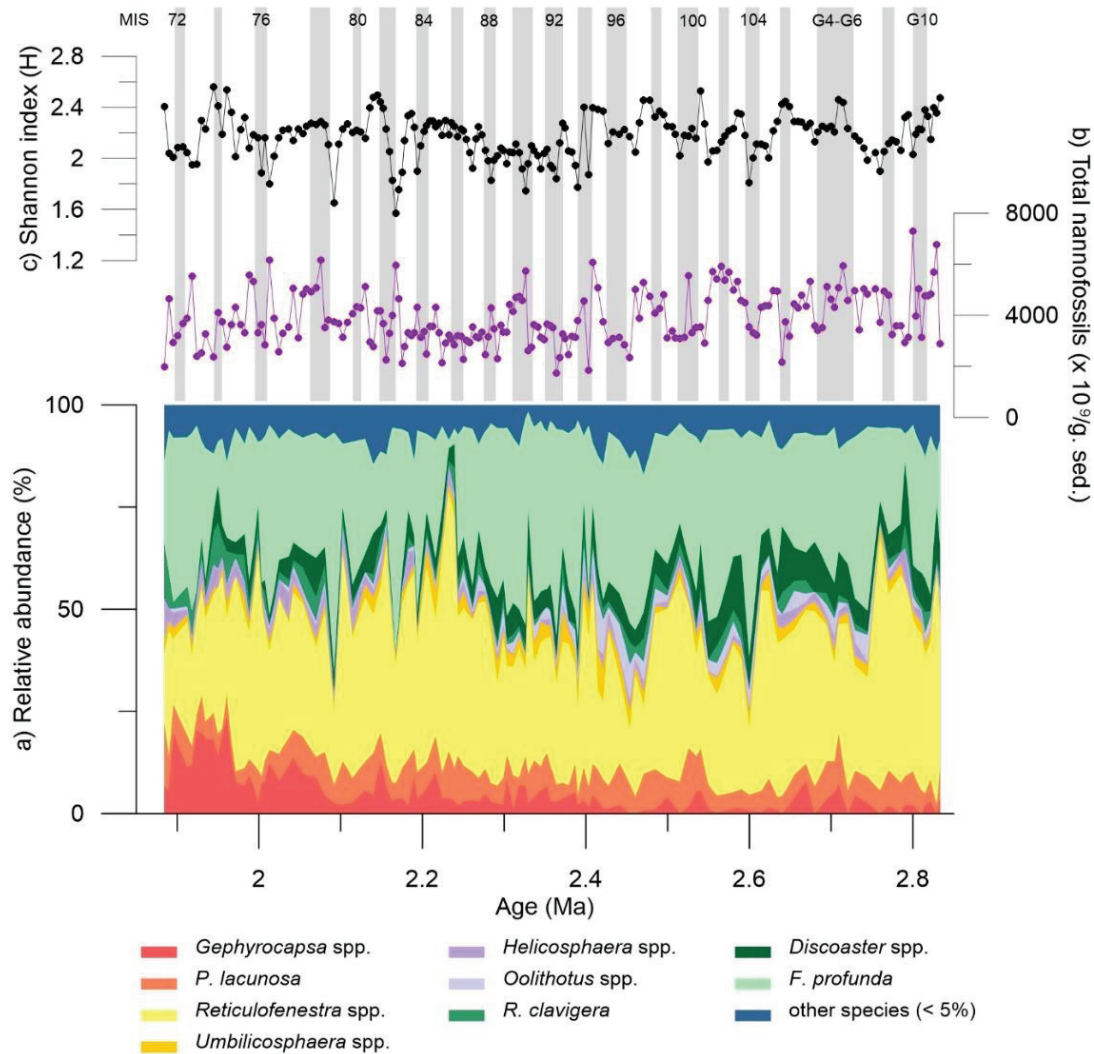


Figure 4.3: Calcareous nannofossils of Site U1476: (a) stack plot of all species; (b) total absolute nannofossil concentration per gram (g) of sediment; (c) Shannon diversity index (H). Glacial stages are marked by gray bars.

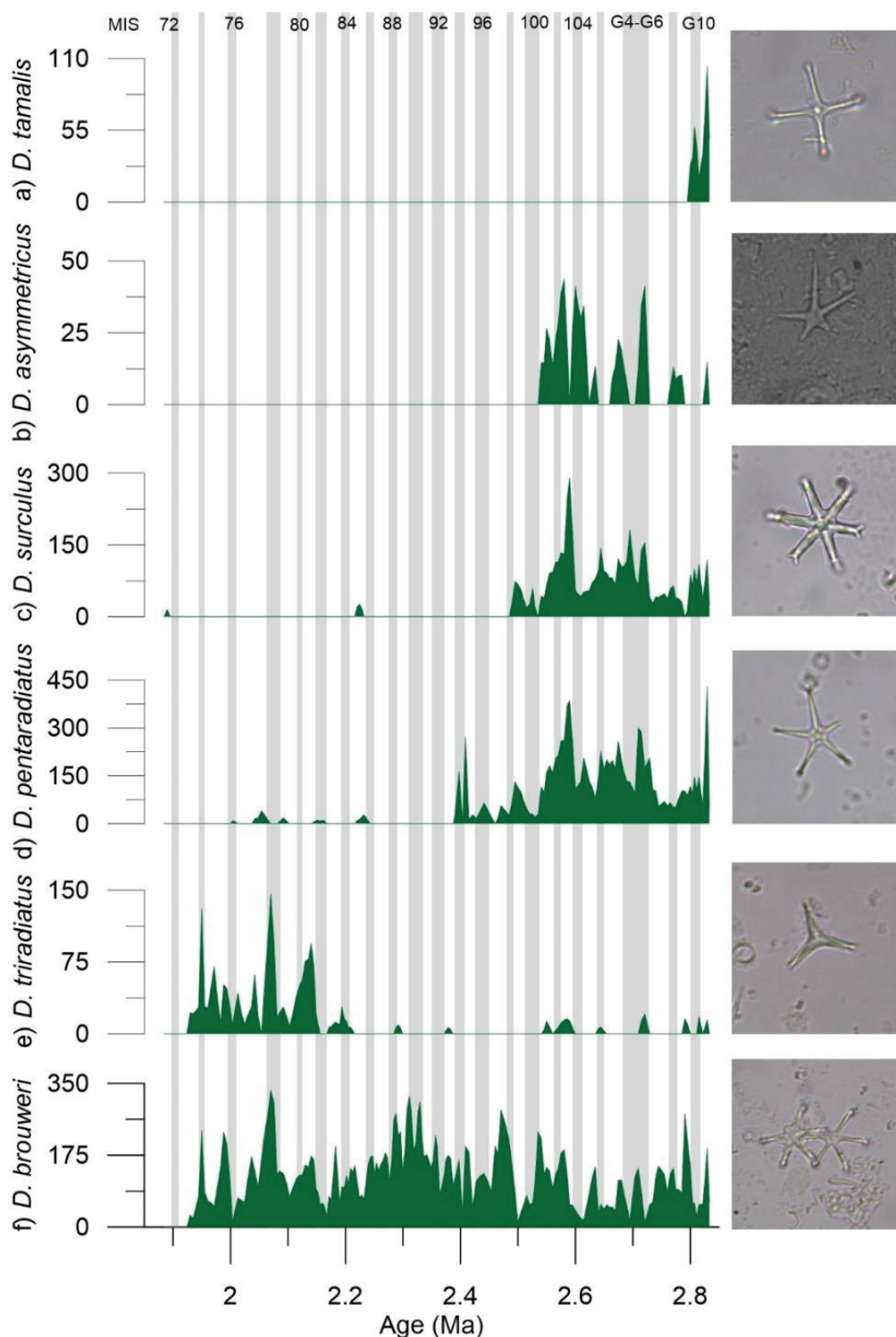


Figure 4.4: Absolute concentrations of the Plio-Pleistocene *Discoaster* species: (a) *D. tamalis*; (b) *D. asymmetricus*; (c) *D. surculus*; (d) *D. pentaradiatus*; (e) *D. triradiatus*; and (f) *D. brouweri*. All concentrations are expressed in number of nannofossils $\times 10^9$ /gram of sediment. Glacial stages are marked by gray bars.

4.5 Discussion

4.5.1 *Discoaster* extinction and paleoenvironment during the Plio-Pleistocene

The successive extinction of *Discoaster* species during the Plio-Pleistocene offers well-established biostratigraphic events (Bukry, 1971; Backman and Pestiaux, 1987), including our record from Site U1476. Efforts on the refinement of these datum events have progressed over the years, including astronomical calibration (e.g., Raffi et al., 2006; Agnini et al., 2017). While the Pliocene nannofossil chronology is rather less studied on a global scale compared to the Miocene or Pleistocene intervals (Raffi et al., 2006), the Plio-Pleistocene *Discoaster* extinction event is widely documented. Despite the reported uncertainties in using the individual datum due to diachronous first and last occurrences of its member taxa between oceans, there is still a general consensus that these group disappeared from the record during the transition from the warm Pliocene to the cold Pleistocene interval.

At Site U1476, a general reduction in the *Discoaster* abundance from 2.85 to 1.85 Myr is observed until it completely vanished from the record (**Figure 4.5c** and **4.6f**). This record contradicts the abundance pattern of the upper photic zone (UPZ) flora showing an increasing abundance towards 1.85 Myr (**Figure 4.5d**). Previous studies have suggested that some *Discoaster* species prefer the LPZ, a behavior similar to *F. profunda* (e.g., Aubry, 1998; Bralower, 2002). In particular, a recent study by Schueth and Bralower (2015) supported this finding through an ecological ordination technique, where the authors suggested that *D. brouweri* and *D. pentaradiatus* have favored a warm and stratified regime with deep nutricline. A distinct shift starting at 2.4 Myr is both observed in the *Discoaster* and UPZ records, after the transition from the Pliocene to the Pleistocene. The increase in abundance of the UPZ flora suggests nutrient enhancement in the photic layer, which is in accordance with the *F. profunda* index indicating a less stratified water column conditions from 2.4 to 1.85 Myr (**Figure 4.5b**). A more intensified water column mixing could have shoaled the nutricline leading to increase in the abundances of the UPZ flora. This shift at 2.4 Myr is coincident to the extreme climatic variability during the Pliocene described by Shackleton et al. (1984) that have triggered the onset of the NH glaciation. The estimated primary productivity (EPP) calculated from the relative abundance of *F. profunda* however

shows a relatively stable pattern throughout the studied time period although higher amplitude fluctuations can be observed starting at 2.25 Myr (**Figure 4.5e**). This is in agreement with previous studies suggesting that gradual cooling coupled with the shallowing of the nutricline/thermocline (Ravelo et al., 2004; Lawrence et al., 2013) resulted to the progressive decline and subsequent demise of the discoasters (Chapman and Chepstow-Lusty, 1997; Schueth and Bralower, 2015).

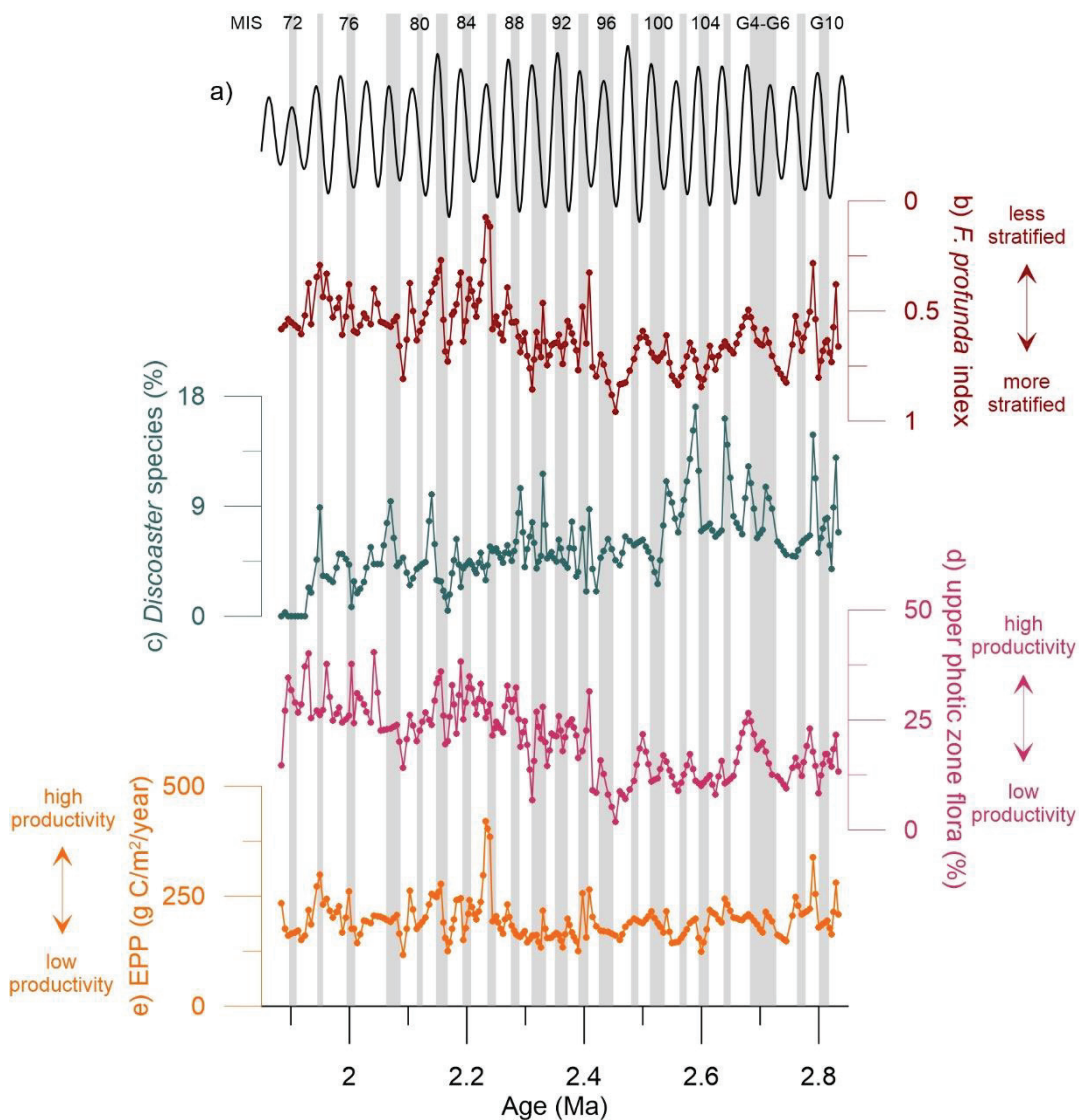


Figure 4.5: Site U1476 coccolithophore productivity and stratification records: **(a)** orbital obliquity sequence (Berger, 1992); **(b)** *Florisphaera profunda* index; **(c)** relative abundance of *Discoaster* spp.; **(d)** upper photic zone flora comprising of small *Gephyrocapsa* and small *Reticulofenestra*; **(e)** estimated primary productivity (EPP) calculated from relative abundance of *F. profunda*. Glacial stages are marked by gray bars.

4.5.2 Productivity fluctuations from indicative taxa

The downcore variations in individual nannoplankton species show differences in abundance patterns, with some species showing a clear trend with the isotope stages (**Figure 4.6**). The co-occurrence of the cold-water species *C. pelagicus* and high nutrient taxon *C. braarudii* in the record suggest that a combination of environmental parameters, and not only SST controlled the coccolithophore productivity at Site U1476 during the Pliocene-Pleistocene (**Figure 4.6a** and **4.6b**). This is corroborated by the increased abundances of the UPZ dwelling taxa (small placoliths; **Figure 4.6d**), which indicate enriched nutrient supply in the upper photic layer (Okada, 2000). Relatively stable abundances of the UPZ group are recorded for the Pliocene sequence, and registered a major change after the transition to the Pleistocene (2.4 Myr), where it reaches minimum and progressively increases thereafter. The interval from 2.4 to 1.85 Myr is characterized by higher surface water productivity conditions, as also shown by the increased abundances of *C. leptoporus*, another taxon with affinity for high-nutrient environment (e.g., Giraudeau, 1992; Winter et al., 1994) (**Figure 4.6c**). While this species is also typified of warm conditions (Winter and Martin, 1990; Flores et al., 1999; Baumann and Freitag, 2004), its contrasting pattern with the warm water taxa (**Figure 4.6g**), especially starting at 2.2 Myr, shows that the abundances of *C. leptoporus* is not a factor of SST but rather by nutrient availability in the water column. Despite the low abundances of the accessory taxa *Oolithotus* spp., *Rhabdosphaera clavigera*, *Syracosphaera* spp., and *Umbellosphaera* spp., the cumulative abundance of these species that we used as warm water proxy shows distinct and regular variations in the record. The high abundances of the tropical species, such as *F. profunda*, *C. leptoporus* coupled with the consistent occurrences of the warm water taxa (*Oolithotus* spp, *Rhabdosphaera clavigera*, *Syracosphaera* spp., and *Umbellosphaera* spp.) reflect prevalence of warm tropical conditions in the study area.

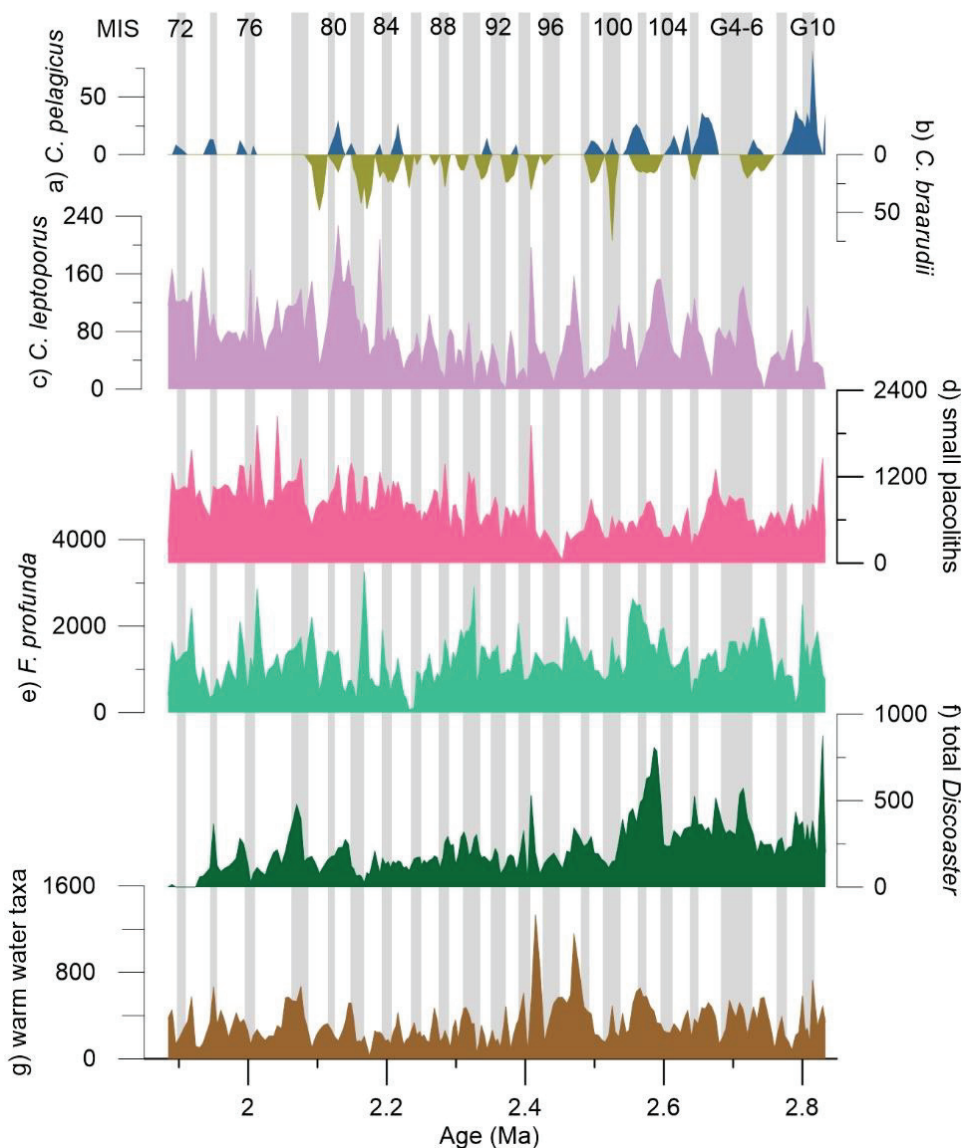


Figure 4.6: Absolute concentrations of selected calcareous nannofossil taxa: (a) *Coccolithus pelagicus*; (b) *C. braarudii*; (c) *Calcidiscus leptoporus*; (d) small placoliths including small *Gephyrocapsa* and small *Reticulofenestra*; (e) *Florisphaera profunda*; (f) total *Discoaster* spp.; (g) warm water taxa comprising of *Oolithotus* spp, *Rhabdosphaera clavigera*, *Syracosphaera* spp., and *Umbellosphaera* spp. All concentrations are expressed in number of nannofossils $\times 10^9$ /gram of sediment. Glacial stages are marked by gray bars.

4.5.3 Implications on the Agulhas Current

We relate the long-term record of paleoproductivity at Site U1476 to be driven by both atmospheric and oceanographic processes, which have influenced variations in the nutricline/thermocline dynamics and nutrient availability in the water column. The present day oceanography of the western Indian Ocean has been suggested to be linked to the Pacific Ocean climate variability (Schouten et al., 2003) and also holds true for Quaternary

climate archives (Kuhnert et al., 2014; Tangunan et al., 2017). The abundance of the LPZ-dwelling species *F. profunda* was a successful proxy for the nutricline/thermocline depth in Quaternary sediments and was also proven useful for late Neogene sequences (Okada, 2000), as well as interpret the Indo-Pacific teleconnections over the past 300 kyr (Tanganan et al., 2017). The regular occurrence of warm water taxa reflects tropical Pacific influence in our study area. This shows that the transport of warm and oligotrophic surface water of the ITF via the SEC across the Indian Ocean was a persistent feature of the last 2.85 Myr, which could be linked to the development of the Agulhas Current downstream, and subsequent leakage into the South Atlantic (Biajoch et al., 2009).

A possible influence of the southern sourced waters into the site is shown by the occurrences of *C. pelagicus* and *C. braarudii*. Both of these species were not encountered in late Quaternary sediments of the equatorial Indian Ocean (Tanganan et al., 2017) but were found in the subtropical region (Tanganan et al., Chapter 3), which was attributed to the entrance of the nutrient-rich SASW during the glacial periods, with the northward migration of the subtropical front (STF). However, the lowest latitude (33°S) migrated by the STF during the glacial periods (Bard and Rickaby, 2009) did not reach our study site in the Mozambique Channel, an area described by Ternon et al. (2014) as one of the most turbulent areas in the world oceans. Enhanced surface water productivity and cooler water conditions resulting in the occurrences of these species could therefore be also due to localized upwelling event, hence intensified water column mixing driven by the mesoscale anticyclonic eddies in the channel (Schouten et al., 2003).

4.5.4 Orbitally-forced variability of calcareous nannoplankton species

Calcareous nannoplankton abundances visually exhibit cyclic variations (**Figure 4.5** and **4.6**), which was confirmed by spectral analysis (**Figure 4.7**). Spectral analysis performed on the nannofossil record demonstrates variations in paleoproductivity primarily driven by the glacial/interglacial variability (100 kyr) and the obliquity-controlled periodicity (41 kyr). The nannofossil group warm water taxa, estimated primary productivity, and *F. profunda* index also show orbital forcing at the precession band (23 kyr). This shows that productivity in the Mozambique Channel is modulated by both the high latitude and the tropical Pacific forcings. The 23 kyr cyclicity in the calcareous

nannofossil record from this site was also observed in the equatorial Indian Ocean, which was linked to a combination of both the boreal monsoon and the El Niño Southern Oscillation (ENSO)-like dynamics (Beaufort et al., 2001).

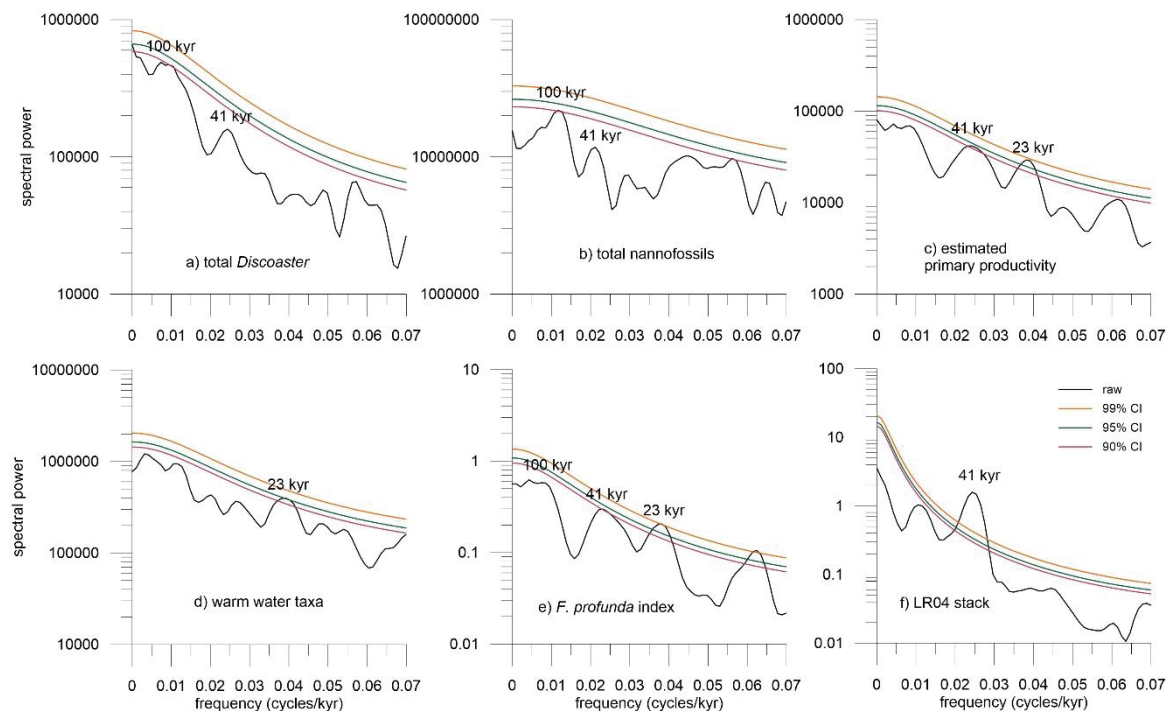


Figure 4.7: Spectral power versus frequency plots of calcareous nannoplankton and global $\delta^{18}\text{O}$ benthic foraminiferal stack (Lisiecki and Raymo, 2005): (a) total *Discoaster* species; (b) total nannofossils; (c) estimated primary productivity calculated from relative abundance of *Florisphaera profunda*; (d) warm water taxa comprising of *Oolithotus* spp., *Rhabdosphaera clavigera*, and *Syracosphaera* spp.; (e) *F. profunda* index; (f) LR04 $\delta^{18}\text{O}$ benthic foraminiferal stack.

4.6 Conclusions

The Plio-Pleistocene paleoenvironment reconstruction of the last 1 Myr before the *Discoaster* extinction using calcareous nannoplankton assemblage at Site U1476 shows that:

1. Both temperature and nutrient availability played a critical role in calcareous nannoplankton productivity at the location.
2. Calcareous nannoplankton taxa showed variations in frequencies, which were at paced with orbital periodicities, suggesting both NH and tropical Pacific forcing in the records.

3. Discoasters declined with cooling across the Plio-Pleistocene, which have initiated at 2.4 Myr. Gradual decline and successive extinction could be due to a more mixed water column and consequent increase in productivity at the Mozambique Channel as shown by the low values of the *F. profunda* index and high abundances of UPZ flora indicative of nutrient-rich surface water conditions.
4. The transport of warm and oligotrophic surface water of the ITF via the SEC across the Indian Ocean was a persistent feature of the last 2.85 Myr, as shown by the consistent occurrences of warm water taxa.
5. A possible influence of the southern sourced sub-Antarctic surface waters into the site exists as shown by the occurrences of *C. pelagicus* and *C. braarudii*, species that are adapted to cold and high-nutrient environments, respectively. The enhanced productivity could also be further amplified by localized upwelling event driven by the Mozambique Channel eddies.

Acknowledgments

This research used samples and data provided by the International Ocean Discovery Program (IODP). We are thankful for much support from the crew of the R/V *JOIDES Resolution*, IODP staff, and Expedition 361 shipboard science party. This work is part of the project Ocean and Climate 2: Land-ocean interaction and climate variability in low latitudes funded thru the German Science Foundation (DFG) Research Center/Cluster of Excellence "The Ocean in the Earth System" MARUM. Data will be archived in the PANGAEA database (www.pangaea.de).

Supplementary information

Table 4.1: Calcareous nannofossil biostratigraphic events recorded at Site U1476.

Calcareous nannofossil event	Age (Ma)	Shipboard		Refined: Splice	
		Hole-Core-Section-interval	CCSF (m)	Hole-Core-Section-interval	CCSF (m)
T <i>C. macintyre</i>	1.60	U1476A-5H2-75 cm	36.63		
B <i>Gephyrocapsa</i> (>4 μ m)	1.73	U1476A-5H2-75 cm	41.13		
T <i>D. brouweri</i>	1.93	U1476A-6H2-75 cm	46.06	U1476D-6H5-81 cm	45.29
T <i>D. triradiatus</i>	1.95	U1476A-6H2-75 cm	46.06	U1476D-6H5-141 cm	45.89
Bc <i>D. triradiatus</i>	2.14	U1476A-6H6-60 cm	51.91	U1476E-6H3-147 cm	51.08
T <i>D. pentaradiatus</i>	2.39	U1476A-7H6-75 cm	61.64	U1476A-7H5-108 cm	60.97
T <i>D. surculus</i>	2.49	U1476A-8H1-75 cm	64.31	U1476D-8H4-125 cm	63.42
T <i>D. tamalis</i>	2.80	U1476A-8H6-75 cm	71.81	U1476D-9H4-6 cm	72.72
T <i>Sphenolithus</i> spp.	3.54	U1476A-11H6-75 cm	103.13		

Table 4.2: Approximate paleomagnetic boundaries at Site U1476.

Boundary	Age (Ma)	CCSF (m)	uncertainty +- (m)
	GPTS 2012		
B Jaramillo	1.07	26.80	0.30
T Olduvai	1.78	38.10	0.90
B Olduvai	1.95	47.00	0.10
T Gauss	2.58	56.30	0.25
T Gilbert	3.60	114.80	0.10

CHAPTER 5
Conclusions

CHAPTER 5 **Conclusions**

Below are the main conclusions drawn from this Ph.D. research:

1. Prevalent regime with deep thermocline and low surface water productivity in the western tropical Indian Ocean

Coccolithophore assemblage off Tanzania (GeoB12613-1) is exclusively composed of tropical species, suggesting that warm tropical conditions with SSTs of at least 20°C occurred over the last 300 kyr. The assemblage is dominated by four species, namely *Florisphaera profunda*, small *Gephyrocapsa*, *E. huxleyi* and *G. oceanica*. Further downstream, a change in the assemblage composition is observed at the Natal Valley (MD96-2077). Here two assemblage groups were recognized: cooler water (*G. muellerae*, *Coccolithus pelagicus*), which suggests the influx of southern sourced sub-Antarctic surface waters (SASW), and warm water taxa (*F. profunda*, *G. oceanica*, small *Gephyrocapsa*), which we inferred to be linked to the intensity of the Agulhas Current. In the Mozambique Channel (IODP Site U1476), consistent occurrence and high abundance of tropical species (e.g., *F. profunda*, *Reticulofenestra* spp.) are recorded, indicating prevalence of warm tropical conditions across the Plio-Pleistocene. Such high abundances of the deep dwelling species *F. profunda* in the western Indian Ocean study sites indicate a prevalent regime with deep thermocline and low surface water productivity throughout the investigated time period.

2. Existence of an analogous to the modern El Niño Southern Oscillation/Indian Ocean Dipole events operating on longer timescales

Comparison with the eastern Indian Ocean coccolithophore data revealed differences in productivity values between the two regions. In particular, during the glacial stages, productivity was generally higher in the east than in the west, whereas during most of the interglacial intervals, higher productivity occurred in the west (**Figure 5.1**). Interestingly, for most of the glacial stage MIS 6, surface water productivity was consistently higher in the eastern tropical region and also in the younger part of the record. These east-west productivity patterns are proposed to be linked to the intensity of the Walker Circulation, suggesting the possible existence of patterns resembling the present day El Niño Southern Oscillation and Indian Ocean Dipole, which are both inter-annual modes of the Walker Circulation, operating on longer timescales. Reduction in surface

water productivity in the western tropical Indian Ocean is interpreted to be a result of a weak Walker Circulation from 160 kyr toward the Holocene. This is consistent with the results from modeling studies, proposing that the Walker Circulation has been slowing over the past century, resulting in a more El Niño-like phase, characterized by higher water stratification and concomitant lower surface water productivity in the western Indian Ocean.

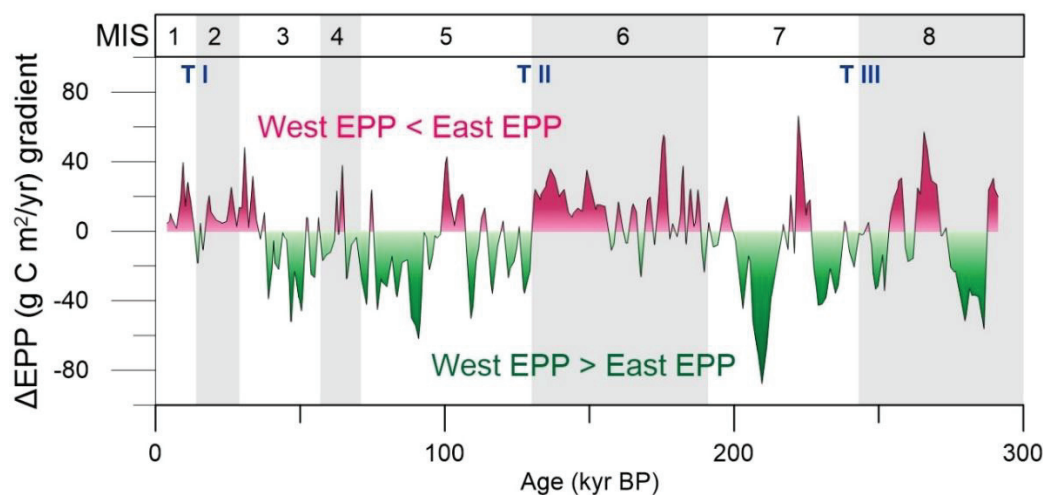


Figure 5.1: Differences in estimated primary productivity (EPP) based upon the relative abundance of *Florisphaera profunda* between the eastern (SO139-74KL; Andruleit et al., 2008) and the western tropical Indian Ocean (GeoB12613-1).

3. Latitudinal shifts in the subtropical front drive variations in coccolithophore productivity

Estimated primary productivity (EPP) at the Natal Valley (MD96-2077) revealed similar trend with the ODP Site 1082 (Benguela upwelling region), having enhanced surface water productivity during the glacial periods and lower productivity during the interglacial stages. This indicates that the equatorward movement of the subtropical front (STF) resulted to a weaker Agulhas Current and a more intense Benguela Current upwelling. For the Natal Valley in the subtropical Indian Ocean (MD96-2077), the increased abundances of *G. muelleriae* reflect cooler surface water conditions driven by the northward STF migration, leading to a weaker Agulhas Current and entrance of nutrient-rich southern sourced SASW. On the other hand, the EPP pattern at the Walvis Ridge (ODP Site 1082), indicates enhanced productivity during the interglacial periods, which contrasts the EPP variations in the Natal Valley and the Benguela upwelling region. We interpret that the higher surface water productivity at the Walvis Ridge during the interglacial periods is due

to the seaward lateral advection of nutrient-rich upwelled waters of the Benguela Current during the weakening of the coastal upwelling process or could also be a result of a local upwelling event in the Walvis Ridge.

4. The Agulhas Current is a persistent feature of the last 500 kyr

The relatively high concentration of warm water taxa (e.g., *F. profunda*, *Gephyrocapsa* spp.) in the Natal Valley (MD96-2077) during the glacial periods indicate that the northward migration of the STF did not completely obstruct the Agulhas Current and the transport of warm water to the South Atlantic. However, the STF shift could have reduced the Agulhas leakage, leading to a decline in the abundances of the warm water species in the eastern South Atlantic site (ODP Site 1266). Nevertheless, the consistent occurrences of these taxa in the study sites suggest that the Agulhas Current is a persistent feature of the past 500 kyr, with reduced magnitude and leakage during the glacial periods.

5. Discoasters declined with global cooling and associated enhancement of surface water productivity across the Plio-Pleistocene

The complete demise of the *Discoaster* species from the geologic record is suggested to be driven by a combination of several environmental parameters. Discoasters declined with cooling across the Plio-Pleistocene, which have initiated at 2.4 Myr. During this time, a more intensified water column mixing as shown by low values of the *F. profunda* index have occurred at the Mozambique Channel, which resulted to increased abundances of the upper photic zone flora indicative of nutrient-rich surface water conditions. These patterns suggest that the ecological preference of Discoasters resembles that of *F. profunda*, i.e., warm and oligotrophic surface waters or deeper nutricline/thermocline.

6. Plio-Pleistocene coccolithophore variations and implications on the Agulhas Current

The consistent occurrences of warm water taxa at the Mozambique Channel indicate that the transport of warm and oligotrophic surface water of the Indonesian Throughflow via the South Equatorial Current across the Indian Ocean is a prevalent feature of the last 2.85 Myr. This could have implications on the development of the Agulhas Current downstream, and subsequent transport of the Agulhas Current waters into the South

Atlantic. Alternatively, a possible influence of the southern sourced surface water into the site is shown by the occurrences of *C. pelagicus* and *C. braarudii*. Both of these species were not encountered in late Quaternary sediments of the equatorial Indian Ocean (GeoB12613-1) but were found in the subtropical region (MD96-2077), which was attributed to the entrance of southern sourced nutrient-rich SASW during the glacial periods, with the northward migration of the STF. The occurrence of these two species could also be due to enhanced surface water productivity and cooler water conditions as a result of a localized upwelling event or intensified mixing driven by the mesoscale anticyclonic eddies in the channel.

CHAPTER 6

Future direction/outlook

CHAPTER 6 **Future direction/outlook**

Results of this Ph.D. thesis show that coccolithophores are valuable paleoceanographic proxies in Quaternary and late Neogene sediments of the western Indian Ocean and the eastern South Atlantic. Thus, this research has contributed to a better understanding of their distribution and how they respond to changing water column properties, driven by atmospheric, oceanographic or orbital processes. However, there is still a large number of questions to be addressed in order to better understand the past productivity dynamics in these two oceans.

One of the new findings from this Ph.D. work is the existence of an analogous to the present day El Niño Southern Oscillation events in the 300 kyr coccolithophore productivity record off Tanzania (western Indian Ocean), the occurrence of which was correlated to the varying intensity of the Walker Circulation. The Walker Circulation is the most prominent feature in the low latitudes coupling the ocean and the atmosphere, as well as revealing a number of east-west patterns, with worldwide teleconnections across all tropical oceans and even in higher latitudes. These patterns/teleconnections across the Indian Ocean are different from the Pacific and the Atlantic oceans and are less well understood than the others. Thus, results of this present research have allowed better understanding of the ocean-atmosphere interactions across the Indian Ocean over the past 300 kyr. One of the questions that can be explored for further studies is: *What happened prior to 300 kyr?* Sediment core GeoB12613-1 spans the last 800 kyr and it would be interesting to look deeper down this record. Moreover, the correlation of our coccolithophore record from the western tropical region was possible because of the previous work carried out by Andruleit et al. (2008) in the eastern tropical region on similar timescale. Despite this, both the eastern and the western regions of the Indian Ocean are understudied, hence additional investigation of the late Neogene sedimentary archives would be necessary in order to have a comprehensive overview of the Indo-Pacific teleconnections.

Another question that could be addressed by climate modelers would be: *Is the modern Indian Ocean a more El Niño- or La Niña-like state of the Walker Circulation compared to the Indian Ocean 300 kyr ago?* Studies dealing with how surface water productivity in the Indian Ocean will change in a warming world are therefore necessary.

This will have important implications on the global carbon cycle (increase of pCO₂ in the atmosphere, ocean acidification, variations in coccolith productivity, enhancement of the oxygen minimum zones, etc.). All these could be tested by modeling studies referring to the long-term (orbital-driven) change as background.

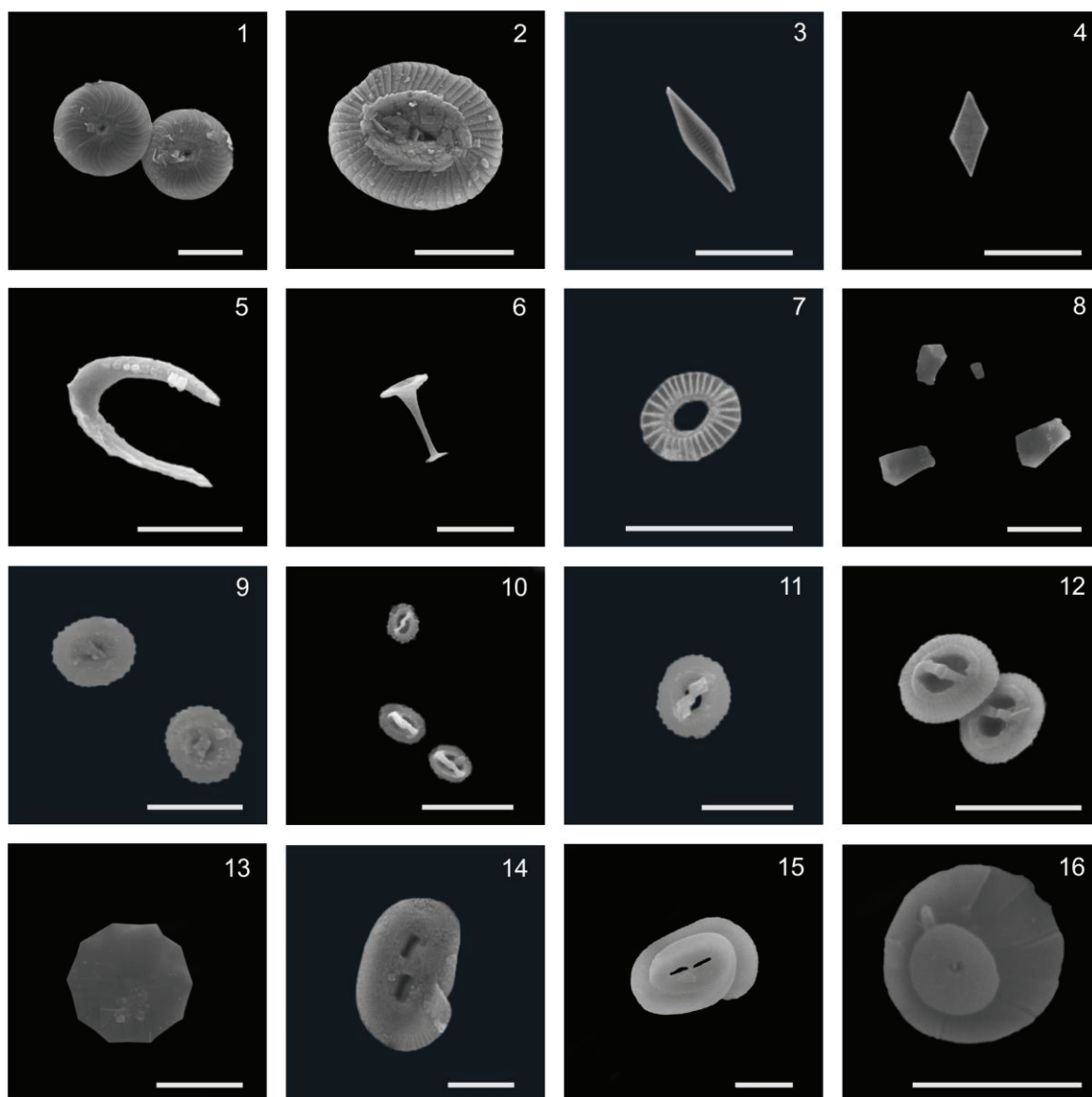
Ultimately, given the robust datasets that were acquired for this thesis, it would also be interesting to perform time series analysis of other coccolith species data and explore correlations between these records. Cross spectral analysis could be done using globally recognized paleoceanographic records (orbital cyclicity, $\delta^{18}\text{O}$ stack, etc.) and calculate the time lead/lags of our records relative to the climatic events in the higher or lower latitudes.

With the recent IODP expeditions in the Indo-Pacific region, new sedimentary archives extending down to key Neogene time intervals are available, providing opportunity to explore the sensitivity of the Walker Circulation in a much deeper timescale. My involvement in one of these research expeditions (Expedition 361 – Southern African Climates) is therefore an advantage. The materials are available and preliminary works in close collaboration with other shipboard scientists are ongoing. The generation of these new records thus offers multiple potentials in addressing the role of the tropical Indo-Pacific in the Earth's climate system, which is at present vulnerable to the impacts of extreme climate events.

Appendices

Appendices

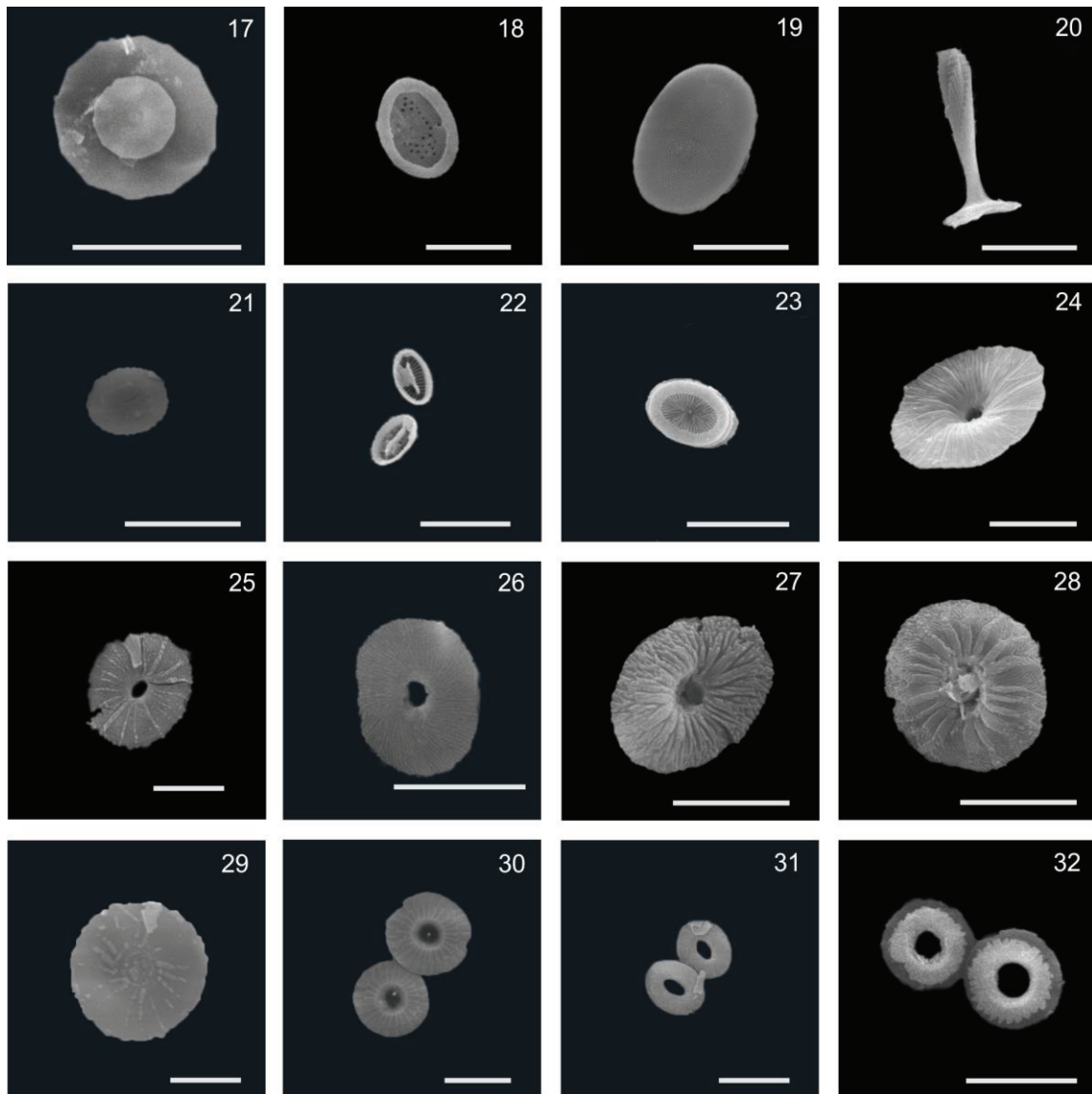
Appendix 1: Scanning electron microscope images of coccolithophores from the western Indian Ocean and the South Atlantic.



Scale bar = 5 μ m

1) *Calcidiscus leptoporus*; 2) *Coccolithus pelagicus*; 3) *Calciosolenia brasiliensis*; 4) *C. murrayi*; 5) *Ceratolithus cristatus*; 6) *Discosphaera tubifera*; 7) *Emiliana huxleyi*; 8) *Florisphaera profunda*; 9) *Gephyrocapsa caribbeanica*; 10) *G. ericsonii*; 11) *G. muellerae*; 12) *G. oceanica*; 13) *Hayaster perplexus*; 14-15) *Helicosphaera carteri*; 16) *Oolithotus antillarum*.

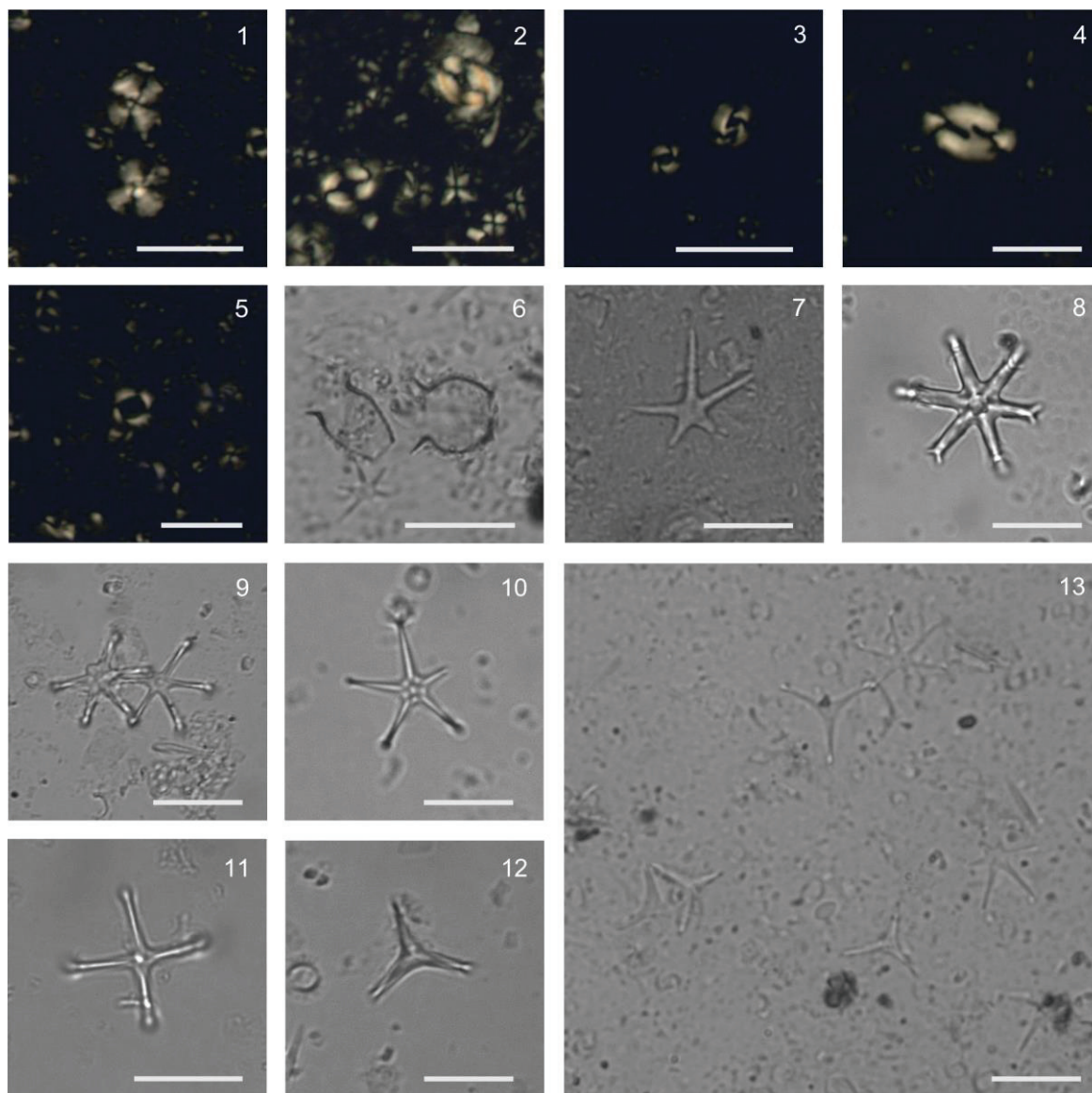
Appendix 1: Scanning electron microscope images of coccolithophores from the western Indian Ocean and the South Atlantic.



Scale bar = 5 μ m

17) *Oolithotus fragilis*; 18) *Pontosphaera discopora*; 19) *Pontosphaera* sp.; 20) *Rhabdosphaera clavigera*; 21) *Reticulofenestra sessilis*; 22) *Syracosphaera lamina*; 23) *S. pulchra*; 24) *Umbellosphaera irregularis*; 25-29) *U. tenuis*; 30) *Umbilicosphaera foliosa*; 31) *U. hulburtiana*; 32) *U. sibogae*.

Appendix 2: Light microscope images of Plio-Pleistocene nannofossils from the Mozambique Channel.



Scale bar = 10 μ m

1) *Calcidiscus leptoporus*; 2) *Coccolithus pelagicus*; 3) medium *Gephyrocapsa* sp.; 4) *Helicosphaera carteri*; 5) *Pseudoemiliana lacunosa*; 6) *Scyphosphaera* spp.; 7) *Discoaster asymmetricus*; 8) *D. surculus*; 9) *D. brouweri*; 10) *D. pentaradiatus*; 11) *D. tamalis*; 12) *D. triradiatus*; 13) *D. triradiatus* and *D. brouweri*.

References

References

- Abram, N.J., Gagan, M.K., Liu, Z., Hantoro, W.S., Mcculloch, M.T. & Suwargadi, B.W. 2007. Seasonal characteristics of the Indian Ocean Dipole during the Holocene epoch. *Nature*: 299-302. <https://doi.org/10.1038/nature05477>
- Acker, J.G. & Leptoukh, G. 2007. Online analysis enhances use of NASA earth science data. *Eos, Transactions American Geophysical Union*, 88(2): 14-17. <https://doi.org/10.1029/2007EO020003>
- Agnini, C., Monechi, S. & Raffi, I. 2017. Calcareous nannofossil biostratigraphy: historical background and application in Cenozoic chronostratigraphy. *Lethaia*, 50(3): 447-463. <https://doi.org/10.1111/let.12218>
- Ahagon, N., Tanaka, Y. & Ujiie, H. 1993. *Florisphaera profunda*, a possible nannoplankton indicator of late Quaternary changes in sea-water turbidity at the northwestern margin of the Pacific. *Marine Micropaleontology*: 255-273. [https://doi.org/10.1016/0377-8398\(93\)90047-2](https://doi.org/10.1016/0377-8398(93)90047-2)
- Andrulleit, H. 1996. A filtration technique for quantitative studies of coccoliths. *Micropaleontology*: 403-406. <https://doi.org/10.2307/1485964>
- Andrulleit, H. 2007. Status of the Java upwelling area (Indian Ocean) during the oligotrophic northern hemisphere winter monsoon season as revealed by coccolithophores. *Marine Micropaleontology*: 36-51. <https://doi.org/10.1016/j.marmicro.2007.02.001>
- Andrulleit, H., Luckge, A., Wiedicke, M. & Stager, S. 2008. Late Quaternary development of the Java upwelling system (eastern Indian Ocean) as revealed by coccolithophores. *Marine Micropaleontology*: 3-15. <https://doi.org/10.1016/j.marmicro.2007.11.005>
- Andrulleit, H. & Rogalla, U. 2002. Coccolithophores in surface sediments of the Arabian Sea in relation to environmental gradients in surface waters. *Marine Geology*: 505-526.
- Andrulleit, H., Rogalla, U. & Stäger, S. 2005. Living coccolithophores recorded during the onset of upwelling conditions off Oman in the western Arabian Sea. *Journal of Nannoplankton Research*, 27(1): 1-14.
- Antoine, D. & Morel, A. 1996. Oceanic primary production: 1. Adaptation of a spectral light-photosynthesis model in view of application to satellite chlorophyll observations. *Global Biogeochemical Cycles*: 43-55. <https://doi.org/10.1029/95GB02831>
- Antonov, J., Seidov, D., Boyer, T., Locarnini, R., Mishonov, A., Garcia, H., Baranova, O., Zweng, M. & Johnson, D. 2010. *World Ocean Atlas 2009, Salinity*. U.S. Government Printing Office: 184.
- Aubry, M.-P. 1998. Early Paleogene calcareous nannoplankton evolution: a tale of climatic amelioration. *Late Paleocene-Early Eocene climatic and biotic events in the marine and terrestrial records*. Columbia University Press, New York: 158-203.
- Aubry, M.-P. 2007. A major Pliocene coccolithophore turnover: Change in morphological strategy in the photic zone. *Geological Society of America Special Papers*, 424: 25-51.
- Backman, J., Hermelin, O., Pestiaux, P. & Zimmerman, H. 1986. Palaeoclimatic and palaeoceanographic development in the Pliocene North Atlantic: *Discoaster* accumulation and coarse fraction data. *Geological Society, London, Special Publications*, 21(1): 231-242. <https://doi.org/10.1144/GSL.SP.1986.021.01.17>
- Backman, J. & Pestiaux, P. 1987. Pliocene *Discoaster* abundance variations, Deep Sea Drilling Project Site 606: Biochronology and palaeoenvironmental implications. *Ruddiman, WE, Kidd, RB, Thomas, E., et al., Initial Reports of the Deep Sea Drilling Project*, 94: 903-909.
- Bairbakhish, A.N., Bollmann, J., Sprengel, C. & Thierstein, H.R. 2010. Disintegration of aggregates and coccospheres in sediment trap samples. *Marine Micropaleontology*, 37(2): 5.
- Bard, E. & Rickaby, R.E. 2009. Migration of the subtropical front as a modulator of glacial climate, *Nature*: 380-383. <https://doi.org/10.1038/nature08189>
- Barker, S., Archer, D., Booth, L., Elderfield, H., Henderiks, J. & Rickaby, R.E. 2006. Globally increased pelagic carbonate production during the Mid-Brunhes dissolution interval and the CO₂ paradox of MIS 11. *Quaternary Science Reviews*, 25(23): 3278-3293. <https://doi.org/10.1016/j.quascirev.2006.07.018>
- Baumann, K.-H., Böckel, B. & Frenz, M. 2004. Coccolith contribution to South Atlantic carbonate sedimentation. *In: H.R. Thierstein & J.R. Young (Eds.), Coccolithophores: from molecular processes to global impact*. Springer Berlin: 367-402.
- Baumann, K.-H., Boeckel, B. & Čeppek, M. 2008. Spatial distribution of living coccolithophores along an east-west transect in the subtropical South Atlantic. *Journal of Nannoplankton Research*, 30(1): 9-21.
- Baumann, K.H., Andrulleit, H.A. & Samtleben, C. 2000. Coccolithophores in the Nordic Seas: comparison of living communities with surface sediment assemblages. *Deep-Sea Research Part II-Topical Studies in Oceanography*, 47(9-11): 1743-1772.

- Baumann, K.H., Čepek, M. & Kinkel, H. 1999. Coccolithophores as Indicators of Ocean Water Masses, Surface-Water Temperature, and Paleoproductivity — Examples from the South Atlantic. In: G. Fischer & G. Wefer (Eds.), *Use of Proxies in Paleoceanography*. Springer Berlin Heidelberg: 117-144.
- Baumann, K.H. & Freitag, T. 2004. Pleistocene fluctuations in the northern Benguela Current system as revealed by coccolith assemblages, *Marine Micropaleontology*: 195-215.
- Beal, L.M., Hormann, V., Lumpkin, R. & Foltz, G.R. 2013. The response of the surface circulation of the Arabian Sea to monsoonal forcing. *Journal of Physical Oceanography*: 2008-2022. <https://doi.org/10.1175/JPO-D-13-033.1>
- Beal, L.M., Ruijter, W.P.M.D., Biastoch, A., Zahn, R. & 136, S.W.I.W.G. 2011. On the role of the Agulhas system in ocean circulation and climate. *Nature*, 472: 429-436. <https://doi.org/10.1038/nature09983>
- Beaufort, L. 1996. Dynamics of the monsoon in the equatorial Indian Ocean over the last 260,000 years. *Quaternary International*: 13-18. [https://doi.org/10.1016/1040-6182\(95\)00017-D](https://doi.org/10.1016/1040-6182(95)00017-D)
- Beaufort, L., De Garidel-Thoron, T., Linsley, B., Oppo, D. & Buchet, N. 2003. Biomass burning and oceanic primary production estimates in the Sulu Sea area over the last 380 kyr and the East Asian monsoon dynamics. *Marine Geology*: 53-65. [https://doi.org/10.1016/S0025-3227\(03\)00208-1](https://doi.org/10.1016/S0025-3227(03)00208-1)
- Beaufort, L., De Garidel-Thoron, T., Mix, A.C. & Pisias, N.G. 2001. ENSO-like forcing on oceanic primary production during the Late Pleistocene. *Science*: 2440-2444. <https://doi.org/10.1126/science.293.5539.2440>
- Beaufort, L., Lancelot, Y., Camberlin, P.C., O., Vincent, E., Bassinot, F.C. & Labeyrie, L. 1997. Insolation cycles as a major control of equatorial Indian Ocean primary production. *Science*: 1451-1454. <https://doi.org/10.1126/science.278.5342.1451>
- Berger, A. 1992. Orbital variations and insolation database. *IGBP PAGES/World Data Center-A for Paleoclimatology Data Contribution Series*, 92(007).
- Bertrand, P. & Al., E. 1997. Les rapport de campagne a la mer a bord du Marion Dufresne—Campagne NAUSICAA—Images II—MD105 du 20/10/96 au 25/11/96. *Inst. Fr. pour la Rech. et la Technol. Polaires, France, Plouzane*.
- Biastoch, A., Böning, C.W., Schwarzkopf, F.U. & Lutjeharms, J. 2009. Increase in Agulhas leakage due to poleward shift of Southern Hemisphere westerlies. *Nature*, 462(7272): 495-498. <https://doi.org/10.1038/nature08519>
- Boeckel, B. & Baumann, K.H. 2004. Distribution of coccoliths in surface sediments of the south-eastern South Atlantic Ocean: ecology, preservation and carbonate contribution. *Marine Micropaleontology*, 51(3-4): 301-320. <https://doi.org/10.1016/j.dsr.2005.11.006>
- Boeckel, B., Baumann, K.H., Henrich, R. & Kinkel, H. 2006. Coccolith distribution patterns in South Atlantic and Southern Ocean surface sediments in relation to environmental gradients. *Deep-Sea Research Part I—Oceanographic Research Papers*, 53(6): 1073-1099.
- Bolli, H.M., Saunders, J.B. & Perch-Nielsen, K. 1989. *Plankton Stratigraphy: Volume 1, Planktic Foraminifera, Calcareous Nannofossils and Calpionellids*, 1. CUP Archive.
- Bollmann, J. 1997. Morphology and biogeography of *Gephyrocapsa* coccoliths in Holocene sediments. *Marine Micropaleontology*, 29(3-4): 319-350. [https://doi.org/10.1016/S0377-8398\(96\)00028-X](https://doi.org/10.1016/S0377-8398(96)00028-X)
- Bollmann, J., Baumann, K.H. & Thierstein, H.R. 1998. Global dominance of *Gephyrocapsa* coccoliths in the late Pleistocene: Selective dissolution, evolution, or global environmental change? *Paleoceanography*, 13(5): 517-529. <https://doi.org/10.1029/98PA00610>
- Bolton, C.T., Chang, L., Clemens, S.C., Kodama, K., Ikehara, M., Medina-Elizalde, M., Paterson, G.A., Roberts, A.P., Rohling, E.J., Yamamoto, Y. & Zhao, X. 2013. A 500,000 year record of Indian summer monsoon dynamics recorded by eastern equatorial Indian Ocean upper water column structure. *Quaternary Science Reviews*: 167-180. <https://doi.org/10.1016/j.quascirev.2013.07.031>
- Bolton, C.T., Hernandez-Sanchez, M.T., Fuertes, M.A., Gonzalez-Lemos, S., Abrevaya, L., Mendez-Vicente, A., Flores, J.A., Probert, I., Giosan, L., Johnson, J. & Stoll, H.M. 2016. Decrease in coccolithophore calcification and CO₂ since the middle Miocene. *Nature communications*, 7. <https://doi.org/10.1038/ncomms10284>
- Bolton, C.T. & Stoll, H.M. 2013. Late Miocene threshold response of marine algae to carbon dioxide limitation. *Nature*, 500(7464): 558-562. <https://doi.org/10.1038/nature12448>
- Bordiga, M., Bartol, M. & Henderiks, J. 2015. Absolute nannofossil abundance estimates: Quantifying the pros and cons of different techniques. *Revue de micropaléontologie*, 58(3): 155-165. <https://doi.org/10.1016/j.revmic.2015.05.002>
- Bordiga, M., Cobianchi, M., Lupi, C., Pelosi, N., Venti, N.L. & Ziveri, P. 2014. Coccolithophore carbonate during the last 450 ka in the NW Pacific Ocean (ODP site 1209B, Shatsky Rise). *Journal of Quaternary Science*, 29(1): 57-69. <https://doi.org/10.1002/jqs.2677>

- Bown, P. 1998. *Calcareous nannofossil biostratigraphy*. Chapman and Hall; Kluwer Academic. <https://doi.org/10.1007/978-94-011-4902-0>
- Bown, P.R., Lees, J.A. & Young, J.R. 2004. Calcareous nannoplankton evolution and diversity through time, *Coccolithophores*. Springer: 481-508.
- Bralower, T.J. 2002. Evidence of surface water oligotrophy during the Paleocene-Eocene thermal maximum: Nannofossil assemblage data from Ocean Drilling Program Site 690, Maud Rise, Weddell Sea. *Paleoceanography*, 17(2). <https://doi.org/10.1029/2001PA000662>
- Bramlette, M. 1958. Significance of coccolithophorids in calcium-carbonate deposition. *Geological Society of America Bulletin*, 69(1): 121-126. [https://doi.org/10.1130/0016-7606\(1958\)69\[121:SOCICD\]2.0.CO;2](https://doi.org/10.1130/0016-7606(1958)69[121:SOCICD]2.0.CO;2)
- Brand, L. 1994. Physiological ecology of marine. In: A. Winter & W. G. Siesser (Eds.), *Coccolithophores*. Cambridge University Press: 39.
- Brassell, S.C., Eglinton, G., Marlowe, I.T., Pflaumann, U. & Sarnthein, M. 1986. Molecular Stratigraphy - a New Tool for Climatic Assessment. *Nature*, 320(6058): 129-133. <https://doi.org/10.1038/320129a0>
- Broerse, A.T.C., Brummer, G.J.A. & Van Hinte, J.E. 2000. Coccolithophore export production in response to monsoonal upwelling off Somalia (northwestern Indian Ocean). *Deep-Sea Research Part II-Topical Studies in Oceanography*: 2179-2205. [https://doi.org/10.1016/S0967-0645\(00\)00021-7](https://doi.org/10.1016/S0967-0645(00)00021-7)
- Bukry, D. 1971. *Discoaster* evolutionary trends. *Micropaleontology*: 43-52. <https://doi.org/10.2307/1485036>
- Caley, T., Giraudeau, J., Malaize, B., Rossignol, L. & Pierre, C. 2012. Agulhas leakage as a key process in the modes of Quaternary climate changes. *Proceedings of National Academy of Science*, 109(18): 6835-6839. <https://doi.org/10.1073/pnas.1115545109>
- Caley, T., Peeters, F.J.C., Biastoch, A., Rossignol, L., Van Sebille, E., Durgadoo, J., Malaizé, B., Giraudeau, J., Arthur, K. & Zahn, R. 2014. Quantitative estimate of the paleo-Agulhas leakage. *Geophysical Research Letters*, 41(4): 1238-1246. <https://doi.org/10.1002/2014GL059278>
- Chapman, M.R. & Chepstow-Lusty, A.J. 1997. Late Pliocene climatic change and the global extinction of the discoasters: an independent assessment using oxygen isotope records. *Palaeogeography, Palaeoclimatology, Palaeoecology*, 134(1): 109-125. [https://doi.org/10.1016/S0031-0182\(97\)00035-7](https://doi.org/10.1016/S0031-0182(97)00035-7)
- Chepstow-Lusty, A., Backman, J. & Shackleton, N.J. 1989. Comparison of upper Pliocene *Discoaster* abundance variations from North Atlantic Sites 552, 607, 658, 659 and 662: further evidence for marine plankton responding to orbital forcing, In: Ruddiman, WF, Sarnthein, M., et al., *Proceedings of. ODP, Scientific Results*: 121-141. <https://doi.org/10.2973/odp.proc.sr.108.122.1989>
- Clemens, S., Prell, W., Murray, D., Shimmield, G. & Weedon, G. 1991. Forcing Mechanisms of the Indian-Ocean Monsoon. *Nature*: 720-725. <https://doi.org/10.1038/353720a0>
- Clemens, S.C., Murray, D.W. & Prell, W.L. 1996. Nonstationary phase of the Plio-Pleistocene Asian monsoon. *Science*, 274(5289): 943. <https://doi.org/10.1126/science.274.5289.943>
- De Boer, A.M., Graham, R.M., Thomas, M.D. & Kohfeld, K.E. 2013. The control of the Southern Hemisphere Westerlies on the position of the Subtropical Front. *Journal of Geophysical Research: Oceans*, 118(10): 5669-5675. <https://doi.org/10.1002/jgrc.20407>
- Dickson, A.J., Leng, M.J., Maslin, M.A., Sloane, H.J., Green, J., Bendle, J.A., McClymont, E.L. & Pancost, R.D. 2010. Atlantic overturning circulation and Agulhas leakage influences on southeast Atlantic upper ocean hydrography during marine isotope stage 11. *Paleoceanography*, 25(3). <https://doi.org/10.1029/2009PA001830>
- Dittert, N., Baumann, K.-H., Bickert, T., Henrich, R., Huber, R., Kinkel, H. & Meggers, H. 1999. Carbonate dissolution in the deep-sea: methods, quantification and paleoceanographic application, *Use of proxies in paleoceanography*. Springer: 255-284.
- Durgadoo, J.V., Loveday, B.R., Reason, C.J.C., Penven, P., Biastoch, A., Durgadoo, J.V., Loveday, B.R., Reason, C.J.C., Penven, P. & Biastoch, A. 2013. Agulhas Leakage Predominantly Responds to the Southern Hemisphere Westerlies. *Journal of Physical Oceanography*, 43(10): 2113-2131. <https://doi.org/10.1175/JPO-D-13-047.1>
- Fedorov, A.V. & Philander, S.G. 2000. Is El Niño Changing?, *Science*, 288(5473): 1997-2002. <https://doi.org/10.1126/science.288.5473.1997>
- Fincham, M.J. & Winter, A. 1989. Paleoceanographic interpretations of coccoliths and oxygen-isotopes from the sediment surface of the southwest Indian Ocean. *Marine Micropaleontology*, 13(4): 26. [https://doi.org/10.1016/0377-8398\(89\)90024-8](https://doi.org/10.1016/0377-8398(89)90024-8)
- Findlay, C.S. & Flores, J.A. 2000. Subtropical Front fluctuations south of Australia (45°09'S, 146°17' E) for the last 130 ka years based on calcareous nannoplankton. *Marine Micropaleontology*, 40(4): 403-416. [https://doi.org/10.1016/S0377-8398\(00\)00045-1](https://doi.org/10.1016/S0377-8398(00)00045-1)

- Fink, C., Baumann, K.H., Groeneveld, J. & Steinke, S. 2010. Strontium/Calcium ratio, carbon and oxygen stable isotopes in coccolith carbonate from different grain-size fractions in South Atlantic surface sediments. *Geobios*: 151-164. <https://doi.org/10.1016/j.geobios.2009.11.001>
- Flores, J.A., Gersonde, R. & Sierro, F.J. 1999. Pleistocene fluctuations in the Agulhas Current Retroflexion based on the calcareous plankton record. *Marine Micropaleontology*: 1-22. [https://doi.org/10.1016/S0377-8398\(99\)00012-2](https://doi.org/10.1016/S0377-8398(99)00012-2)
- Friedinger, P.J. & Winter, A. 1987. Distribution of modern coccolithophore assemblages in the southwest Indian Ocean off southern Africa. *Journal of Micropalaeontology*, 6(1): 49-56. <https://doi.org/10.1144/jm.6.1.49>
- Gibbs, S., Shackleton, N. & Young, J. 2004. Orbitally forced climate signals in mid-Pliocene nannofossil assemblages. *Marine Micropaleontology*, 51(1-2): 39-56. <https://doi.org/10.1016/j.marmicro.2003.09.002>
- Giraudeau, J. 1992. Distribution of Recent nannofossils beneath the Benguela System - Southwest African continental margin. *Marine Geology*: 219-237. [https://doi.org/10.1016/0025-3227\(92\)90174-G](https://doi.org/10.1016/0025-3227(92)90174-G)
- Giraudeau, J. & Bailey, G.W. 1995. Spatial Dynamics of Coccolithophore Communities during an Upwelling Event in the Southern Benguela System. *Continental Shelf Research*, 15(14): 1825-1852. [https://doi.org/10.1016/0278-4343\(94\)00095-5](https://doi.org/10.1016/0278-4343(94)00095-5)
- Giraudeau, J., Monteiro, P.M.S. & Nikodemus, K. 1993. Distribution and Malformation of Living Coccolithophores in the Northern Benguela Upwelling System Off Namibia. *Marine Micropaleontology*, 22(1-2): 93-110. [https://doi.org/10.1016/0377-8398\(93\)90005-1](https://doi.org/10.1016/0377-8398(93)90005-1)
- Giraudeau, J., Grelaud, M., Solignac, S., Andrews, J. T., Moros, M., & Jansen, E. 2010. Millennial-scale variability in Atlantic water advection to the Nordic Seas derived from Holocene coccolith concentration records. *Quaternary Science Reviews*, 29(9): 1276-1287. <https://doi.org/10.1016/j.quascirev.2010.02.014>
- Gordon, A.L., Weiss, R.F., Smethie, W.M. & Warner, M.J. 1992. Thermocline and Intermediate Water Communication between the South-Atlantic and Indian Oceans. *Journal of Geophysical Research-Oceans*, 97(C5): 7223-7240. <https://doi.org/10.1029/92JC00485>
- Gradstein, F.M., Ogg, G. & Schmitz, M. 2012. *The Geologic Time Scale 2012*, 117. Elsevier: 6 pp.
- Graham, R.M. & De Boer, A.M. 2013. The Dynamical Subtropical Front. *Journal of Geophysical Research: Oceans*, 118(10): 5676-5685. <https://doi.org/10.1002/jgrc.20408>
- Hall, I.R., Hemming, S.R. & Levay, L.J. 2016. *Expedition 361 Preliminary Report: South African Climates (Agulhas LGM Density Profile)*. International Ocean Discovery Program.
- Hall, I.R., Hemming, S.R., Levay, L.J., Barker, S., Berke, M.A., Brentegani, L., Caley, T., Cartagena-Sierra, A., Charles, C.D., Coenen, J.J., Crespin, J.G., Franzese, A.M., Gruetzner, J., Han, X., Hines, S.K.V., Jimenez Espejo, F.J., Just, J., Koutsodendris, A., Kubota, K., Lathika, N., Norris, R.D., Periera Dos Santos, T., Robinson, R., Rolinson, J.M., Simon, M., Tanguan, D., Van Der Lubbe, J.J.L., Yamane, M. & Zhang, H. 2017a. Expedition 361 methods. In: I. R. Hall, Hemming, S.R., LeVay, L.J., and the Expedition 361 Scientists (Ed.), *South African Climates (Agulhas LGM Density Profile)*. International Ocean Discovery Program. <https://doi.org/10.14379/iodp.proc.361.102.2017>
- Hall, I.R., Hemming, S.R., Levay, L.J., Barker, S., Berke, M.A., Brentegani, L., Caley, T., Cartagena-Sierra, A., Charles, C.D., Coenen, J.J., Crespin, J.G., Franzese, A.M., Gruetzner, J., Han, X., Hines, S.K.V., Jimenez Espejo, F.J., Just, J., Koutsodendris, A., Kubota, K., Lathika, N., Norris, R.D., Periera Dos Santos, T., Robinson, R., Rolinson, J.M., Simon, M., Tanguan, D., Van Der Lubbe, J.J.L., Yamane, M. & Zhang, H. 2017b. Site U1476. In: I. R. Hall, Hemming, S.R., LeVay, L.J., and the Expedition 361 Scientists (Ed.), *South African Climates (Agulhas LGM Density Profile)*. International Ocean Discovery Program. <https://doi.org/10.14379/iodp.proc.361.105.2017>
- Hammer, Ø., Harper, D. & Ryan, P. 2009. PAST-PAlaeontological STatistics, ver. 1.89, *University of Oslo, Oslo*: 1-31.
- Haq, B.U. & Lohmann, G. 1976. Early Cenozoic calcareous nanoplankton biogeography of the Atlantic Ocean. *Marine Micropaleontology*, 1: 119-194. [https://doi.org/10.1016/0377-8398\(76\)90008-6](https://doi.org/10.1016/0377-8398(76)90008-6)
- Hastenrath, S., Nicklis, A. & Greischar, L. 1993. Atmospheric-hydrospheric mechanisms of climate anomalies in the western equatorial Indian Ocean. *Journal of Geophysical Research*, 98(C11): 20219. <https://doi.org/10.1029/93JC02330>
- Hay, W.W. 2004. Carbonate fluxes and calcareous nanoplankton, *Coccolithophores*. Springer: 509-528.
- Honjo, S., & Okada, H. 1974. Community structure of coccolithophores in the photic layer of the mid-Pacific. *Micropaleontology*: 209-230. <https://doi.org/10.2307/1485061>
- Hutson, W.H. 1980. The agulhas current during the late pleistocene: analysis of modern faunal analogs. *Science*, 207(4426): 64-66. <https://doi.org/10.1126/science.207.4426.64>

- Jasper, J.P. & Hayes, J.M. 1990. A carbon isotope record of CO₂ levels during the late Quaternary. *Nature*, 347(6292): 462-464. <https://doi.org/10.1038/347462a0>
- Jordan, R. W., Zhao, M., Eglinton, G., & Weaver, P. P. E. 1996. Coccolith and alkenone stratigraphy and palaeoceanography at an upwelling site off NW Africa (ODP 658C) during the last 130,000 years. *Microfossils and Oceanic Environments*. University of Wales, Aberystwyth Press, Aberystwyth: 111-130.
- Kennett, J.P. 1983. Paleo-oceanography: Global ocean evolution. *Reviews of Geophysics*, 21(5): 1258-1274. <https://doi.org/10.1029/RG021i005p01258>
- Kinkel, H., Baumann, K.H. & Cepek, M. 2000. Coccolithophores in the equatorial Atlantic Ocean: response to seasonal and Late Quaternary surface water variability. *Marine Micropaleontology*: 87-112. [https://doi.org/10.1016/S0377-8398\(00\)00016-5](https://doi.org/10.1016/S0377-8398(00)00016-5)
- Knorr, G. & Lohmann, G. 2003. Southern Ocean origin for the resumption of Atlantic thermohaline circulation during deglaciation. *Nature*, 424(6948): 532-536. <https://doi.org/10.1038/nature01855>
- Kohfeld, K., Graham, R., De Boer, A., Sime, L., Wolff, E., Le Quéré, C. & Bopp, L. 2013. Southern Hemisphere westerly wind changes during the Last Glacial Maximum: paleo-data synthesis. *Quaternary Science Reviews*, 68: 76-95. <https://doi.org/10.1016/j.quascirev.2013.01.017>
- Koné, V., Aumont, O., Lévy, M. & Resplandy, L. 2013. Physical and biogeochemical controls of the phytoplankton seasonal cycle in the Indian Ocean: a modeling study, *Indian Ocean Biogeochemical Processes and Ecological Variability*. American Geophysical Union: 147-166.
- Krammer, R., Baumann, K.H. & Hennich, R. 2006. Middle to late Miocene fluctuations in the incipient Benguela Upwelling System revealed by calcareous nannofossil assemblages (ODP Site 1085A). *Palaeogeography Palaeoclimatology Palaeoecology*, 230(3-4): 319-334. <https://doi.org/10.1016/j.palaeo.2005.07.022>
- Kuhnert, H., Kuhlmann, H., Mohtadi, M., Meggers, H., Baumann, K.H. & Patzold, J. 2014. Holocene tropical western Indian Ocean sea surface temperatures in covariation with climatic changes in the Indonesian region. *Paleoceanography*: 423-437. <https://doi.org/10.1002/2013PA002555>
- Kwiatkowski, C., Prange, M., Varma, V., Steinke, S., Hebbeln, D. & Mohtadi, M. 2015. Holocene variations of thermocline conditions in the eastern tropical Indian Ocean. *Quaternary Science Reviews*, 114: 33-42. <https://doi.org/10.1016/j.quascirev.2015.01.028>
- Lawrence, K.T., Sigman, D., Herbert, T.D., Riihimaki, C., Bolton, C., Martinez-Garcia, A., Rosell-Mele, A. & Haug, G. 2013. Time-transgressive North Atlantic productivity changes upon Northern Hemisphere glaciation. *Paleoceanography*, 28(4): 740-751. <https://doi.org/10.1002/2013PA002546>
- Lévy, M., Shankar, D., André, J.M., Shenoi, S.S.C., Durand, F. & De Boyer Montégut, C. 2007. Basin-wide seasonal evolution of the Indian Ocean's phytoplankton blooms. *Journal of Geophysical Research*: 112(C12). <https://doi.org/10.1029/2007JC004090>
- Lisiecki, L.E. & Raymo, M.E. 2005. A Pliocene-Pleistocene stack of 57 globally distributed benthic $\delta^{18}\text{O}$ records. *Paleoceanography*, 20(1). <https://doi.org/10.1029/2004PA001071>
- Little, M.G., Schneider, R.R., Kroon, D., Price, B., Bickert, T. & Wefer, G. 1997. Rapid palaeoceanographic changes in the Benguela Upwelling System for the last 160,000 years as indicated by abundances of planktonic foraminifera. *Palaeogeography Palaeoclimatology Palaeoecology*, 130(1-4): 135-161. [https://doi.org/10.1016/S0031-0182\(96\)00136-8](https://doi.org/10.1016/S0031-0182(96)00136-8)
- Locarnini, R., Mishonov, A., Antonov, J., Boyer, T., Garcia, H., Baranova, O., Zweng, M. & Johnson, D. 2010. World Ocean Atlas 2009, *Temperature*. U. S. Government Printing Office: 184.
- Lückge, A., Mohtadi, M., Rühlemann, C., Scheeder, G., Vink, A., Reinhardt, L., Fairbanks, R.G. & Wiedicke, M. 2009. Monsoon versus ocean circulation controls on paleoenvironmental conditions off southern Sumatra during the past 300,000 years. *Paleoceanography*: 24(1). <https://doi.org/10.1029/2008PA001627>
- Luo, J.J., Sasaki, W. & Masumoto, Y. 2012. Indian Ocean warming modulates Pacific climate change. *Proceedings of National Academy of Science USA*, 109(46): 18701-18706. <https://doi.org/10.1073/pnas.1210239109>
- Lutjeharms, J. 1996. The exchange of water between the South Indian and South Atlantic Oceans, *The South Atlantic*. Springer: 125-162.
- Lutjeharms, J. 2006. The agulhas current. *African Journal of Marine Science*, 28(3-4): 729-732.
- Lutjeharms, J.R.E. & Stockton, P.L. 1987. Kinematics of the Upwelling Front Off Southern-Africa. *South African Journal of Marine Science-Suid-Afrikaanse Tydskrif Vir Seewetenskap*, 5(1): 35-49. <https://doi.org/10.2989/025776187784522612>
- Marino, M., Maiorano, P. & Flower, B.P. 2011. Calcareous nannofossil changes during the Mid-Pleistocene Revolution: Paleocologic and paleoceanographic evidence from North Atlantic Site 980/981.

- Palaeogeography Palaeoclimatology Palaeoecology*, 306(1-2): 58-69.
<https://doi.org/10.1016/j.palaeo.2011.03.028>
- Marino, M., Maiorano, P., Tarantino, F., Voelker, A., Capotondi, L., Gironi, A., Lirer, F., Flores, J.-A. & Naafs, B.D.A. 2014. Coccolithophores as proxy of seawater changes at orbital-to-millennial scale during middle Pleistocene Marine Isotope Stages 14-9 in North Atlantic core MD01-2446. *Paleoceanography*, 29(6): 518-532. <https://doi.org/10.1002/2013PA002574>
- Martin, A., Goodlad, S. & Salmon, D. 1982. Sedimentary basin in-fill in the northernmost Natal Valley, hiatus development and Agulhas Current palaeo-oceanography. *Journal of the Geological Society*, 139(2): 183-201. <https://doi.org/10.1144/gsjgs.139.2.0183>
- Martínez-Méndez, G., Zahn, R., Hall, I.R., Peeters, F.J.C., Pena, L.D., Cacho, I. & Negre, C. 2010. Contrasting multiproxy reconstructions of surface ocean hydrography in the Agulhas Corridor and implications for the Agulhas Leakage during the last 345,000 years. *Paleoceanography*, 25(4). <https://doi.org/10.1029/2009PA001879>
- Martini, E. 1971. Standard Tertiary and Quaternary calcareous nannoplankton zonation, *Proceedings of the Second Planktonic Conference, Roma 1970*. Tecnoscienza: 739-785.
- McIntyre, A., & Molino, B. 1996. Forcing of Atlantic equatorial and subpolar millennial by precession. *Science*, 274(5294), 1867. <https://doi.org/10.1126/science.274.5294.1867>
- McIntyre, A. & Bé, A.W. 1967. Modern coccolithophoridae of the Atlantic Ocean—I. Placoliths and cyrtoliths, *Deep Sea Research and Oceanographic Abstracts*. Elsevier: 561IN3565IN9567-3564IN8566IN20597.
- Mejia, L.M., Ziveri, P., Cagnetti, M., Bolton, C., Zahn, R., Marino, G., Martinez-Mendez, G. & Stoll, H. 2014. Effects of midlatitude westerlies on the paleoproductivity at the Agulhas Bank slope during the penultimate glacial cycle: Evidence from coccolith Sr/Ca ratios. *Paleoceanography*: 697-714. <https://doi.org/10.1002/2013PA002589>
- Meng, Q.J., Latif, M., Park, W., Keenlyside, N.S., Semenov, V.A. & Martin, T. 2012. Twentieth century Walker Circulation change: data analysis and model experiments. *Climate Dynamics*, 38(9-10): 1757-1773. <https://doi.org/10.1007/s00382-011-1047-8>
- Mohtadi, M., Luckge, A., Steinke, S., Groeneveld, J., Hebbeln, D. & Westphal, N. 2010. Late Pleistocene surface and thermocline conditions of the eastern tropical Indian Ocean. *Quaternary Science Reviews*: 887-896. <https://doi.org/10.1016/j.quascirev.2009.12.006>
- Molino, B. & McIntyre, A. 1990. Precessional forcing of nutricline dynamics in the equatorial Atlantic. *Science*: 766-769. <https://doi.org/10.1126/science.249.4970.766>
- Müller, P.J., Kirst, G., Ruhland, G., Von Storch, I. & Rosell-Melé, A. 1998. Calibration of the alkenone paleotemperature index U^K₃₇ based on core-tops from the eastern South Atlantic and the global ocean (60°N-60°S). *Geochimica et Cosmochimica Acta*, 62(10): 1757-1772. [https://doi.org/10.1016/S0016-7037\(98\)00097-0](https://doi.org/10.1016/S0016-7037(98)00097-0)
- Naqvi, S.W.A. 2008. The Indian Ocean, *Nitrogen in the Marine Environment*. Elsevier: 631-681.
- Niedermeyer, E.M., Sessions, A.L., Feakins, S.J. & Mohtadi, M. 2014. Hydroclimate of the western Indo-Pacific Warm Pool during the past 24,000 years. *Proceedings of the National Academy of Science USA*: 9402-9406. <https://doi.org/10.1073/pnas.1323585111>
- Okada, H. 2000. 33. Neogene and Quaternary calcareous nannofossils from the Blake Ridge, Sites 994, 995, and 9971, *Proceedings of the Ocean Drilling Program. Scientific Results*. Ocean Drilling Program: 331-341.
- Okada, H., & Wells, P. 1997. Late Quaternary nannofossil indicators of climate change in two deep-sea cores associated with the Leeuwin Current off Western Australia. *Palaeogeography, Palaeoclimatology, Palaeoecology*, 131(3-4): 413-432. [https://doi.org/10.1016/S0031-0182\(97\)00014-X](https://doi.org/10.1016/S0031-0182(97)00014-X)
- Okada, H. & Bukry, D. 1980. Supplementary modification and introduction of code numbers to the low-latitude coccolith biostratigraphic zonation (Bukry, 1973; 1975). *Marine Micropaleontology*, 5: 321-325. [https://doi.org/10.1016/0377-8398\(80\)90016-X](https://doi.org/10.1016/0377-8398(80)90016-X)
- Okada, H., & McIntyre, A. 1979. Seasonal distribution of modern coccolithophores in the western North Atlantic Ocean. *Marine Biology*, 54(4): 319-328. <https://doi.org/10.1007/BF00395438>
- Okada, H. & Honjo, S. 1975. Distribution of coccolithophores in marginal seas along the western Pacific Ocean and in the Red Sea. *Marine Biology*: 271-285. <https://doi.org/10.1007/BF00387154>
- Orsi, A.H., Whitworth, T. & Nowlin, W.D. 1995. On the Meridional Extent and Fronts of the Antarctic Circumpolar Current. *Deep-Sea Research Part I-Oceanographic Research Papers*, 42(5): 641-673. [https://doi.org/10.1016/0967-0637\(95\)00021-W](https://doi.org/10.1016/0967-0637(95)00021-W)
- Paillard, D., Labeyrie, L. & Yiou, P. 1996. Macintosh program performs time-series analysis. *Eos, Transactions American Geophysical Union*: 379-379. <https://doi.org/10.1029/96EO00259>

- Parente, A., Cachao, M., Baumann, K.H., De Abreu, L. & Ferreira, J. 2004. Morphometry of *Coccolithus pelagicus* s.l. (Coccolithophore, Haptophyta) from offshore Portugal, during the last 200 kyr. *Micropaleontology*, 50: 107-120. https://doi.org/10.2113/50.Suppl_1.107
- Peeters, F.J., Acheson, R., Brummer, G.J., De Ruijter, W.P., Schneider, R.R., Ganssen, G.M., Ufkes, E. & Kroon, D. 2004. Vigorous exchange between the Indian and Atlantic oceans at the end of the past five glacial periods. *Nature*, 430(7000): 661-665. <https://doi.org/10.1038/nature02785>
- Peterson, R.G. & Stramma, L. 1991. Upper-Level Circulation in the South-Atlantic Ocean. *Progress in Oceanography*, 26(1): 1-73. [https://doi.org/10.1016/0079-6611\(91\)90006-8](https://doi.org/10.1016/0079-6611(91)90006-8)
- Petrack, B.F., Mcclymont, E.L., Marret, F. & Van Der Meer, M.T.J. 2015. Changing surface water conditions for the last 500 ka in the Southeast Atlantic: Implications for variable influences of Agulhas leakage and Benguela upwelling. *Paleoceanography*, 30(9): 1153-1167. <https://doi.org/10.1002/2015PA002787>
- Pienaar, R. 1994. Ultrastructure and calcification of coccolithophores. *Coccolithophores*. Cambridge University Press, Cambridge: 13-37.
- Piotrowski, A.M., Banakar, V.K., Scrivner, A.E., Elderfield, H., Galy, A. & Dennis, A. 2009. Indian Ocean circulation and productivity during the last glacial cycle. *Earth and Planetary Science Letters*: 179-189. <https://doi.org/10.1016/j.epsl.2009.06.007>
- Power, S.B. & Kociuba, G. 2011. What caused the observed twentieth-century weakening of the Walker circulation? *Journal of Climate*, 24(24): 6501-6514. <https://doi.org/10.1175/2011JCLI4101.1>
- Prell, W.L. & Kutzbach, J.E. 1992. Sensitivity of the Indian Monsoon to forcing parameters and implications for its evolution. *Nature*: 647-652. <https://doi.org/10.1038/360647a0>
- Pujos, A. 1992. Calcareous nannofossils of Plio-Pleistocene sediments from the northwestern margin of tropical Africa. *Geological Society, London, Special Publications*, 64(1): 343-358. <https://doi.org/10.1144/GSL.SP.1992.064.01.23>
- Raffi, I., Backman, J., Fornaciari, E., Pälike, H., Rio, D., Lourens, L. & Hilgen, F. 2006. A review of calcareous nannofossil astrobiochronology encompassing the past 25 million years. *Quaternary Science Reviews*, 25(23): 3113-3137. <https://doi.org/10.1016/j.quascirev.2006.07.007>
- Rau, A., Rogers, J. & Chen, M.T. 2006. Late Quaternary palaeoceanographic record in giant piston cores off South Africa, possibly including evidence of neotectonism. *Quaternary International*, 148: 65-77. <https://doi.org/10.1016/j.quaint.2005.11.007>
- Ravelo, A.C., Andreasen, D.H., Mitchell, L., Lyle, A.O. & Wara, M.W. 2004. Regional climate shifts caused by gradual global cooling in the Pliocene epoch. *Nature*, 429(6989): 263. <https://doi.org/10.1038/nature02567>
- Raymo, M.E., Hodell, D. & Jansen, E. 1992. Response of Deep Ocean Circulation to Initiation of Northern Hemisphere Glaciation (3-2 Ma). *Paleoceanography*, 7(5): 645-672. <https://doi.org/10.1029/92PA01609>
- Read, J.F., Lucas, M.I., Holley, S.E. & Pollard, R.T. 2000. Phytoplankton, nutrients and hydrography in the frontal zone between the Southwest Indian Subtropical gyre and the Southern Ocean. *Deep-Sea Research Part I-Oceanographic Research Papers*, 47(12): 2341-2368. [https://doi.org/10.1016/S0967-0637\(00\)00021-2](https://doi.org/10.1016/S0967-0637(00)00021-2)
- Reason, C. & Mulenga, H. 1999. Relationships between South African rainfall and SST anomalies in the southwest Indian Ocean. *International Journal of Climatology*, 19(15): 1651-1673. [https://doi.org/10.1002/\(SICI\)1097-0088\(199912\)19:15<1651::AID-JOC439>3.0.CO;2-U](https://doi.org/10.1002/(SICI)1097-0088(199912)19:15<1651::AID-JOC439>3.0.CO;2-U)
- Reimer, P.J., Bard, E., Bayliss, A., Beck, J.W., Blackwell, P.G., Bronk, R.C., Buck, C.E., Cheng, H., Edwards, R.L. & Friedrich, M. 2013. IntCal13 and Marine13 radiocarbon age calibration curves 0-50,000 years cal BP. *Radiocarbon*: 1869-1887. https://doi.org/10.2458/azu_js_rc.55.16947
- Rickaby, R.E.M., Bard, E., Sonzogni, C., Rostek, F., Beaufort, L., Barker, S., Rees, G. & Schrag, D.P. 2007. Coccolith chemistry reveals secular variations in the global ocean carbon cycle?. *Earth and Planetary Science Letters*: 83-95. <https://doi.org/10.1016/j.epsl.2006.10.016>
- Rickaby, R.E.M., Schrag, D.P., Zondervan, I. & Riebesell, U. 2002. Growth rate dependence of Sr incorporation during calcification of *Emiliania huxleyi*. *Global Biogeochemical Cycles*, 16(1). <https://doi.org/10.1029/2001GB001408>
- Rippert, N., Baumann, K.H. & Patzold, J. 2015. Thermocline fluctuations in the western tropical Indian Ocean during the past 35 ka. *Journal of Quaternary Science*: 201-210. <https://doi.org/10.1002/jqs.2767>
- Rogalla, U. & Andruleit, H. 2005. Precessional forcing of coccolithophore assemblages in the northern Arabian Sea: Implications for monsoonal dynamics during the last 200,000 years. *Marine Geology*: 31-48. <https://doi.org/10.1016/j.margeo.2005.02.028>

- Romero, O.E., Kim, J.H., Bárcena, M.A., Hall, I.R., Zahn, R. & Schneider, R. 2015. High-latitude forcing of diatom productivity in the southern Agulhas Plateau during the past 350 kyr. *Paleoceanography*, 118-132. <https://doi.org/10.1002/2014PA002636>
- Rost, B. & Riebesell, U. 2004. Coccolithophores and the biological pump: Responses to environmental changes. *Coccolithophores: from molecular processes to global impact*: 99-125.
- Roth, P. H., & Berger, W. H. 1975. Distribution and dissolution of coccoliths in the south and central Pacific. *Special Publication Cushman Foundation Foraminiferal Research*, 13: 87-113.
- Roxy, M.K., Modi, A., Murtugudde, R., Valsala, V., Panickal, S., Prasanna Kumar, S., Ravichandran, M., Vichi, M. & Lévy, M. 2016. A reduction in marine primary productivity driven by rapid warming over the tropical Indian Ocean. *Geophysical Research Letters*, 43(2): 826-833. <https://doi.org/10.1002/2015GL066979>
- Roxy, M.K., Ritika, K., Terray, P. & Masson, S. 2014. The curious case of Indian Ocean warming. *Journal of Climate*: 8501-8509. <https://doi.org/10.1175/JCLI-D-14-00471.1>
- Saavedra-Pellitero, M., Baumann, K.-H., Ullermann, J. & Lamy, F. 2017. Marine Isotope Stage 11 in the Pacific sector of the Southern Ocean; a coccolithophore perspective. *Quaternary Science Reviews*, 158: 1-14. <https://doi.org/10.1016/j.quascirev.2016.12.020>
- Samtleben, C., Schäfer, P., Andruleit, H., Baumann, A., Baumann, K. H., Kohly, A., Matthiessen, J., & Schröder-Ritzrau, A. 1995. Plankton in the Norwegian-Greenland Sea: from living communities to sediment assemblages—an actualistic approach. *Geologische Rundschau*, 84(1), 108-136. <https://doi.org/10.1007/BF00192245>
- Savoie, B., Ridderinkhof, H., Pätzold, J. & Schneider, R. 2013. Western Indian Ocean Climate and Sedimentation - Cruise No. M75 - December 29, 2007 - April 08, 2008 - Port Louis (Mauritius) - Cape Town (South Africa). METEOR-Berichte, M75. DFG Senatskommission für Ozeanographie, doi: 10.2312/cr_m75: 196.
- Schonten, M.W., Ruijter, W.P., Leeuwen, P.J. & Lutjeharms, J.R. 2000. Translation, decay and splitting of Agulhas rings in the southeastern Atlantic Ocean. *Journal of Geophysical Research: Oceans*, 105(C9): 21913-21925. <https://doi.org/10.1029/1999JC000046>
- Schott, F.A. & McCreary, J.P. 2001. The monsoon circulation of the Indian Ocean. *Progress in Oceanography*: 1-123. [https://doi.org/10.1016/S0079-6611\(01\)00083-0](https://doi.org/10.1016/S0079-6611(01)00083-0)
- Schott, F.A., Xie, S.P. & McCreary, J.P. 2009. Indian Ocean circulation and climate variability. *Reviews of Geophysics*, 47(1). <https://doi.org/10.1029/2007RG000245>
- Schouten, M.W., De Ruijter, W.P.M., Van Leeuwen, P.J. & Ridderinkhof, H. 2003. Eddies and variability in the Mozambique Channel, *Deep-Sea Research Part II-Topical Studies in Oceanography: 1987-2003*. [https://doi.org/10.1016/S0967-0645\(03\)00042-0](https://doi.org/10.1016/S0967-0645(03)00042-0)
- Schueth, J.D. & Bralower, T.J. 2015. The relationship between environmental change and the extinction of the nannoplankton *Discoaster* in the early Pleistocene. *Paleoceanography*, 30(7): 863-876. <https://doi.org/10.1002/2015PA002803>
- Schulz, M. & Mudelsee, M. 2002. REDFIT: estimating red-noise spectra directly from unevenly spaced paleoclimatic time series. *Computers & Geosciences*: 421-426. [https://doi.org/10.1016/S0098-3004\(01\)00044-9](https://doi.org/10.1016/S0098-3004(01)00044-9)
- Shackleton, N.J., Backman, J., Zimmerman, H.T., Kent, D.V., Hall, M., Roberts, D.G., Schnitker, D., Baldauf, J., Desprairies, A. & Homrighausen, R. 1984. Oxygen isotope calibration of the onset of ice-rafting and history of glaciation in the North Atlantic region. *Nature*, 307(5952): 620-623. <https://doi.org/10.1038/307620a0>
- Shannon, L.V., Lutjeharms, J.R.E. & Agenbag, J.J. 1989. Episodic Input of Sub-Antarctic Water into the Benguela Region. *South African Journal of Science*, 85(5): 317-322.
- Simon, M.H., Arthur, K.L., Hall, I.R., Peeters, F.J.C., Loveday, B.R., Barker, S., Ziegler, M. & Zahn, R. 2013. Millennial-scale Agulhas Current variability and its implications for salt-leakage through the Indian-Atlantic Ocean Gateway. *Earth and Planetary Science Letters*, 383: 101-112. <https://doi.org/10.1016/j.epsl.2013.09.035>
- Simpson, E. & Schlich, R. 1974. Initial reports of the Deep Sea Drilling Project, vol. 25. *Washington, DC: US Government Printing Office*. <https://doi.org/10.2973/dsdp.proc.25.1974>
- Song, Q. & Gordon, A.L. 2004. Significance of the vertical profile of the Indonesian Throughflow transport to the Indian Ocean. *Geophysical Research Letters*, 31(16). <https://doi.org/10.1029/2004GL020360>
- Southon, J., Kashgarian, M., Fontugne, M., Metivier, B. & Yim, W.W.S. 2002. Marine reservoir corrections for the Indian Ocean and southeast Asia. *Radiocarbon*: 167-180. <https://doi.org/10.1017/S0033822200064778>
- Stoll, H., Shimizu, N., Arevalos, A., Matell, N., Banasiak, A. & Zeren, S. 2007. Insights on coccolith chemistry from a new ion probe method for analysis of individually picked coccoliths. *Geochemistry Geophysics Geosystems*, 8(6). <https://doi.org/10.1029/2006GC001546>

- Stoll, H.M., Klaas, C.M., Probert, I., Encinar, J.R. & Alonso, J.I.G. 2002a. Calcification rate and temperature effects on Sr partitioning in coccoliths of multiple species of coccolithophorids in culture. *Global and Planetary Change*: 153-171. [https://doi.org/10.1016/S0921-8181\(02\)00112-1](https://doi.org/10.1016/S0921-8181(02)00112-1)
- Stoll, H.M. & Schrag, D.P. 2000. Coccolith Sr/Ca as a new indicator of coccolithophorid calcification and growth rate. *Geochemistry Geophysics Geosystems*, 1(5). <https://doi.org/10.1029/1999GC000015>
- Stoll, H.M. & Ziveri, P. 2002. Separation of monospecific and restricted coccolith assemblages from sediments using differential settling velocity. *Marine Micropaleontology*: 209-221. [https://doi.org/10.1016/S0377-8398\(02\)00040-3](https://doi.org/10.1016/S0377-8398(02)00040-3)
- Stoll, H.M. & Ziveri, P. 2004. Coccolithophorid-based geochemical paleoproxies, *Coccolithophores*. Springer: 529-562.
- Stoll, H.M., Ziveri, P., Geisen, M., Probert, I. & Young, J.R. 2002b. Potential and limitations of Sr/Ca ratios in coccolith carbonate: new perspectives from cultures and monospecific samples from sediments. *Philosophical Transactions of the Royal Society A Mathematical, Physical and Engineering Sciences*, 360(1793): 719-747. <https://doi.org/10.1098/rsta.2001.0966>
- Stolz, K., Baumann, K.-H. & Mersmeyer, H. 2015. Extant coccolithophores from the western equatorial Indian Ocean off Tanzania and coccolith distribution in surface sediments. *Micropaleontology*: 473-488.
- Stuiver, M., Reimer, P.J. & Reimer, R.W. 1993. Extended 14C data base and revised Calib 3.0 14C age calibration program. *Radiocarbon*: 215-230. <https://doi.org/10.1017/S0033822200013904>
- Su, X., Liu, C., Beaufort, L., Barbarin, N. & Jian, Z. 2015. Differences in Late Quaternary primary productivity between the western tropical Pacific and the South China Sea: Evidence from coccoliths. *Deep-Sea Research Part II-Topical Studies in Oceanography*: 131-141. <https://doi.org/10.1016/j.dsr2.2015.07.008>
- Summerhayes, C.P., Kroon, D., Rosell-Mele, A., Jordan, R.W., Schrader, H.J., Hearn, R., Villanueva, J., Grimali, J.O. & Eglinton, G. 1995. Variability in the Benguela Current upwelling system over the past 70,000 years. *Progress in Oceanography*, 35(3): 207-251. [https://doi.org/10.1016/0079-6611\(95\)00008-5](https://doi.org/10.1016/0079-6611(95)00008-5)
- Takahashi, K. & Okada, H. 2000. The paleoceanography for the last 30,000 years in the southeastern Indian Ocean by means of calcareous nannofossils. *Marine Micropaleontology*: 83-103. [https://doi.org/10.1016/S0377-8398\(00\)00033-5](https://doi.org/10.1016/S0377-8398(00)00033-5)
- Tangunan, D., Baumann, K.-H., Pätzold, J., Henrich, R., Kucera, M., De Pol-Holz, R. & Groeneveld, J. 2017. Insolation forcing of coccolithophore productivity in the western tropical Indian Ocean over the last two glacial-interglacial cycles. *Paleoceanography*, 32: 692-709. <https://doi.org/10.1002/2017PA003102>
- Ternon, J.F., Bach, P., Barlow, R., Huggett, J., Jaquemet, S., Marsac, F., Menard, F., Penven, P., Pontier, M. & Roberts, M.J. 2014. The Mozambique Channel: From physics to upper trophic levels. *Deep Sea Research Part II: Tropical Studies in Oceanography*, 100: 9. <https://doi.org/10.1016/j.dsr2.2013.10.012>
- Thierstein, H.R., Geitzenauer, K.R. & Molfino, B. 1977. Global synchronicity of Late Quaternary coccolith datum levels - validation by oxygen isotopes. *Geology*: 400-404. [https://doi.org/10.1130/0091-7613\(1977\)5<400:GSOLQC>2.0.CO;2](https://doi.org/10.1130/0091-7613(1977)5<400:GSOLQC>2.0.CO;2)
- Tokinaga, H., Xie, S.P., Deser, C., Kosaka, Y. & Okumura, Y.M. 2012. Slowdown of the Walker circulation driven by tropical Indo-Pacific warming. *Nature*, 491(7424): 439-443. <https://doi.org/10.1038/nature11576>
- Vecchi, G.A. & Soden, B.J. 2007. Global warming and the weakening of the tropical circulation. *Journal of Climate*, 20(17): 4316-4340. <https://doi.org/10.1175/JCLI4258.1>
- Vecchi, G.A., Soden, B.J., Wittenberg, A.T., Held, I.M., Leetmaa, A. & Harrison, M.J. 2006. Weakening of tropical Pacific atmospheric circulation due to anthropogenic forcing. *Nature*, 441(7089): 73-76. <https://doi.org/10.1038/nature04744>
- Wang, Y.M.V., Leduc, G., Regenberg, M., Andersen, N., Larsen, T., Blanz, T. & Schneider, R.R. 2013. Northern and southern hemisphere controls on seasonal sea surface temperatures in the Indian Ocean during the last deglaciation. *Paleoceanography*: 619-632. <https://doi.org/10.1002/palo.20053>
- Wells, P., & Okada, H. 1996. Holocene and Pleistocene glacial palaeoceanography off southeastern Australia, based on foraminifers and nannofossils in Vema cored hole V18-222. *Australian Journal of Earth Sciences*, 43(5): 509-523. <https://doi.org/10.1080/08120099608728273>
- Westbroek, P., Brown, C.W., Van Bleijswijk, J., Brownlee, C., Brummer, G.J., Conte, M., Egge, J., Fernández, E., Jordan, R. & Knappertsbusch, M. 1993. A model system approach to biological climate forcing. The example of *Emiliana huxleyi*. *Global and Planetary Change*, 8(1-2): 27-46. [https://doi.org/10.1016/0921-8181\(93\)90061-R](https://doi.org/10.1016/0921-8181(93)90061-R)
- Winter, A., Jordan, R.W. & Roth, P.H. 1994. Biogeography of living coccolithophores in ocean waters. In: A. Winter & W. G. Siesser (Eds.), *Coccolithophores*. Cambridge University Press: 37.
- Winter, A. & Martin, K. 1990. Late Quaternary history of the Agulhas Current. *Paleoceanography*: 479-486. <https://doi.org/10.1029/PA005i004p00479>

- Xie, S.P., Annamalai, H., Schott, F.A. & McCreary, J.P. 2002. Structure and mechanisms of South Indian Ocean climate variability. *Journal of Climate*: 864-878.
[https://doi.org/10.1175/1520-0442\(2002\)015<0864:SAMOSI>2.0.CO;2](https://doi.org/10.1175/1520-0442(2002)015<0864:SAMOSI>2.0.CO;2)
- Young, J.R. 1994. Functions of coccoliths. In: A. Winter & W. G. Siesser (Eds.), *Coccolithophores*. Cambridge University Press: 63-82.
- Young, J.R., Geisen, M., Cros, L., Kleijne, A., Sprengel, C., Probert, I. & Østergaard, J. 2003. A guide to extant coccolithophore taxonomy. *Journal of Nannoplankton Research Special*: 1-124.
- Young, J.R. & Ziveri, P. 2000. Calculation of coccolith volume and its use in calibration of carbonate flux estimates. *Deep-Sea Research Part II-Topical Studies in Oceanography*: 1679-1700.
[https://doi.org/10.1016/S0967-0645\(00\)00003-5](https://doi.org/10.1016/S0967-0645(00)00003-5)
- Ziveri, P., Baumann, K.-H., Böckel, B., Bollmann, J. & Young, J.R. 2004. Biogeography of selected Holocene coccoliths in the Atlantic Ocean, *Coccolithophores*. Springer: 403-428.
https://doi.org/10.1007/978-3-662-06278-4_15

Acknowledgments

This research endeavor would not have been possible if not for the following people and institutions who have doled out as support, mentors, collaborators or inspirations:

For his constant guidance and support throughout the conduct of this thesis, I thank **Dr. Karl-Heinz Baumann**. For all the advice, discussions, time and boost to finish this endeavor, thank you. I would not have survived in Bremen without your help since the very beginning.

To my supervisor **Prof. Dr. Rüdiger Henrich** for his valuable comments and suggestions from the conception of this project, manuscript writing, to finishing this dissertation, thank you.

To the members of my thesis committee **Dr. Jürgen Pätzold** and **Prof. Dr. Michal Kucera**, I am deeply honored to be working with the both of you. I am thankful for your time and input in this project. Our thesis committee meetings have provided me with the much needed direction and have kept me on track.

To **Prof. José Abel Flores Villarejo**, for being one of the reviewers, thank you. I am grateful for the opportunity to discuss this work with you.

To the **Paleoceanography-Sedimentology Research Group**, especially to the “cocco girls” **Mariem Saavedra-Pellitero**, **Catarina Guerreiro** and **Catarina Cavaleiro**, thank you. I consider myself quite lucky to have shared the “coccoworld” with you, guys! I thank my officemate **Grit Warratz**, for sharing with me three wonderful working years in the office. Big thanks is especially due to **Mariem and Catarina G.** for their time (and patience) reading and commenting on my first drafts, may it be manuscripts, posters, reports, figures, drawings, presentations, etc. and for being there to help in any and in every way.

To **Brit Kockisch** for all the laboratory assistance, providing me with every laboratory supplies I need, thank you very much. To **Susanne Müller-Wünsch**, thank you for your help in all the administrative matters.

To the **Bremen International Graduate School for Marine Sciences (GLOMAR)** and **MARUM – Center for Marine Environmental Sciences** for the funding support and the opportunity to present results of this project to local and international scientific conferences, thank you.

To the **Meteor 2008, IMAGES-2, ODP Leg 208**, and the **IODP Expedition 361 Science Party** for the sediments used for this study, thank you.

To the **Once Upon a Time** team, especially to **Dharma Reyes-Macaya** and **Gema Martinez Mendez** for the opportunity to share my science to the general audience, thank you.

This thesis is dedicated to **my family members** who know nothing about the contents of this thesis but tried to help in anyway.

And to all the **scientists, professors, colleagues, former and present labmates** and **friends** who have inspired me to learn, thank you.

Versicherung an Eides Statt
gem. § 5 Abs. 5 der Promotionsordnung vom 15.07.2015

Ich, **Deborah Tangunan**, Eduard-Grunow-Str. 31, 28203 Bremen, 3069065
(Vorname, Name, Anschrift, ggf. Matr.-Nr.)

versichere an Eides Statt durch meine Unterschrift, dass ich die vorstehende Arbeit selbständig und ohne fremde Hilfe angefertigt und alle Stellen, die ich wörtlich dem Sinne nach aus Veröffentlichungen entnommen habe, als solche kenntlich gemacht habe, mich auch keiner anderen als der angegebenen Literatur oder sonstiger Hilfsmittel bedient habe, und die zu Prüfungszwecken beigelegte elektronische Version der Dissertation mit der abgegebenen gedruckten Version identisch ist.

Ich versichere an Eides Statt, dass ich die vorgenannten Angaben nach bestem Wissen und Gewissen gemacht habe und dass die Angaben der Wahrheit entsprechen und ich nichts verschwiegen habe. Die Strafbarkeit einer falschen eidesstattlichen Versicherung ist mir bekannt, namentlich die Strafandrohung gemäß § 156 StGB bis zu drei Jahren Freiheitsstrafe oder Geldstrafe bei vorsätzlicher Begehung der Tat bzw. gemäß § 161 Abs. 1 StGB bis zu einem Jahr Freiheitsstrafe oder Geldstrafe bei fahrlässiger Begehung.

Ort, Datum

Unterschrift

